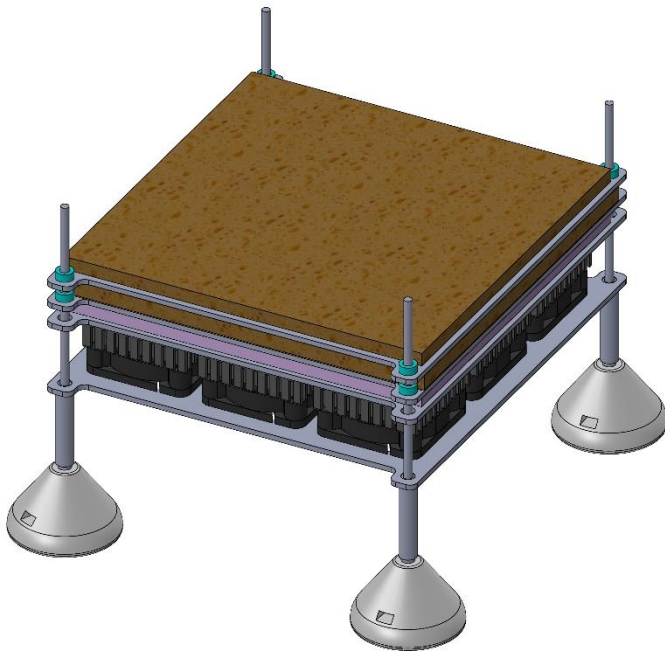


Therminus-K2: A Thermal Conductivity Measurement Device for Textile Layers at a Crime Scene



Charlotte I. Kaanen
Delft University of Technology

Therminus-K2: A Thermal Conductivity Measurement Device for Textile Layers at a Crime Scene

Design and Development

By

Charlotte I. Kaanen

in partial fulfilment of the requirements for the degree of

Master of Science

in the field of

**BioMedical Engineering:
Medical Devices and Bioelectronics**

to be defended publicly on the 17th of June, 2022 at 9:30 AM.

Student number:	4453719	
Supervisors:	dr. ir. A.J. Loeve (chair), drs. C.A.W. Pellemans,	TU Delft, Dept. BioMechanical Engineering Politie Nederland, Forensics Department
Committee member:	dr. ir. T. Horeman	TU Delft, Dept. BioMechanical Engineering

An electronic version of this thesis is available at <http://repository.tudelft.nl/>.



Preface

This thesis marks the end of my wonderful time at TU Delft: a time in which I have grown from an 18 year old high school student to a real Biomedical Engineer.

I would like to thank everybody that made my time in Delft such a great experience. First and foremost, I would like to thank my parents for their unconditional support and for making it possible for me to finish my studies. Furthermore, I would like to thank everybody I had the opportunity to meet during my time in Delft: de Butsers, Féliz, Oras, Rabarbers, and all the others! I'm very lucky to have met you all and I smile back to all the beautiful memories we have made together.

In this final thesis project, I had the chance to develop a thermal conductivity measurement device for textile layers. The device specifically measures textile layers that were present surrounding a deceased at a crime scene. The thermal conductivity coefficients of these layers are needed in the calculation of the post mortem interval: the time passed shortly after death. It was extremely interesting to be working on this project, and to learn about the crime scene investigation process as a graduate intern at the Dutch Police.

I would gratefully like to thank dr. ir. Arjo J. Loeve and drs. Chris A.W. Pellemans for their supervision and support. In particular, I would like to thank Arjo for his thorough feedback throughout my thesis.

Enjoy reading!

*Charlotte Kaanen
Rotterdam, May 28, 2022*

Abstract

Introduction

Each year, many people die due to non-natural causes of death, such as accidents, suicide, and murder and manslaughter. In these cases it is often necessary to investigate the cause, manner and time of death, which are investigated by forensic pathologists and the Police. To determine the time of death, the post mortem interval (PMI), the time passed shortly after death, should then be determined.

Wilk et al. (2020) developed a new method to determine the early PMI (3 – 72 hours). An input parameter in this method is the Thermal Conductivity Coefficient (k-value) of the textile layers surrounding the deceased. A method to determine the k-value of textile layers at, or around, a crime scene is needed. Therefore, this study aimed to design and develop a Thermal Conductivity (TC) measurement device for textile layers at a crime scene.

Method

A functional decomposition chart of the device and a morphologic overview were created to design a suitable concept which was used for further development of the final prototype. SolidWorks was used to perform heat transfer simulations that were required to make the right design decisions and subsequently a final design and prototype were developed.

Tests were performed to assess the performance of the prototype in terms of device configuration, accuracy, precision and measurement time. Furthermore, the effects of moisture content of the sample and sample compression during measurement on the calculated k-value were investigated.

Results

A Guarded Hot Plate (GHP) based prototype was developed: Therminus-K2. This prototype was equipped with a back heater and four guard heaters to ensure one dimensional heat flow from the main heater through the sample towards the cold plate to eliminate other heat flows.

Therminus-K2 obtains a precision of < 5% in TC measurements within 30 minutes. A steady-state measurement is achieved within a maximum of 7 minutes.

Increasing the moisture content (2 states: dried and wetted) in the sample resulted in an increase in determined k-value (205 – 415 %). However, the uncertainty in sample thickness measurement was high (up to 16.7%) and complicated measurement of the sample compression effect on determined k-values.

Discussion and Conclusion

Therminus-K2 delivers precise and fast TC measurements of textile samples: impressive results considering the simple components that were used. The future development of Therminus-K2 should focus on improving sample thickness measurement and improve user friendliness in order to make the device suitable to use in PMI estimation at actual crime scenes.

Nomenclature

Abbreviations

PMI	P ost M ortem I nterval
CSI	C rime S cene I nvigation
TC	T hermal C onductivity
GHP	G uarded H ot P late
GH	G uard H heater
BH	B ack H heater
CMR	C onduction M easurement R egion
SS	S teady-State
PWM	P ulse W idth M odulation
NTC	N egative T emperature C oefficient
PID	P roportional I ntegral D erivative
MOSFET	M etal– O xide– S emiconductor F ield- E ffect T ransistor
EMI	E lectro M agnetic I nterference

Materials

PC	Polycarbonate
NY6	Nylon 6 (Polyamide 6)
CO	Cotton
PES	Polyester
PAN	Acrylic

Symbols

k	$[\frac{W}{mK}]$	Thermal Conductivity Coefficient (often referred to as k-value)
dT or ΔT	$[^{\circ}C]$	Temperature Difference between the plates
\dot{Q}	$[Watt]$	Power to the main heater
A	$[m^2]$	Measuring Area
L	$[m]$	Sample Thickness
R	$[\frac{m^2K}{W}]$	Thermal Resistance

Table of Contents

1. INTRODUCTION	1
1.1 Time of Death Estimation and Problem in Thermal Conductivity Determination	1
1.2 A Thermal Conductivity Measurement Device	3
1.2.1 Design Objectives	3
1.2.2 Design Requirements	3
2. PRINCIPLES OF THERMAL CONDUCTIVITY MEASUREMENT OF TEXTILE	7
2.1 Measurement principle	7
2.2 Factors affecting Thermal Conductivity measurement of Textile Layers	8
3. CONCEPT DEVELOPMENT	10
3.1 Concept Design Method	10
3.2 Concept Design Result	11
3.2.1 Sub-solutions and Morphologic Chart	11
3.2.2 Concept Selection	13
4. SIMULATIONS FOR DESIGN DECISIONS	15
4.1 Ratio of Main Heater to Guard Heater Dimensions	15
4.2 Minimum Aluminum Plate Thickness required for Temperature Uniformity	17
5. THERMINUS-K2 PROTOTYPE	19
5.1 Construction Methods	19
5.2 The Therminus-K2 Prototype	19
5.2.1 Overview	19
5.2.2 Temperature Control	23
5.2.3 Electronics and Software	24
5.2.4 Specifications	27
6. THERMINUS-K2 TESTS	29
6.1 Therminus-K2 Validation and Performance	29
6.1.1 Device Configuration Test	29
6.1.2 Performance Test	32
6.2 Error Sensitivity Test	34
6.3 Therminus-K2 Case Study	37
6.3.1 Moisture Content Effect Test	37
6.3.2 Sample Compression Effect Test	38
7. DISCUSSION	41
7.1 Interpretation of the Experimental Results	41
7.2 Evaluation of the Design Requirements	42
7.3 Limitations	44

7.4 Recommendations	45
8. CONCLUSION.....	47
REFERENCES	49
APPENDICES	54
A. Extension to the Morphologic Chart: sub-solutions to Position Textile Sample.....	54
B. Established Temperature Distributions in Simulation 4.2.....	55
C. Preparation, Calibration and Validation of the Temperature Sensors	57
D. Sensor Positioning Cold Plate	62
E. Full Electronics Scheme.....	64
F. Photographs of the Terminus-K2 prototype	65
G. Visualization of the Terminus-K2 layers and electronics	66
H. Measurement Protocol.....	68
I. Original Textile Samples used for Measurements.....	69
J. Extended List of Components used in Terminus-K2	70
K. Technical Drawings of Custom-designed Components	72
L. Data Sheets of some (electronic) components.....	85
M. Arduino Code used for Data Acquisition.....	91
N. Full MATLAB Code	95
O. Output of post-processing data in MATLAB.....	100
P. Literature Study.....	103

1. INTRODUCTION

1.1 Time of Death Estimation and Problem in Thermal Conductivity Determination

The Post Mortem Interval

In 2020, 168.678 people died in the Netherlands, of which 9.030 died due to non-natural causes of death, such as accidents (6.433, of which 633 in transport), suicide (1.823) and, murder and manslaughter (107) [1]. The mortal remains that are found in these cases are investigated by forensic pathologists, the Dutch Police and sometimes by the Netherlands Forensic Institute. The reason, manner and time of death are often unknown and should thus be investigated.

For this investigation, an estimation of the post mortem interval (PMI), the time passed after death, is important as it helps to determine the actual time of death. An estimation of the PMI assists in death investigation by drafting a temporal reconstruction of the events. A narrowed time frame of PMI estimations could help the Police in proceeding with their investigations with more focus, making the investigations more efficient [2]. For this purpose, it would be most beneficial to determine the PMI as early as possible at the crime scene.

The PMI is categorized into an immediate (0 – 3 hours), early (3 – 72 hours) and late (> 72 hours) phase [3]. The PMI estimation is easily done within the immediate phase, as the body undergoes rapid physiological and biochemical changes are particularly detectable in the eyes and the skin. In the subsequent early phase, estimation of the PMI is not so evident. However, the mortal remains are still cooling down and measurements can be performed to estimate the PMI. After this period the late PMI phase is entered, in which the body has substantially cooled down, starts disintegrating and undergoes decomposition. In the late phase, no proper measurements to estimate the PMI can be performed.

Methods for early Post Mortem Interval Estimation

Currently, the early PMI is primarily determined via the Henssge method [4]. However, this method is not very precise, having a maximum error of the PMI estimation of ± 7 hours (tested on 53 bodies, maximum true PMI: 75 hours) [5]. The method, used as a nomogram, only includes one correction factor for cooling conditions deviating from the standard (unclothed, uncovered, still air) [4]. However, factors to correct for differences in environment or posture conditions are lacking.

Therefore, Wilk et al. (2020) developed a new method to determine the early PMI that utilizes a thermodynamic finite-difference model, called PHOEBE, combined with skin thermometry [6]. The PHOEBE model, while still being in its development stage, already shows great promises. 83.3 % of the reconstructed PMIs deviated less than ± 1 hour from their equivalent real PMIs, tested on 4 bodies (total of 80 data points) with true PMIs ranging from 5 – 50 hours [6]. This method could therefore help in a better early PMI determination, compared to the golden standard's Henssge method.

One of the input parameters in the PHOEBE model is the thermal conductivity coefficient (k-value) of textile layers surrounding the deceased. Thermal conductivity (TC) indicates the ability of a material to conduct heat; a lower k-value means better insulation. Thermal clothing insulation around a human body reduces the heat transfer (the thermal energy transfer between two objects due to a temperature difference) between the body and the environment. Therefore, the k-value of these textile layer is an important input parameter in the PHOEBE model. To determine the PMI as soon as possible and continue the forensic investigation with an accurately estimated PMI, the k-value of the textile layers should be determined directly at the crime scene, where the mortal remains are.

Determination of Thermal Conductivity of Textile Layers

TC of textile layers could either be estimated, or determined through measurement. The k-value could be estimated based on the material composition of clothing, as indicated in its garment label. This however might not give the most reliable results for insulating fabrics, as it excludes the effect of factors like fabric thickness, moisture and compression on TC of clothing [7]. Furthermore, non-adjustable intrinsic fabric parameters, such as microstructure, density, (fibre) composition, layering,

long-time wear, and weaving pattern of the sample may also affect TC [8]. In addition to that, pre-processing techniques (e.g. coatings, spraying and nano-soldering) affect TC of textile layers [9-14]. Therefore, it is desirable to determine the k-value of textile layers through measurement instead of estimating it.

Existing TC measurement systems, like the λ -Meter EP500e (Lambda-Meßtechnik, Dresden, Germany), the HFM-100 Heat Flow Meter (Thermtest Inc., Fredericton, Canada), the TPS 3500 (Hot Disk, Göteborg, Sweden) and the Trident (C-Therm Technologies Ltd., Fredericton, Canada) seem not to be fit for use at a crime scene [15-19]. The main problem is that these systems are too large and complex to move to a crime scene, as these systems are generally fabricated to test 'large' samples of building insulation materials. Besides this, existing devices are rather expensive (\pm €40.000,-), which makes them unsuitable for broad use by the Police.

Therefore, a new TC measurement device is needed for on-site TC determination of the textile layers found on mortal remains. Previous studies by the BioMedical Engineering Department (Delft, University of Technology) resulted in the basis of the development of a Guarded Hot Plate (GHP) based measurement device. In a series of student assignments [20-25], a first prototype has been developed, called Therminus-K1 (Project name (Therminus) -Variable (k) -Version (1)) (**Figure 1**) [24]. However, this prototype is still only a proof of principle, having the following limitations [25]:

- Low accuracy
- Low precision
- Fragile
- Difficult to use

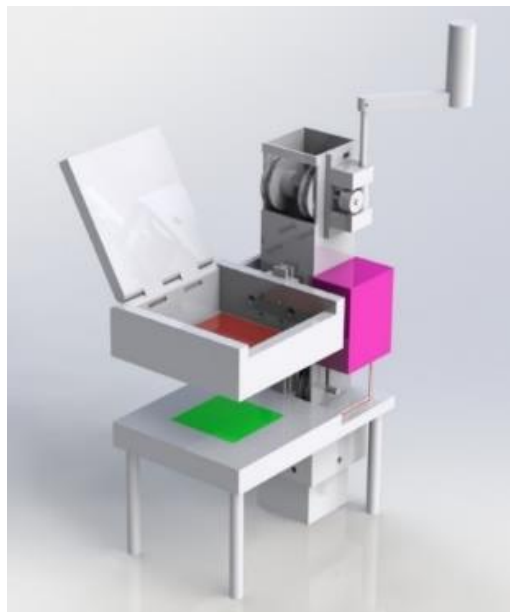


Figure 1. Therminus-K1 SolidWorks drawing: A concept for measuring TC of textile, adapted from [24].

The low accuracy and precision in Therminus-K1 are likely to be attributed to:

- Parasitic heat flows (generated heat that does not flow through the sample, but in lateral or backward directions),
- Incomplete system coding, and
- A fragile and limited electronics configuration.

However, even though the device does not yet meet the design requirements, the feasibility and operation of the concept have been demonstrated and remain very promising. Therefore, it is aimed to improve Therminus-K1 to a new, more precise, compact and user-friendly prototype.

1.2 A Thermal Conductivity Measurement Device

1.2.1 Design Objectives

In improving Thermanus-K1 to a new prototype, hereinafter referred to as Thermanus-K2, first the major limitations of Thermanus-K1 should be solved. Therefore, the main focus of this design study lies in improving the performance of the device in terms of accuracy and precision. This is needed in order to use the TC measurement results in PMI estimation and eventually in court. Besides this, its final application in forensic practice is considered throughout the processes in this design study. The TC measurement device should be used by forensic investigators during crime scene investigation (CSI) processes, in which the device and its use should be easily incorporated. The measurements shouldn't take long or interfere with CSI workflows and the results should be usable as an input in the PHOEBE model.

Intended use: measuring TC of textile samples at a crime scene.

Intended user: forensic investigators (Netherlands Forensic Institute) and/or forensic investigation Police employees.

1.2.2 Design Requirements

A list of design requirements for Thermanus-K2 was compiled based on discussions with the Dutch Police (dep. Forensic Investigation), the Netherlands Forensic Institute (dep. Crime Scene Investigation), the Amsterdam Medical Centre (PHOEBE development team) and the TU Delft (dep. BioMedical Engineering). Several expert sessions were held with the intended users and the developers of the PHOEBE model to quantify the requirements. Later, the requirements were specified according to literature values, NEN/ISO norms and insights from the previously conducted literature study about factors affecting TC measurement of textile layers [7]. The list of design requirements is provided in **Table 1**.

Requirement 1

In studies investigating TC of clothing samples, k -values at standard conditions ($\pm 23\text{ }^{\circ}\text{C}$, $\sim 40\text{ }\%$ humidity) ranged from 0.057 to 0.52 W/mK [24]. In conditions which increased apparent k -values these ranged from 0.022 – 0.7 W/mK, due to amongst others an increased moisture content [7, 26-48]. Layers surrounding the deceased with k -values above 0.7 W/mK don't affect PMI determination, as investigated by Dessing (2018) [21]. Therefore, the device should at least be able to identify k -values of clothing under standard conditions (0.057 to 0.52 W/mK) and should ideally also be able to determine k -values over the range from 0.022 to 0.7 W/mK.

Requirement 2

The device should at least be able to measure textile samples with thicknesses from 0.44 – 28 mm, as 99.73 % of clothing pieces has thicknesses within this range [24]. Ideally, the device could measure a wider range of textile layer thicknesses. This is as during forensic investigations even thicker textile layers may be found, according to 5 interviewed forensic investigation coordinators (FOCO Den Haag, Rotterdam, Amsterdam, Limburg and Noord-Nederland).

Requirements 3 and 4

The device should be able to obtain TC measurement results with high accuracy ($\leq 8\text{ }\%$) and high precision ($\leq 5\text{ }\%$). This is needed to minimize the error in PMI estimation by the PHOEBE model to $\leq 3\%$, which is required to use the final PMI estimation in court. The accuracy is defined as the error of the measurement, the difference between the measured k -value and the exact k -value, as a percentage of the measured k -value. The precision, the repeatability of the measurement, is defined as the standard deviation of the k -values over repeated measurements ($n = 5$) as a percentage of the average k -value over these measurements.

Requirement 5

Forensic investigation coordinators highly prefer keeping the textile samples used for TC measurement intact, to be able to use them in further investigations (e.g. for DNA). If, however, a sample is to be cut from the clothing, maximum sample dimensions of 100 by 100 mm are accepted. Additionally, the cut clothing sample should not be destroyed, as it is a piece of evidence in the investigation and in the PMI estimation.

Requirements 6, 7 and 8

The TC measurement should be done by an autonomous device, that is capable of operating by itself, without direct human control. The operator just starts and ends the measurement. The time to set up the device before measurement should be less than 5 minutes, to minimally interrupt the further CSI process (**Requirement 6**). The measurement time should at least be less than 90 minutes and ideally less than 30 minutes, as requested by forensic investigation coordinators (**Requirement 7**). Furthermore, the device must be reusable over time with low maintenance (**Requirement 8**).

Requirement 9

It is important to prevent cross-contamination (e.g. of DNA) between tested textile samples. Especially when measured samples are used for further investigation after TC determination, decontamination of the measurement device to avoid cross-contamination is essential. Besides this, the device should be cleanable to ensure proper measurements as left-over material from one sample could influence the measurement results of the following.

Requirements 10, 11, 12 and 13

External influences of wind, water, changing environment temperatures and thermal radiation affect TC measurement [7]. Therefore, shielding of the measurement is needed to prevent this (**Requirement 10**). Shielding should be done in a way that enables performing measurements both in the lab and at, or around a crime scene. Performing measurement at these different locations requires different power supplies. Therefore, the device should at least allow powering by a common wall outlet and should ideally allow powering by either batteries or power outlets available in a Police car or forensic investigation van (**Requirement 11**).

The encased device should be robust since it will be used in different types of environments during hectic CSI processes (**Requirement 12**). The device should be able to handle transport between crime scenes and Police offices. In addition to this, the device should have dimensions allowing for transport in a Police van (**Requirement 13**).

Requirements 14, 15 and 16

Communication of the results of the TC measurement should be fit for use in the PHOEBE model (**Requirement 14**). Furthermore, operating the device should be intuitive (**Requirement 15**). Otherwise, the intended users of the device won't use it or would use it incorrectly.

Requirement 16 is added as staying below the European tender limit simplifies the purchase of new devices for Police units. The Dutch Police has a total of 11 Police units throughout the country, with on average 10 forensic investigation vans each. As each van would need one TC measurement device, the maximum costs per device would be €1.945,-.

In this thesis, the focus lies on the performance requirements of the device and the wish to make a device with simple solutions. One first needs a well-performing device before further developing it in terms of the requirements for physical parameters, user interface parameters and costs. These requirements had lower priority for now.

Table 1. Design requirements for the Thermanus-K2 TC measurement device.

The requirements were organised into the categories: performance parameters, physical parameters, user interface and others. For each requirement, minimal and target terms were listed and the reasons for the specific requirements were shortly explained. When minimal and target values of a requirement were equal, cells were merged.

Mind: the requirements within a category were not ordered on importance.

Requirement		Minimal	Target	Reason
Performance parameters				
1	Range of k-values able to measure	0.057 – 0.52 W/mK [24]	0.022 – 0.7 W/mK [26, 27, 37]	K-values in this range should be measured and identified.
2	Range of sample thicknesses able to measure	0.44 – 28 mm [24]	0.17 – 150 mm	Minimal values cover 99.73% of clothing pieces. Target values as found during CSI processes.
3	Accuracy error of TC measurement	≤ 8 % [21, 24]	≤ 3 % [21]	Results need to be used in court later
4	Precision error of TC measurement	≤ 5 % [21]	≤ 1 % [21]	Results need to be used in court later
5	Sample dimensions needed for measurement	100 x 100 mm ²	Keep textile intact	Textile should preferably be kept intact. If the textile does need to be cut, a small sample is accepted.
6	Setup time	< 5 minutes		Minimal interference with CSI process.
7	Measurement time	< 90 minutes	< 30 minutes [21]	Minimal interference with CSI process, assuming an autonomous device.
8	Lifetime without recalibration	≥ 3 months	≥ 12 months	Low maintenance is requested.
Physical parameters				
9	Decontamination	The device should allow frequent (up to 5 times a day) cleaning with agents based on alcohol and with RNA purification products and should otherwise be partly disposable.		Cross-contamination (e.g. of DNA) between crime scenes must be prevented and proper measurements should be ensured.
10	Shielding	The measurements should be performed in an environment without external influences from wind, water, changing temperatures (max ± 5°C) or thermal radiation.		Measurements should not be affected by external influences.
11	Power supply	The device should allow powering by a common 230V-16A AC wall outlet.	The device should allow powering by either batteries and/or a 12V-10A DC (car) outlet as well as by a 230 V-16A DC (CS van).	Ideally, the device should enable performing measurements at, or around the crime scene.
12	Robustness	The encased device should meet the test for rough handling shocks (NEN-EN-IEC 60069-2-31:2008) and (non)repetitive shocks (NEN-EN-IEC 60068-2-27:2008) [49, 50].		The device will be used in different types of environment during hectic CSI processes.
13	Mobility	Dimensions ≤ 330x330x330 mm and weight ≤ 8 kg [21].	Dimensions ≤ 250x250x250 mm and weight ≤ 2 kg [21].	To allow for transport of the device to a crime scene.
User interface				
14	Results communication	The device should deliver both a file with the raw measurement data and a PDF with a description of the measurement and its outcome*.		It should be possible to use the results of the TC measurements in the PHOEBE model.

	Requirement	Minimal	Target	Reason
15	Simplicity	The device should be intuitive and fit to use for forensic investigators and/or forensic investigation Police employees.		Operating the device should be intuitive, otherwise it will either not be used or it will be used in the wrong way.
Others				
16	Costs per device	≤ 1.945 euros		Staying below the European tender limit of €214.000,- simplifies the purchase of new devices by the Police.

*: The outcome of the measurement should at least contain determined k-value [W/mK], sample thickness [mm] and time duration in which a steady state measurement was established [minutes].

Combining all requirements resulted in the following design goal:

Design, develop and test a fast (< 90 minutes), accurate ($\leq 8\%$) and precise ($\leq 5\%$) measurement device that can determine the thermal conductivity coefficient of textile layers at, or around a crime scene and deliver measurements fit for use in the PHOEBE model.

2. PRINCIPLES OF THERMAL CONDUCTIVITY MEASUREMENT OF TEXTILE

2.1 Measurement principle

Heat conduction through a volume of a material driven by a temperature gradient, results in a linear temperature distribution across the material when the system reaches a steady state (**Figure 2**). In a steady state system with one dimensional heat flow, the k-value of the material can be determined via the formula

$$k = \frac{\dot{Q} * L}{A * \Delta T} \quad [W/mK] \quad (1)$$

Where

- \dot{Q} [W] is the rate of heat flow through the material,
- L [m] is the material's thickness,
- A [m²] is the measured surface area, and
- ΔT [°C] is the temperature difference between the face at $x = 0$ [m] and $x = L$ [m].

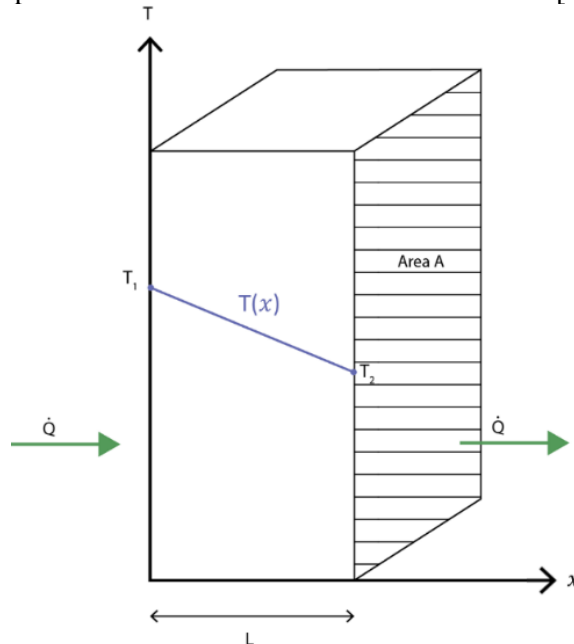


Figure 2. One-dimensional heat transfer across a plane wall by conduction, showing the temperature distribution, adapted from [7].

The often-used guarded hot plate (GHP) method is chosen as the base technique to use to determine TC of textile layers at a crime scene, for two reasons; First of all, the GHP method is denoted by the American Society for Testing and Materials (ASTM) as the most accurate TC measurement method for textile and indeed appears to be the most used and most often reported method in literature [28-33, 35, 51-59]. It is the only absolute method for steady state TC measurement of homogeneous materials that can achieve an overall measurement uncertainty below 2% [60]. Secondly, the GHP method, being a steady state method, is based on simple physics and requires straightforward signal processing. This results in simpler manufacturing and maintenance which is favourable compared to the more complex transient state methods.

In the GHP method a steady state temperature difference is generated over a sample material. This generally is realized via a hot plate on one side of the sample, acting as a heater, and a cold plate on the other side of the sample, acting as a cooler. The plates are controlled to maintain specific temperatures. The electrical power needed to heat the hot plate indicates the heat flow rate through the sample. The sample thickness and the surface area should be determined and resultingly the k-value of

the sample material is determined through Equation 1. A simplified scheme of the principle of the GHP method is provided in **Figure 3**.

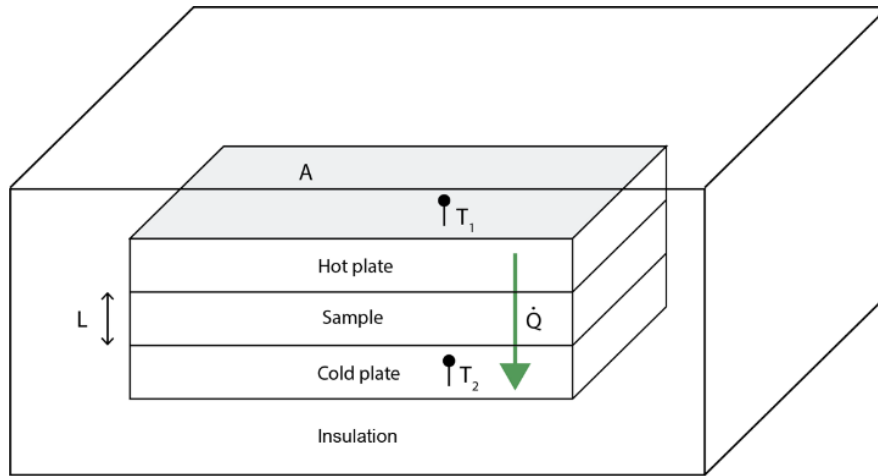


Figure 3. Schematic general GHP method for TC measurement of flat samples, adapted from [7].

T_1 and T_2 : indicating temperature measurement; L : sample thickness; \dot{Q} : heat flow per unit area; A : horizontal area hot plate = horizontal area sample = horizontal area cold plate [7]

In order to use Equation 1 to determine a sample material's k -value, a uniform one directional and steady state heat flow should be established through a flat homogeneous sample sandwiched between two isothermal plates. The electrical power delivered to the hot plate only corresponds to the heat flow through the sample if all produced heat actually only flows through the sample in a straight line. Therefore, in the design of a TC measurement device, parasitic heat flows should be eliminated: heat flow in backward and lateral direction on the edges of the hot plate.

Besides this, the hot and cold plates require adequate temperature control and should achieve and maintain a uniform temperature distribution. Furthermore, the material's thickness and the horizontal hot plate area should be determined.

Altogether, the Terminus-K2 prototype will have to consist of at least some basic components, in order to comply with the operation of a GHP measuring method. These basic components are:

- A heating module to generate and maintain a uniformly heated hot plate
- A cooling module to generate and maintain a uniformly cooled cold plate
- Modules to measure temperatures at the hot and cold plates
- A module to determine the sample material's thickness
- A module to eliminate lateral and backward heat flow from the hot plate to the environment
- A sample chambre enclosed by the heating and cooling module

2.2 Factors affecting Thermal Conductivity measurement of Textile Layers

It is indispensable to get insight into factors possibly affecting a TC measurement system for textile layers. In a previously conducted systematic review, thickness of a clothing sample, its moisture content, the air layer thickness between clothing and the measurement device, and the sample compression appeared to be the most dominant factors affecting the apparent TC of textile [7, 26-48]. An extensive overview of factors affecting TC measurement of textile layers is shown in **Figure 4**.

In developing a TC measurement device, adequate measurement of a sample's fabric thickness is indispensable to ensure correct TC determination [7]. To avoid the presence of air layers between the textile sample and the measuring device plates, a system that encloses the sample with a controllable compression on the sample would be needed. However, it should be determined what compression is needed to achieve this, as this parameter also influences TC.

Regarding the moisture content of a sample, it is advised to measure the textile sample in the same moisture conditions as it was worn by the deceased (e.g. directly at the crime scene), as moisture content highly influences the k-value of textile layers. This is particularly relevant at a crime scene, as blood and urine often wet the textile layers surrounding the deceased. When textile layers are only partly wetted, both a sample from the wetted and from the dry region should be measured to achieve two separate k-values. Consequently, both k-values can be inputted into the PHOEBE model to deduce the most accurate results.

Furthermore the effect of environment temperature on TC should be considered during measurement, although the conducted systematic review labelled the effect as negligible for forensic purposes. This is, as the environment temperature influences the rate and the ease of heating and cooling to reach certain temperatures. Therefore, the target temperatures for the hot and cold plate should be set to $\pm 0.5 \cdot \Delta T$.

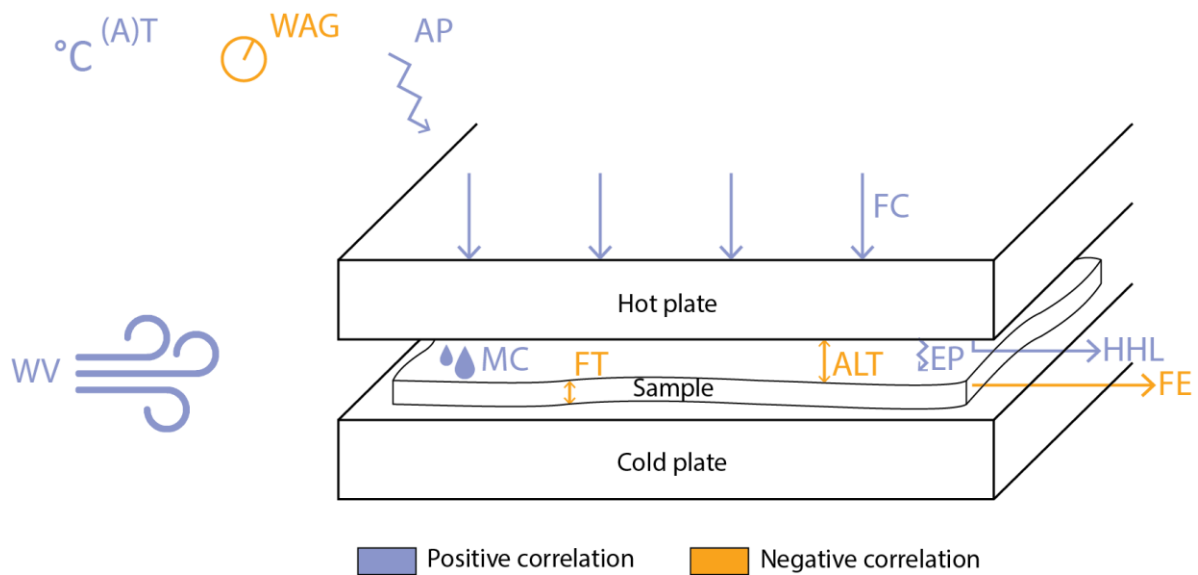


Figure 4. Visualization of factors influencing the TC measurement of clothing, specified for a GHP set-up, adopted from [7] Abbreviations: ALT, air layer thickness; AP, air pressure; (A)T, (ambient) temperature; EP, emissivity of the plates; FC, fabric compression; FE, fabric extension; FT, fabric thickness; HHL, horizontal heat leakage; MC, moisture content. WAG, weight ambient gas; WV, wind velocity [7].

3. CONCEPT DEVELOPMENT

3.1 Concept Design Method

A functional decomposition chart was composed, displaying sub-functions needed to achieve the main function of Thermanus-K2: measuring the k-value of a textile layer. The sub-functions were used for brainstorming about their sub-solutions, which were then merged into a Morphologic Chart.

The sub-solutions were holistically scored on their applicability in a TC measurement device:

- **Applicable – high performance:** the solution is safe to use during CSI processes, is practical in terms of size (Requirement 13) and simplicity (Requirement 15) and has a high performance (Requirement 3).
- **Applicable – low performance:** the solution is safe to use during CSI processes and is practical in terms of size and simplicity.
- **Unapplicable:** the solution might cause dangerous situations during CSI processes and/or is impractical in terms of size and simplicity.

The solutions determined as applicable were used to compile three concept designs. Subsequently, the three concept designs were evaluated through a Harris Profile to decide upon the concept to continue the final design.

The requirements for a TC measurement device (section 1.2.2) were grouped into 6 different criteria that were used in the Harris profile. These criteria were holistic descriptions, as the concepts could not be quantitatively evaluated. The criteria were ordered on importance (high to low = 1 to 6). In drafting the criteria of the Harris profile, **requirements 10, 11, 13 and 14** were omitted, because these only become relevant in a later design step of the device. At first, it is aimed to keep the concept as simple as possible and distinguish on a more fundamental level.

The criteria in the Harris Profile were:

1. Ability to ensure correct heat flow

The ability of the concept to ensure that all generated heat in the main heater only flows vertically through the textile sample(s) (k-values: 0.057 – 0.7 W/mK – **Requirement 1**) towards the cold plate(s) and does not flow in any other direction. This is needed to ensure a high accuracy and precision of the measurement (**Requirement 3 and 4**).

2. Applicability for measuring textile samples

The concept device should be able to measure and identify samples with a variety of thicknesses (0.17 – 150 mm) (**Requirement 2**). Furthermore, it is desired to keep the textile sample, representative for the bulk material, intact (**Requirement 5**).

3. Use for forensic investigators

The concept device should be simple in use for forensic investigators (**Requirement 15**) during PMI determination at a crime scene. The set and measurement time of the device should be short (**Requirement 6 and 7**).

4. Ease of decontamination

The concept device should allow frequent and thorough decontamination (**Requirement 9**).

5. Durability

The expected lifetime of the concept device without need for recalibration (**Requirement 8**) and its expected robustness (**Requirement 12**).

6. Feasibility

This is defined as the ease of development and manufacturing of a single prototype within the scope of this thesis.

The concepts were holistically scored on these criteria by the author. The scores were verified by some of the users (Dutch Police).

3.2 Concept Design Result

3.2.1 Sub-solutions and Morphologic Chart

Figure 5 shows the functional decomposition chart of Therminus-K2, with at the right-most column the lowest level functions to be used in the Morphologic Chart (**Table 2**).

The sub-functions of Therminus-K2 were:

- Correct **positioning** of a textile sample between the heating and cooling modules
 - The textile sample should be enclosed by the heating and cooling modules and make mechanical and thermal contact with these modules on a microscopic level.
- Feedback **controlled TC measurements**
 - The hot and cold plate should achieve specified temperatures by heating and cooling elements. These temperatures should be measured and controlled. Besides this, the sample material's thickness should be measured.
- Ensuring only a **one directional heat flow** from the main heater through the sample towards the cold plate
 - Parasitic heat flows should be eliminated in order to correctly determine k-values (section 2.1).

It was prioritized to find solutions on how to control the measurement and ensure a one directional heat flow through the sample. Solutions on how to position the sample should be investigated once a well-performing prototype has been established (Appendix A: Extension to the Morphologic Chart).

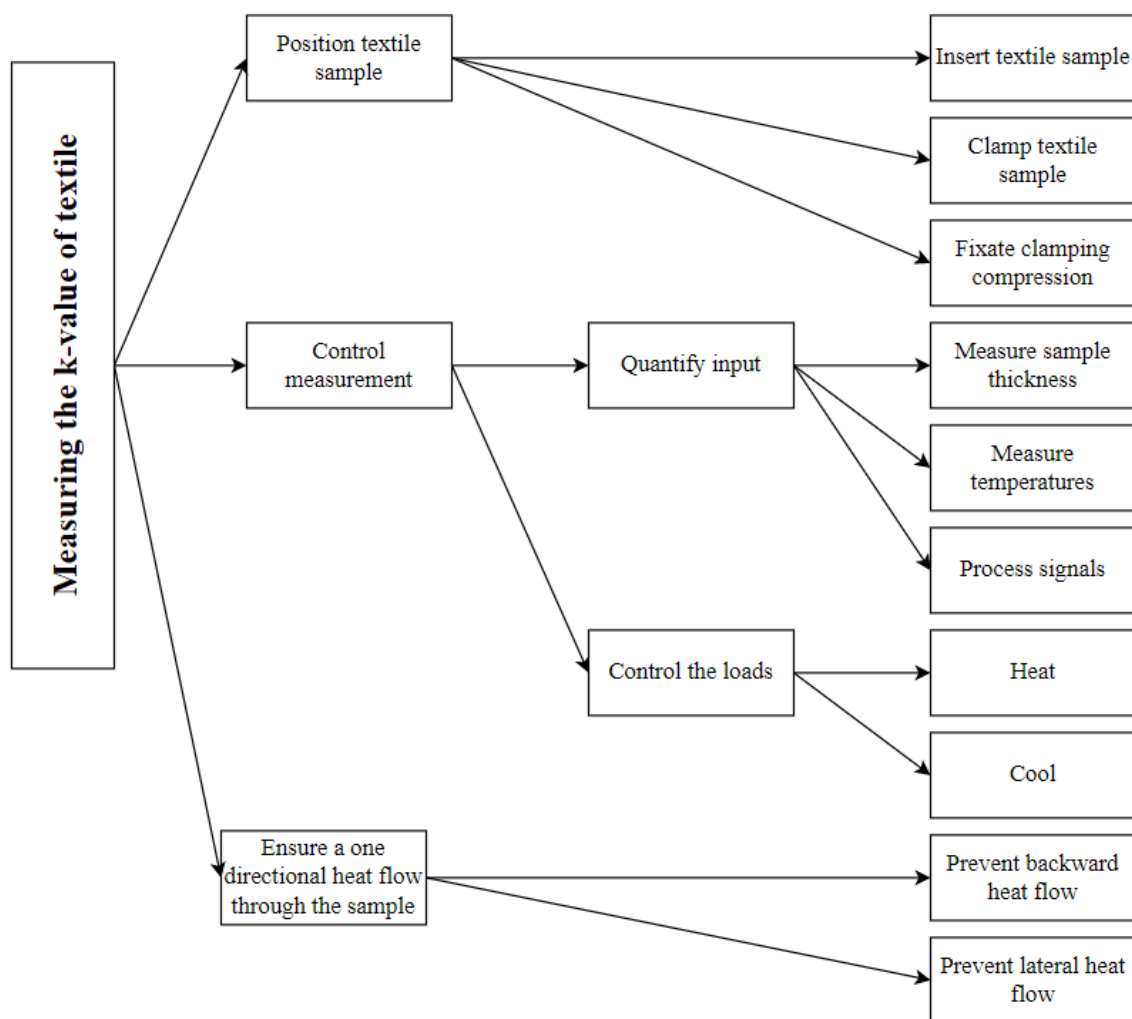











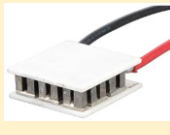







Figure 5. Functional decomposition chart of the Therminus-K2 design.

Morphologic Chart



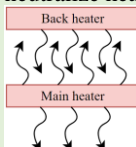



In the Morphologic Chart, the applicable solutions with a predicted high performance in their functionality are circumscribed (**Table 2**).

Table 2. Morphologic Chart of the lowest level sub-functions for measurement control and heat flow direction for a TC measurement device with their corresponding possible sub-solutions. Sub-solutions were scored on applicability: Applicable-High performance: green circumscribed, Applicable-Low performance: yellow, unapplicable: no color fill.

Sub-solutions → Sub-functions ↓		1	2	3	4
Control measurement	Measure sample thickness	Distance sensors between the hot and cold plates (Ultrasonic, Infrared, Laser or LED time-of-flight) 	Displacement sensor between the hot and cold plates (Magneto-strictive or Linear potentiometer) 	Thickness measurement over sample (ruler/caliper) 	
	Measure temperatures	Thermocouples 	Semiconductor based integrated circuits (ICs) 	Thermistor (NTC or PTC) 	Thermopile 
	Process signals	Microcontroller (Arduino) 	Microprocessor (Raspberry pi) 	Data Acquisition (DAQ) card + computer 	
	Heat	Joule effect* (Kapton film or PTC ceramic resistors) 	Peltier effect** 	Chemical Heat Source 	Dynamic Heat Source (liquid flow) 
	Cool	Peltier effect** 	Active heat sink (ice, liquid/ airflow) 	Passive heat sink 	

* Joule effect: the heating of a resistor due to a current.

** Peltier effect: electrical current is converted in a temperature difference at a junction between two different semiconductors.

Sub-solutions → Sub-functions ↓		1	2	3
Ensure one directional heat flow through the sample	Eliminate backward heat flow	Extended modelling for heat loss 	Insert strong insulators behind the main heater 	Use a back heater to neutralize heat flow 
	Eliminate lateral heat flow	Extended modelling for heat loss 	Insert strong insulators around the sample and the main heater 	Use guard heaters around the main heater 

All proposed sub-solutions to measure sample thickness were rated as applicable. A caliper would be the simplest measurement method, although it could induce inter- and intra-observer errors. Using automatic distance or displacement sensors is likely to result in more precise measurements.

For temperature measurement, semiconductor based integrated circuits and thermistors achieve higher accuracies than thermocouples and thermopiles [61]. In signal processing, a Data Acquisition Card combined with a computer is unapplicable for signal processing due to the size of the computer that is needed.

For heating, chemical and dynamic heat sources are unapplicable for safety reasons and dimensions needed. The Peltier effect can be used to heat, although the Joule effect has a higher performance in heating. For cooling however using the Peltier element would be suitable, eventually combined with a fan and heatsink to enhance cooling of the element itself.

Eliminating backward and lateral heat flow by extended modelling is impractical as it would be too complicated to model. Using insulators or heaters neutralizing heat flow could both be implemented with good performance.

3.2.2 Concept Selection

Three design concepts were composed based on the sub-solutions in the Morphologic Chart (Table 2) and are visualized in Figure 6. All concepts consist of at least a main heater plate and a cold plate sandwiching the sample, to create a temperature difference over the sample through which heat can flow (section 2.1).

The hot plate with the main heater will be realized by attaching a thin film resistor to a thermal conducting plate, that resultingly heats when a current flows through the resistor (Joule effect). The cold plate will be made up of a similar thermal conducting plate to which Peltier elements, combined with heat sinks and fans are connected. In all concepts, temperatures will be measured with thermistors, as these have much lower costs compared to semiconductor based ICs [61]. Even though distance sensors and displacement sensors would achieve more accurate thickness measurements, in this project thickness measurement is to be performed directly over the sample with a digital caliper. This is for simplicity reasons in the rapid design process and the fact that sample thickness is a constant value during measurement.

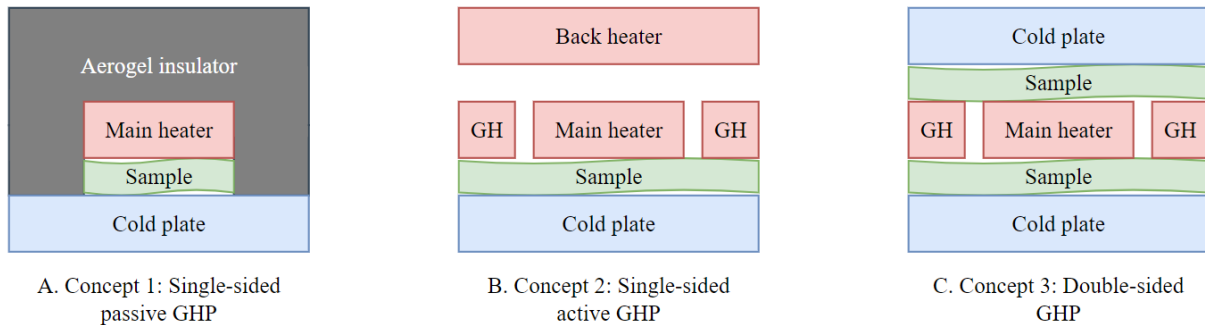


Figure 6. Cross-sections of three concept designs for a TC measurement device, split in configurations A) Concept 1: Single-sided passive GHP, B) Concept 2: Single-sided active GHP and C) Concept 3: Double-sided GHP. GH indicates a guard heater surrounding the main heater.

Concept 1: Single-sided passive GHP

Concept 1, the single-sided passive GHP, is the simplest GHP configuration. The concept consists of a hot plate being surrounded by highly insulating material, such as aerogel ($k \approx 0.01 - 0.02 \text{ W/mK}$) [62]. This insulation layer should avoid backward and lateral heat flow departing from the main heater.

Concept 1 scores good for most of the criteria in the Harris Profile (Table 3). However, the use of an insulator to eliminate parasitic heat flows might result in inaccurate measurements. This is, as textile generally has a k -value (e.g. polyester: 0.05 W/mK) in the same order size as the insulating material. Therefore heat produced by the main heater might also flow through the aerogel insulation. Besides this, the configuration of the insulator makes measuring intact clothing samples with varying thicknesses impossible.

However, Concept 1 has a simple working principle, which is favorable for use by forensic investigators. This predicts a high durability and feasibility to be developed within this thesis.

Concept 2: Single-sided active GHP

Concept 2 uses active heating elements (guard heaters) surrounding the main heater to eliminate lateral heat flow from the main heater. Heating the guard heaters to the same temperature as the main heater ensures a temperature difference of zero between the main and guard heaters, resulting in zero heat flow between those. This way, lateral heat leakage from the conduction measurement region (CMR: main heater – sample – cold plate) through the sample to the environment is prevented. Similarly, a back heater is added to prevent a temperature difference and heat flow between the main heater and the back heater.

Concept 2 seems to be able to ensure the correct heat flow by using the extra heaters. Furthermore, the wish for measuring intact samples can still be fulfilled, as the sample doesn't need to be shielded on the sides. When correctly programmed, the concept is likely to be easy to use by forensic investigators and to deliver fast measurements. However, the concept needs multiple measures for temperature control which might increase the complexity during prototyping.

Concept 3: Double-sided GHP

Concept 3 is a solution based on the double-sided GHP method, consisting of a main heater guarded in lateral direction by guard heaters similar to Concept 2. Concept 3 is however different as two samples are simultaneously needed to perform measurements on. Around the heater configuration, two identical flat samples should be inserted, that are sandwiched between the heaters and cold plates.

Concept 3 could ensure a correct direction of heat flow through the samples by using guard heaters. However, the concept has some disadvantages due to its two-sided configuration. Two identical textile samples would be needed for a single measurement, which in addition to that it is difficult to obtain, is also highly undesirable in forensics, since as little sample material as possible should be used (**Requirement 5**). Furthermore, the development process might encounter difficulties due to the two-sided configuration. The measurement circumstances at both sides should be identical. Making sure the measuring distance between the hot and cold plates is identical at both sides might be difficult to achieve.

Besides this, the concept exists of two cold plates, consisting of two Peltier elements with fin-formed heat sinks, which are hard to clean. Last, the two-sided configuration might need a longer setup time, and could increase the complexity for use by forensic investigators.

Table 3. Harris Profile of the criteria rated for each concept as visualized in Figure 6. The rating scale (- - to + +) indicates how a concept scores on a criteria, with (- -) as a very poor score and + + as a very good score.

	1. Single-sided passive GHP					2. Single-sided active GHP					3. Double-sided GHP			
	- -	-	+	++		- -	-	+	++		- -	-	+	++
1. Ability to ensure correct heat flow														
2. Applicability for measuring textile														
3. Use for forensic investigators														
4. Ease of decontamination														
5. Durability														
6. Feasibility														

Concept 2 scores best in the Harris profile assessment (**Table 3**), as the concept has the most positive (+ or ++) score. The concept seems to be able to ensure a correct heat flow direction and is suitable for forensic purposes. Therefore, this concept is chosen to continue the final design.

4. SIMULATIONS FOR DESIGN DECISIONS

In order to further design the previously selected Final Concept 2, the Single Sided Active GHP, into a prototype, some design decisions had to be made first. The concept eliminates parasitic heat flows by using guard heaters and a back heater. In order to design that configuration properly, one must know what the dimension ratio of guard heaters to the main heater should be (section 4.1). Furthermore, the minimum thickness of the hot plate needed to establish a uniform temperature distribution by using Thermal foil BN 1384113 60x60 mm (Conrad Electronic SE, Germany) should be determined (section 4.2). To decide on these design choices, heat transfer simulations were performed in SolidWorks (Dassault Systèmes).

4.1 Ratio of Main Heater to Guard Heater Dimensions

Introduction

To ensure correct TC measurement, a one dimensional heat flow should be realized through the sample (see section 2.1). However, a two dimensional heat flow through the sample is most likely to be present in the x-y plane, due to the created temperature differences between the sample and the environment (**Figure 7**).

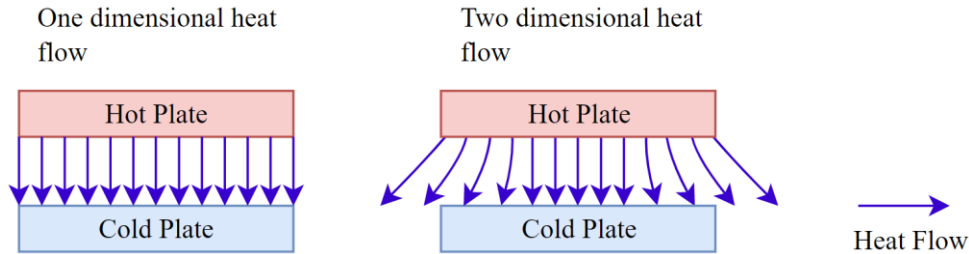


Figure 7. Cross-section (x-y plane) of a hot and a cold plate with arrows indicating the direction of heat flow across the plates due to a temperature difference between these plates.

Using guard heaters would ensure one dimensional heat flow in the middle of the sample while still having a two dimensional heat flow at its edges. Then, an almost one-dimensional heat flow is provided within the area between main heater and cold plate. Therefore, the goal of the first simulations was to determine the required dimensions of the guard heaters relative to the main heater in which a one-dimensional heat flow in the area between main heater and cold plate is established.

Method

In SolidWorks 2021 (Dassault Systèmes, France) a steady state thermal simulation of heat conduction through a squared sample with fixed size (50x50 mm) and varying thicknesses (5, 25 and 50 mm) was performed, to visualize the effect of thickness on temperature distribution over a broad range. Thermal loads were inserted representing temperatures of 30 °C (hot plate: T_{hot}), 20 °C (cold plate: T_{cold}) and 25 °C (environment; $(T_{hot} + T_{cold})/2$), which represent a standard GHP measurement. The sample was meshed and a thermal simulation was performed that resulted in the heat distribution that would be achieved in steady state. Cotton ($k = 0.04$ W/mK) was used as sample material to perform the simulations with, as it is a very common clothing material [63, 64]. Afterwards, the simulations were repeated using air ($k = 0.025$ W/mK) and Aluminum 7075 ($k = 130$ W/mK) as a sample material [65-67].

Results

The simulations resulted in multiple figures showing the heat distribution across a cotton sample. It appeared that for thin samples (50x50x5 mm), the area over which one dimensional heat flow is established was large (**Figure 8**). When simulating heat distribution in thick samples (50x50x50 mm), no area with an established one dimensional heat flow could be differentiated (**Figure 8**).

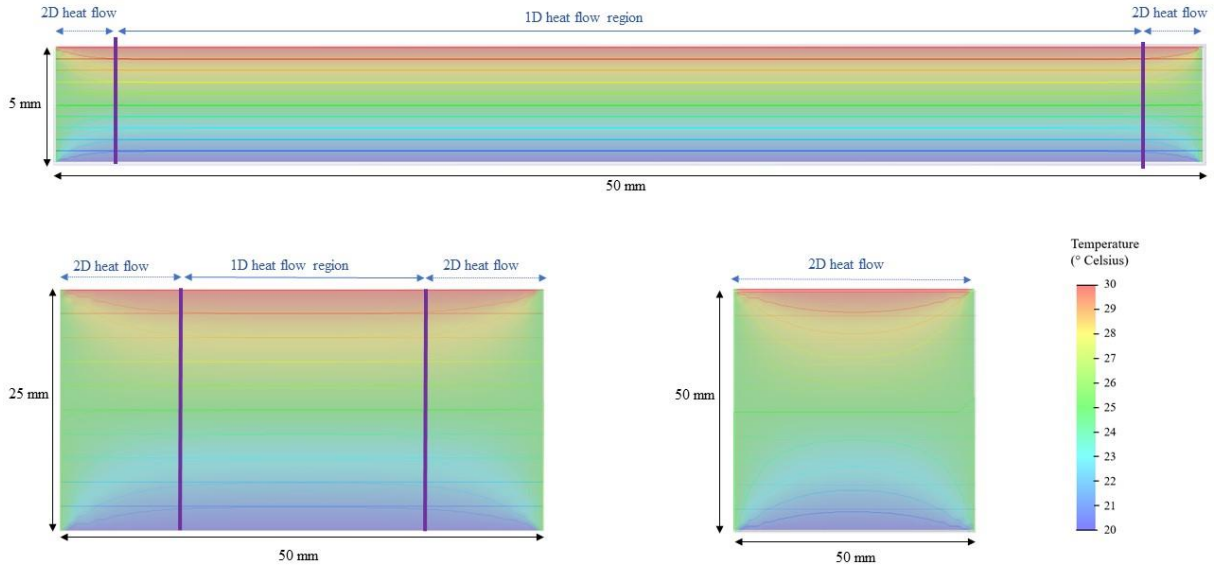


Figure 8. Cross sections of heat distributions in cotton samples ($k = 0.04 \text{ W/mK}$) exposed to $\Delta T = 10^\circ\text{C}$. The region between the vertical lines indicates the region in which one-dimensional heat flow through the sample is established. The regions outside these lines indicate the two-dimensional heat flow regions. In the 50×50 sample no region of one-dimensional heat flow could be enclosed; all heat flow was two dimensional.

The heat distribution in air and aluminum samples ($25 \times 50 \times 50 \text{ mm}$) showed a very similar pattern (**Figure 9**). However, aluminum showed a smooth heat distribution whereas heat distribution in air and cotton samples gets more wrinkled.

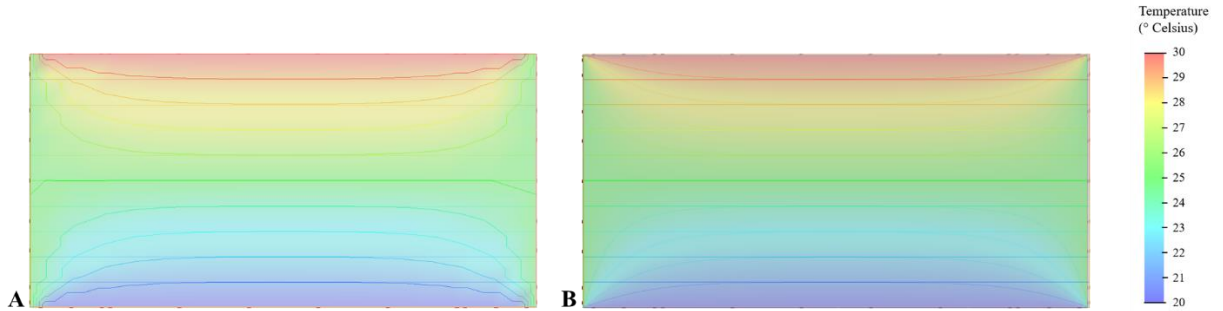


Figure 9. Cross sections of heat distributions in A) Al 7075 ($k = 130 \text{ W/mK}$) and B) air ($k = 0.4 \text{ W/mK}$) samples ($25 \times 50 \times 50 \text{ mm}$) exposed to $\Delta T = 10^\circ\text{C}$.

Conclusion

When having a maximum sample thickness of 0.5 times the sample width, the area of one dimensional heat flow is more than 0.5 times the sample width (**Figure 10**). Therefore, in order to achieve an area in which a one dimensional heat flow through the sample is realized, the sample height (thickness) should be

$$\text{Sample height (thickness)} \leq 2 * \text{sample length (when sample length = sample width)}.$$

The guard heaters should be placed all around the main heater (horizontal axis) with a width of 0.5 times the length of the main heater, in the $a - 2a - a$ configuration (**Figure 8** and **Figure 10**). In this configuration, the $2a$ area is equipped with the main heater and the power delivered to this heater will be used in TC measurement.

Furthermore, no differences in one dimensional heat flow region size were present when using materials with different thermal conductivities ($0.4 - 130 \text{ W/mK}$). This is as in steady state, the q/k

ratio remains the same for different materials. This allows applicability of the proposed $a - 2a - a$ configuration for a wide range of materials.

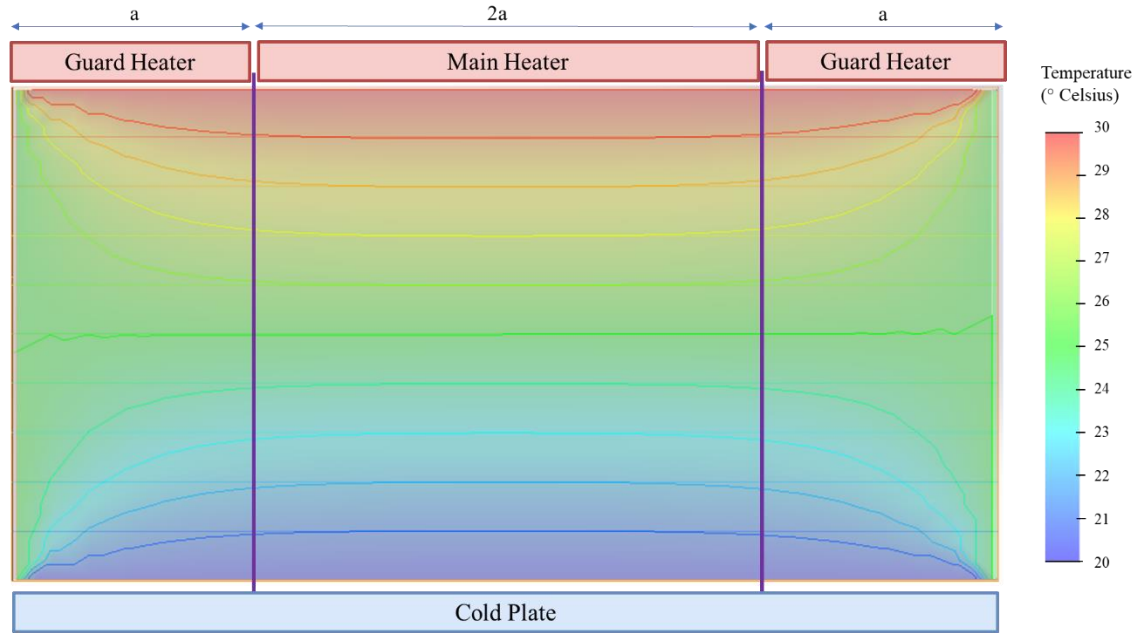


Figure 10. Cross section of heat distribution in a cotton sample exposed to a 10°C temperature difference. The main heater and guard heater configuration ($a - 2a - a$) is visualized, which is needed in a TC measurement device to ensure one dimensional heat flow through the sample in the conduction measurement region (CMR: $2a$).

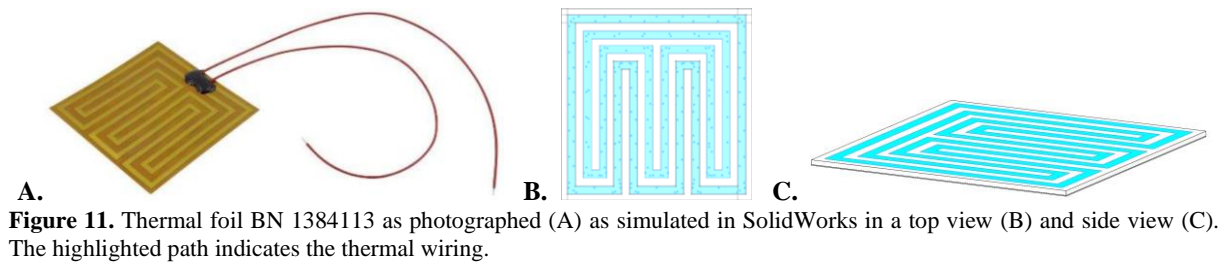
4.2 Minimum Aluminum Plate Thickness required for Temperature Uniformity

Introduction

In the Therminus-K2 prototype, thermal foil BN 1384113 60x60 mm (Conrad Electronic SE, Germany) is used as the main heater, consisting of several wires in which heat is generated and a polyimide foil that keeps everything together (**Figure 11A**). The wires result in a difference in heat concentration along the foil. Therefore, the thermal foil will be attached to a Al7075 plate, acting as a diffuser to achieve a uniform temperature distribution at the other side of the plate. It is desirable to use a plate thickness that is as small as possible, so that the system can be controlled quickly and a steady state is achieved fast. This would shorten the needed measurement time (**Requirement 7**). The research question resultingly is: What is the minimal thickness the Al7075 plate should have to get a uniform temperature distribution at the surface of the lower side of the plate (assuming the heating foils are placed on top)?

Method

In SolidWorks 2021 (Dassault Systèmes, France) a steady state thermal simulation of heat conduction was performed through a Thermal foil – Aluminum Plate – Sample Assembly. The heating pattern as in Thermal foil BN 1384133 was drawn in SolidWorks to use during heat simulations (**Figure 11B**). Temperatures were set to 30 °C (thermal foil wires), 20 °C (lower side sample) and 25 °C (the environment temperature set as average of the hot and cold plate temperatures). Cotton ($k = 0.04$ W/mK) was used as sample material to perform the simulations with. Thicknesses of the aluminum plate (1, 2 and 5 mm) and thicknesses of the sample (0.17 and 25 mm) varied, as these thicknesses are the minimum and maximum thicknesses Therminus-K2 should be able to measure (**Requirement 2**). The results showed the established steady state temperature distributions through the aluminum plate and the sample. It was assessed whether the uniform temperature distribution was reached within the thickness of the aluminum plate.



Results

When measuring thin (0.17 mm) cotton samples (0.04 W/mK), always a steady state uniform temperature distribution within the hot plate's thickness is established (hot plate thicknesses: 1, 2 and 5 mm). When measuring thick (25 mm) cotton samples, a uniform temperature distribution in the hot plate is only established in plates with thicknesses above 2 mm (**Figure 12**).

Cross-sections of the established steady state temperature distributions of all tested configurations were displayed in Appendix B.

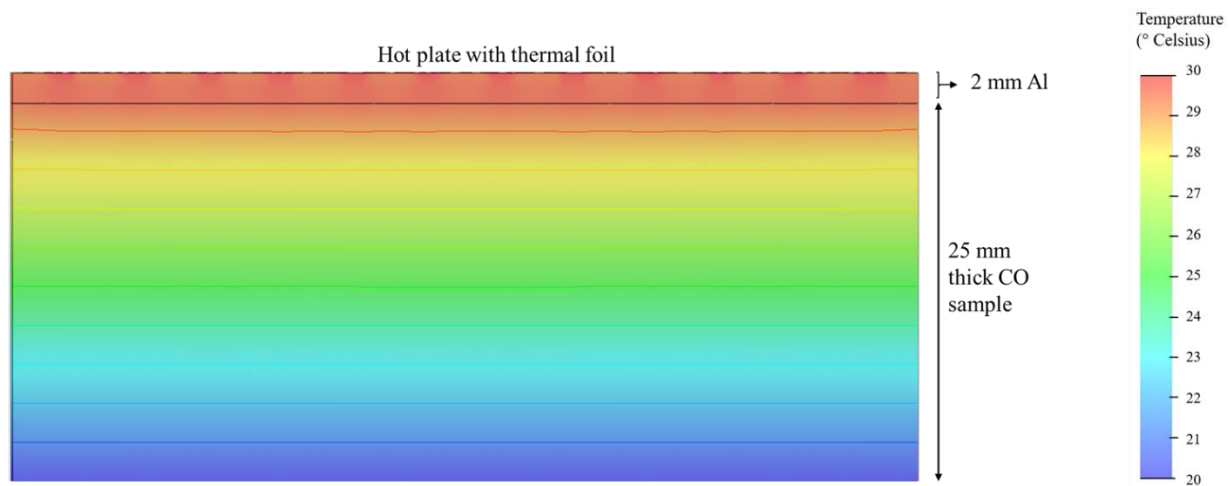


Figure 12. Cross-section of the temperature distribution in a thermal foil – Al7075 plate – cotton sample configuration.

Conclusion

Al7075 is a very conductive material and easily generates a uniform temperature distribution during steady state measurements. When simulating heat flow in a hot plate with a 2 mm thickness, a uniform temperature distribution is achieved.

This is, as a thick (25 mm) sample increases the length over which a 10 °C temperature difference should be established, compared to a thin (0.17 mm) sample. At the lower side of the sample (at the cold plate), a uniform temperature distribution (20°C) is imposed. At the upper side of the aluminum hot plate, the thermal foil causes a non-uniform temperature distribution with high heat fluxes near the thermal foil wires and low heat fluxes between the wires. The line at which a uniform temperature distribution is achieved pulls down towards the bottom of the sample (20°C) with increasing sample thicknesses (0.17 – 25 mm).

As a thinner plate increases the speed of the temperature control (see Section 5.2.2), the thickness of the hot plate was chosen to be 2 mm.

5. THERMINUS-K2 PROTOTYPE

5.1 Construction Methods

In Chapter 4 some design decisions were made, supported by simulations. In this chapter, the Single Sided Active GHP Concept was further developed into a prototype through multiple iterations.

SolidWorks (Dassault Systèmes) was used to make a 3D design of the mechanical embodiments. Fritzing (Version 0.9.9) was used to design the electronic circuit. Software for data acquisition with Arduino was written using the open-source Arduino Software (IDE) version 1.8.13. Received data was post-processed in MATLAB R2021a (MathWorks).

5.2 The Thermanus-K2 Prototype

5.2.1 Overview

A SolidWorks drawing of the final design of Thermanus-K2 is shown in **Figure 13**. Photographs of Thermanus-K2 together with all electronics is visualized in Appendix F. **Figure 14** visualizes a schematic vertical cross-section of the resulted working principle in the Thermanus-K2 prototype. **Figure 15** visualizes the same vertical cross-section in the Thermanus-K2 SolidWorks drawing. In **Table 4** SolidWorks drawings of the top and bottom view of individual layers are shown. A similar table is visualized in Appendix G, showing actual photographs of the top and bottom views of the layers of Thermanus-K2. An extensive list of the components used in the prototype is provided in Appendix J. Appendix K provides technical drawings of the custom-made components with their exact dimensions and Appendix L contains datasheets of the main electronic components used.

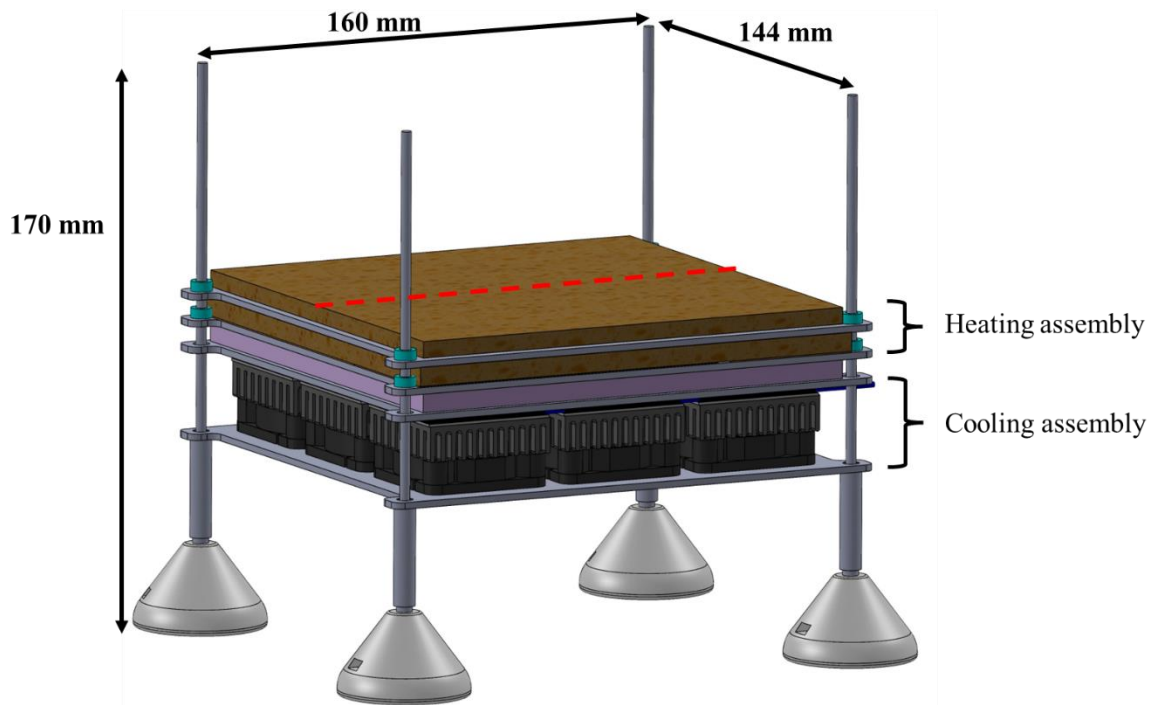


Figure 13. Visualization of the final Thermanus-K2 prototype with a sample inserted between the heating and cooling assembly, in which the dotted line indicates the cross-section used in Figure 15.

In general, Thermanus-K2 is made up of the following assemblies:

- Heating assembly: main heater, guard heaters, back heater, rubber and aerogel layer
- Cooling assembly: Peltier elements, heatsinks and fans
- Frame
- Electronics

The hot plate (**H, Figure 15**) produces a uniform distributed temperature with a temperature difference ΔT ($^{\circ}\text{C}$) towards the cold plate (**I, Figure 15**), similarly having a equithermal surface. The area over which the k-value of the textile sample is determined is the conduction measurement region (CMR), which is the region from the main heater, through the sample towards the underlying cold plate (**Figure 15**).

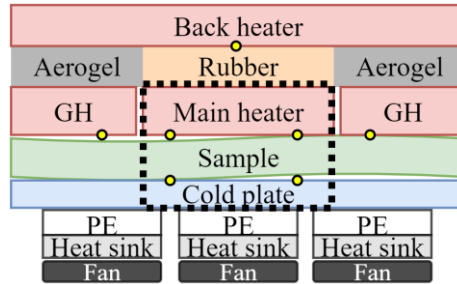


Figure 14. Schematic vertical cross-section (see dotted line **Figure 13**) of Thermanus-K2. The dotted line indicates the conduction measurement region (CMR) and the yellow circles indicate temperature sensors. GH = guard heater, PE = Peltier Element.

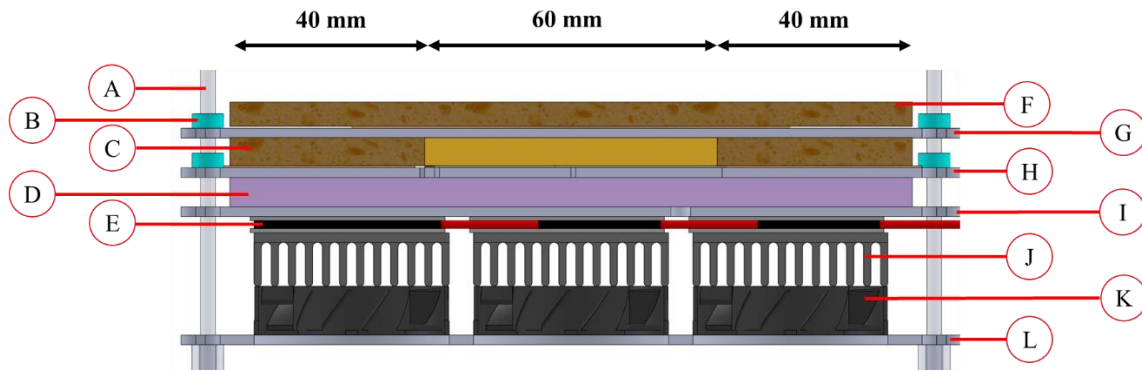


Figure 15. Cross-section (see dotted line **Figure 13**) of the SolidWorks drawing of Thermanus-K2, in which the assigned labels mean:

- | | | |
|----------------------------|---------------------------|--------------------|
| A. Pillar | E. Peltier elements layer | I. Cold plate |
| B. Insulating cap | F. Aerogel layer | J. Heat sink layer |
| C. Aerogel - rubber layer | G. Back heater plater | K. Fan layer |
| D. Inserted textile sample | H. Hot plate | L. Fan plate |

Heating assembly

The main heating element (Thermal foil BN 1384113 0.3x60x60 mm – 12V/DC 48 W - Conrad Electronic SE, Germany) is surrounded by four guard heating elements (Adhesive Thermal foil 0.4x40x100 mm – 12V/DC 10 W – Conrad Electronics SE, Germany) to eliminate lateral heat flow and ensure one dimensional heat flow through the sample (section 4.1). These heating elements are attached with adhesive tape to the upper surface of a 2x144x144 mm Al7075 plate (section 4.2). A 1 mm laser cut air gap is realized between the main and guard section (**Table 4** Top View Hot Plate). The air gap minimizes horizontal heat flow over the plate between the main and guard heater section and ensures that the heat from the main heater flows in vertical direction.

Along the hot plate (**H, Figure 15**), 6 Negative Temperature Coefficient (NTC) thermistors (-40 - +100 $^{\circ}\text{C}$ – 10 k Ω - TTF3A103F34D3AY – TRU Components) are placed in milled groves filled with thermal grease (GD900, Hackerstore). Thermal grease is added ($k \sim 1.22 \text{ W/mK}$) to replace air surrounding the thermistor, which would otherwise act as an extra thermal insulator. which is added to avoid extra thermal insulation by air present around the thermistor. The thermistors, within the thermal grease, are then covered with aluminum tape (see **Table 4** Bottom View Hot Plate). These NTC thermistors measure the generated temperatures of all individual heaters. The temperature of the main heater, heating the CMR, is determined by two temperature sensors, as recommended by ISO ASTM C177 [58]. The guard heaters are equipped with one temperature sensor each.

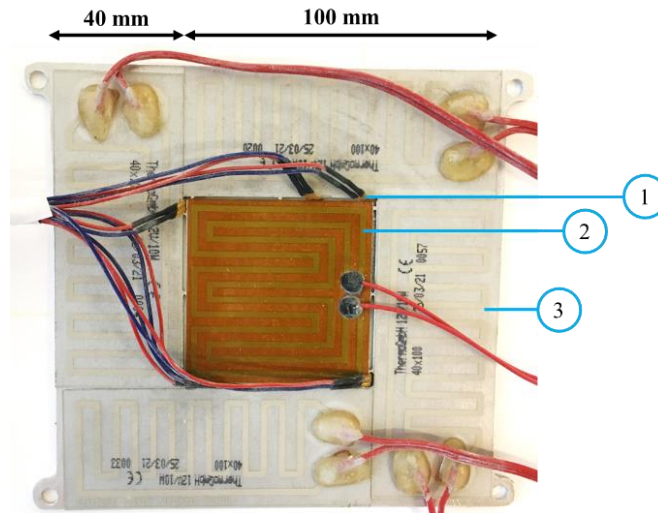


Figure 16. A top view photograph of the configuration of the hot plate. The assigned labels mean: 1) Temperature sensor, 2) Main heater and 3) Guard heater.

The dimensions of the hot plate (**Figure 16**) guarantee the right circumstances for measurement of flat textile samples (120x120 to 140x140 mm) with maximum thicknesses of 60 mm (see Section 4.1).

The back heating element (Adhesive Thermal foil Ø 90 mm, thickness 0.4 mm – 12V/DC 15W – Conrad Electronic SE, Germany) is taped to the centre of the top of the back heater plate (Al7075 2x144x144 mm) (**Table 4**, Top View Back Heater Plate). Between the back and the main heater, a layer of rubber (~0.5 W/mK – 5x60x60 mm) is placed (**Table 4**, Top View Aerogel – Rubber layer) [68]. The area between the back heater and the guard heaters is filled with aerogel (0.02 W/mK – 5x140x140 mm) [68]. On the upper side of the back heater plate a layer of aerogel (5x140x140 mm) is placed to ensure that the heat produced by the back heater does not unnecessarily heat the environment and mainly heats the rubber situated between the back and the main heater.

	LAYER	TOP VIEW	BOTTOM VIEW
Heating Assembly	Back Heater Plate		
	Aerogel – Rubber layer		

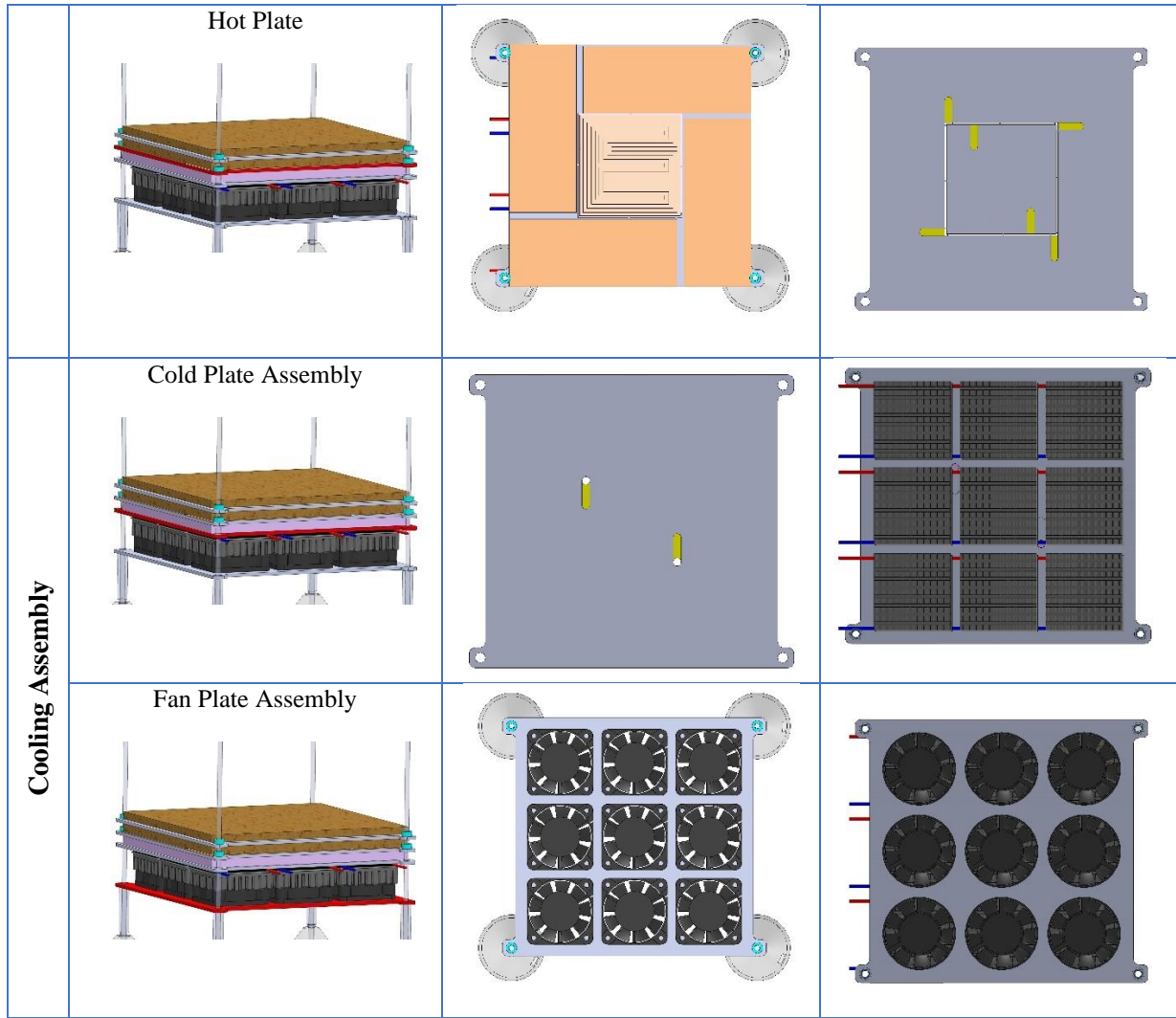


Table 4. Schematic representation of the top and bottom view in SolidWorks of individual layers within Terminus-K2. Details about the dimensions are given in Appendix K with SolidWorks drawings of the custom-made components. The locations for temperature sensors are highlighted in the back heater bottom view, hot plate bottom view and cold plate top view.

Cooling assembly

Peltier elements (3.9x40x40 mm – 12V/DC 50 W – Hackerstore), combined with heat sinks (12x40x40 mm – Hackerstore) and fans (10x40x40 mm – 12V/DC 0.08 A – Hackerstore) were used in order to cool the cold plate (2x144x144 mm) (**I, Figure 15**). The Peltier - heat sink - fan construction is repeated 9 times (3x3) (**Figure 17**). The Peltier elements (**E, Figure 17**) were glued (1.8 W/mK - Electrolube TCOR75S Thermal Adhesive – RS Components) to the cold plate (**I, Figure 15**) using a 3D printed mold (Appendix K, part I) to ensure correct positioning of the parts. The heat sinks (**J, Figure 17**) were attached to the Peltier elements using self-adhesive tape. The 9 fans (**K, Figure 17**) were attached to the Al7077 laser-cut fan plate (**L, Figure 15**) which consisted of 9 open circles to enable heat flow through the fans. The fans direct the air through the heat sinks towards the bottom of the entire assembly.

The cold plate suffices with only two temperature sensors along the middle of the plate in the CMR (**Table 4**), as the Peltier elements function equally and no individual management of the Peltier elements is needed (Appendix D). The Peltier elements generate an equal (max ± 0.1 °C deviation) heat distribution across the aluminum plate as determined with a thermal infrared camera (see Appendix D).

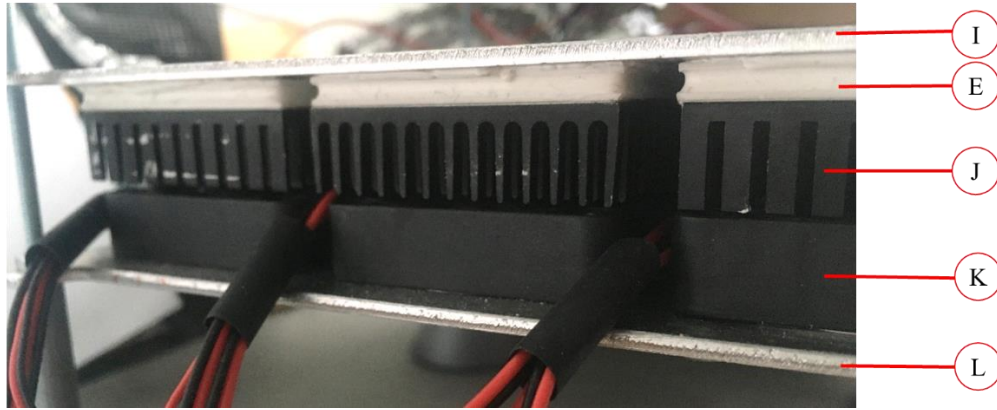


Figure 17. A side view photograph of the full cold plate assembly.

Frame

The heating and cooling assemblies were positioned on top of each other, in such a way that only vertical movement over steel screw thread pillars (**A**, **Figure 15**) was allowed. 3D-printed thermally insulating caps (**B**, **Figure 15**) were placed between the plates and the vertical pillars to avoid conductive heat transfer from the hot to the cold plate through these pillars. 3D-printed supports and lower stands were placed to offset the construction from the base, in order to avoid obstruction of the air flow from the fans (**Figure 13**).

5.2.2 Temperature Control

9 NTC thermistors were placed at the positions as indicated in **Table 4**. The thermistors were calibrated prior to securing them in Therminus-K2 (see Appendix C).

The control system diagram in **Figure 18** illustrates the temperature control implemented in the prototype.

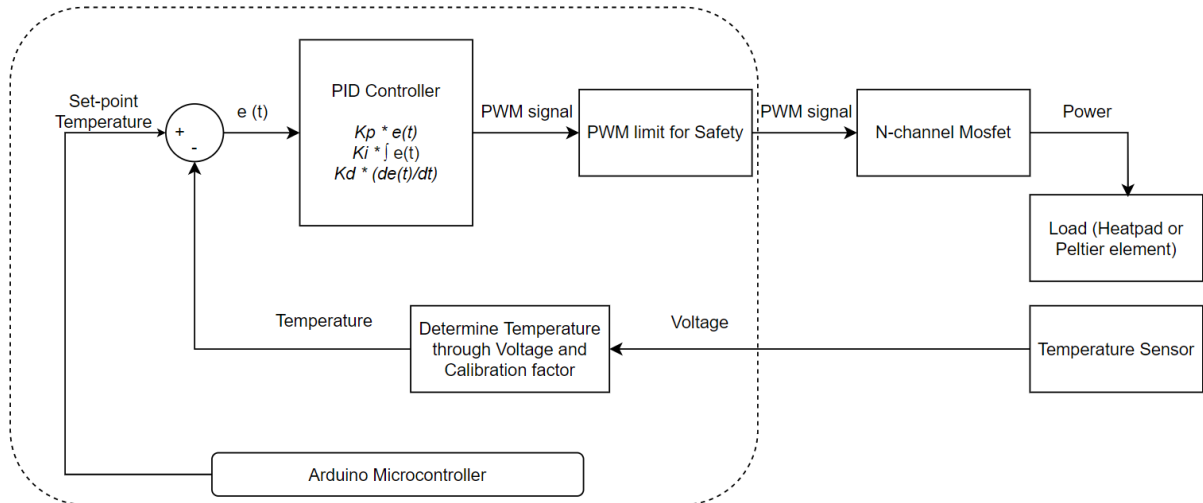


Figure 18. Scheme of the Temperature Control of the surface plates, by regulating heating and Peltier elements based on temperature readouts and resulting PID controlled PWM signals.

A Proportional Integral Derivate (PID) control system that outputs a Pulse Width Modulated (PWM) signal was used to control the temperatures of both the hot and the cold plate. This is, as a PID controller can enable a system to quickly reach the desired temperatures and come to a steady state. During iterative trial and error, the PID constants for the heaters, guard heaters, back heater and Peltier elements were determined (see Appendix M for Full Arduino Code with PID constants). All heaters

were individually controlled, whereas every Peltier element just received the same PWM output, as the cold plate is controlled by two temperature sensors only. During the iterative process of defining the PID constants, it was important to avoid an initial overshoot as this could cause the guard heaters to heat the area of the main heater. This is undesirable, as the power to the main heater would then be disturbed and errors in TC calculation would occur.

5.2.3 Electronics and Software

5.2.3.1 Circuitry

The electronic circuit used in Thermanus-K2 is visualized in Appendix E. A simplified overview of the electronics configuration is shown in **Figure 19**. In this figure, the electronics configuration is simplified into three circuits: the fans circuitry, the heating circuitry, and the temperature sensors' circuitry. As the cooling circuitry is similar to the heating circuitry, for simplicity reasons only the heating circuitry is visualized.

During measurement, temperatures at the thermistors are continuously measured by the Arduino. Once the external power supply is turned on, the fans start running. The heaters and Peltier elements are controlled by the PWM signals from the Arduino. In the current configuration, the Arduino is connected to a PC to visualize temperature sensor data and PWM output data during measurement.

The main modules of the full electronic circuit are:

- 3 Power sources (max 30V 5 A DC)
- Micro-controller (Arduino Mega 2560)
- LCD 2004A display
- 9 Temperature sensor circuitries: sensor and resistance
- 15 circuitries for heating or cooling: load (heater or Peltier), MOSFET and resistance
- 9 fans
- PC

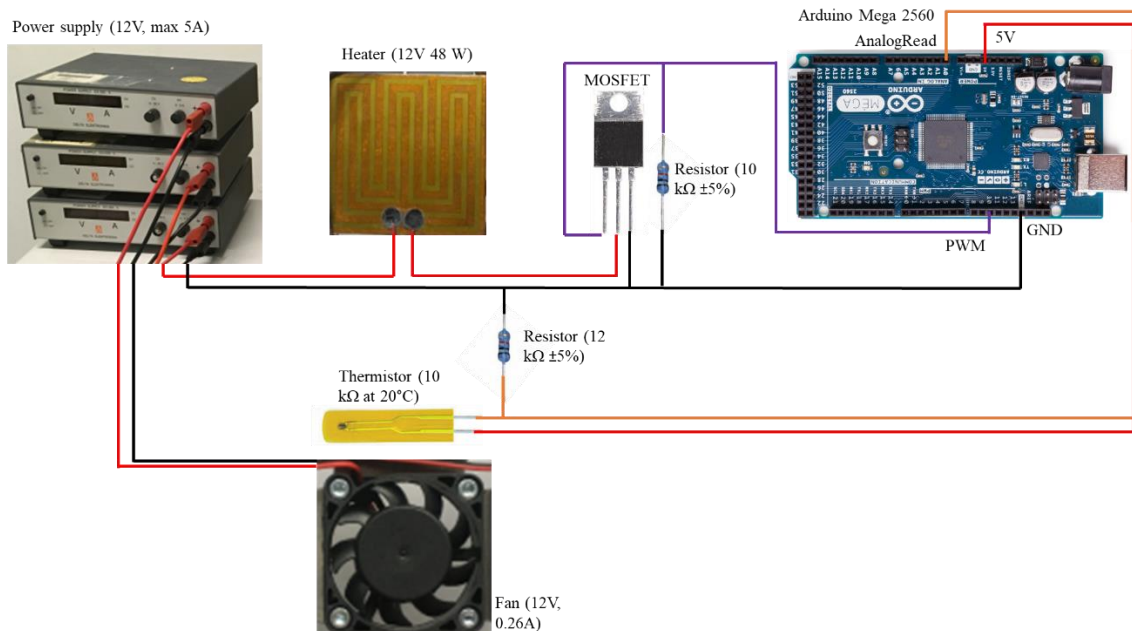


Figure 19. Simplified scheme of the electronics configuration in Thermanus-K2.

Pulse Width Modulation (PWM) is used to control the power delivered to the 15 heating and cooling circuitries. It controls the pulse width of a fixed frequency square wave (490 Hz) towards the gate of a N-channel MOSFET (IRLZ44NPbF – International Rectifier) and resultingly controls the average

power towards the load, see **Figure 20** [69]. A PID controller is used to control the duty cycle of the PWM signal, in which the duty cycle is defined as:

$$\text{duty cycle} = \frac{\text{Pulse Width}}{\text{Period (T) of the pulse}} * 100 \% \quad (2)$$

The PWM signals for the individual heating and cooling circuitries are limited in the Arduino coding by maximum duty cycle, specific per circuitry (see Appendix M for Full Arduino Code with circuitry specific duty cycle limitations). This is done in order to prevent excessive currents (> 5A) from damaging the system.

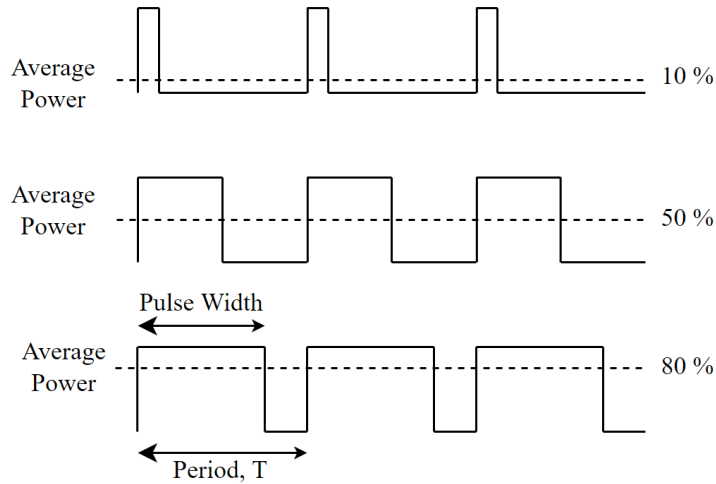


Figure 20. A typical PWM waveform

5.2.3.2 Software design

Figure 21 schematically visualizes the custom-made Arduino code used to control the TC measurement. During the entire measurement, the output parameters (time, temperatures and PWM signals) were visualized (each 500 ms) on the PC screen after each measurement. These parameters should be written to an Excel file. This Excel file is then imported in MATLAB for further post-processing to calculate the thermal conductivity coefficient (k-value) of the measured sample (**Figure 22**).

Arduino code (Figure 21)

The Arduino first initializes all variables (e.g. temperatures and PWM) and ascribes the input and output pins as used in the electronics configuration (Appendix E). In the Thermanus-K2 prototype, the ambient temperature is not continuously measured, but it is measured manually before each measurement to be inserted in the Arduino code. This was done to simplify the design process since it doesn't affect the measurements. The temperature isn't likely to change more than a maximum of 1 °C during measurement and the effect of temperature on TC measurement at ambient temperatures is negligible (see section 2.2) [7].

The void setup runs once after each power-up or reset of the Arduino Board. Subsequently the main code to regulate temperature control and measurement readouts is executed.

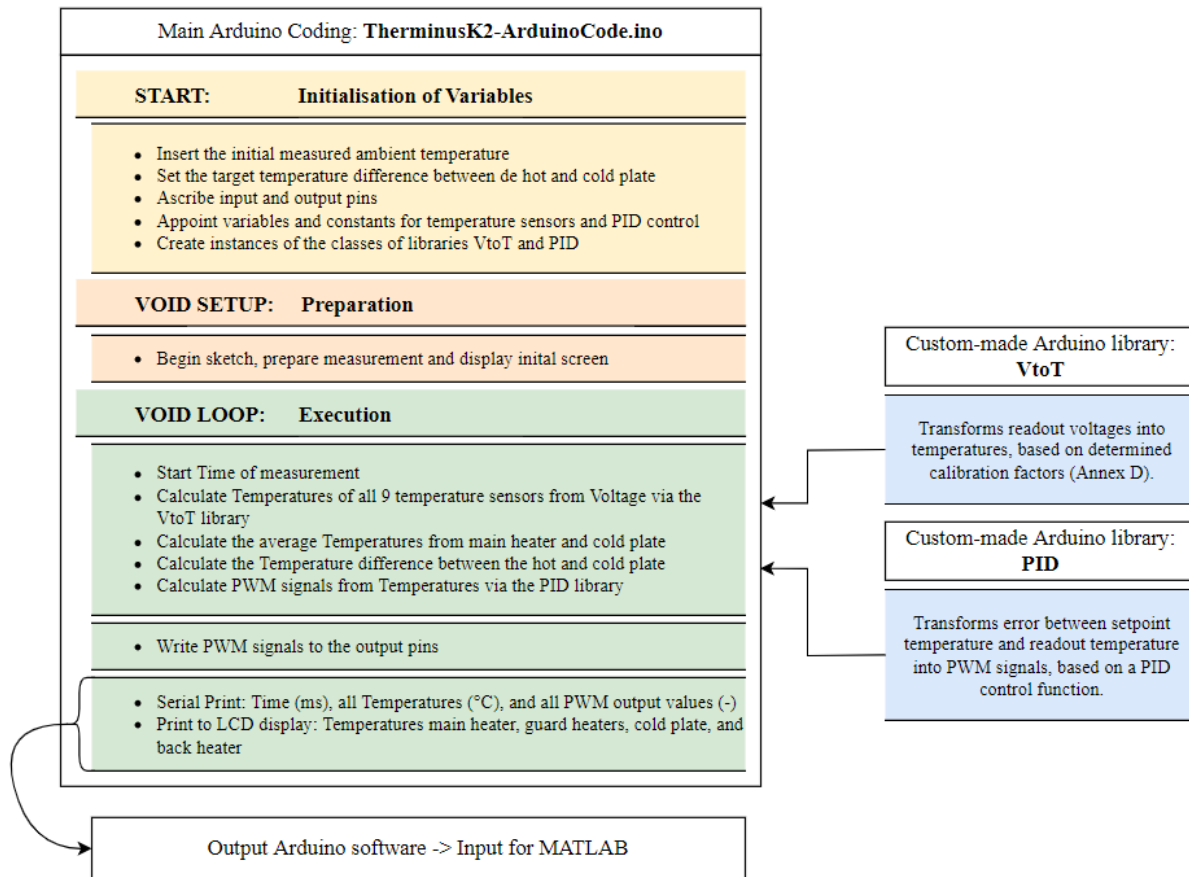


Figure 21. Arduino Pseudo Code to regulate the temperature control and the measurement readouts.

Data filtering

During post-processing, data filtering was needed. In the unfiltered data, sharp transients in temperature and PWM output data were present. Physically it is impossible to measure such rapid temperature changes in this setup. This suggests that the outliers come from an unresolved source of error, which could be due to electromagnetic interference (EMI), sensor readout errors or other sources of interference.

Since a moving average or Butterworth filter could not fully remove the outliers on their own, a custom made outlier removal method was applied to the data. The filter was applied on the data obtained after the initialization phase of each measurement (< 1 minute).

To use the outlier removal method, the measurement resolution for temperature data and PWM output data for the power to the main heater were determined. When the difference in output value between two consecutive data points was more than six times the resolution, the second data point was classified as an outlier. The outlier and three successive data points were filled with the average of the four previous data points. Subsequently, a moving average with a [10,10] window was applied in order to smooth the outlier free data. This custom-made data filtering would be short enough to track changes in the data and long enough to filter out the outliers.

Determine Steady State and calculate the Thermal Conductivity Coefficient

The thermal equilibrium must be reached before the k -value of the sample can be determined (section 2.1). The steady state of the thermal equilibrium is defined using the following criteria:

- 1) The heat flow rate Q remains constant over time (derivative $Q < 0.001$), and
- 2) The temperature distribution dT remains constant over time (derivative $dT < 0.001$).

In measurements with Therminus-K2, an extra condition should be added to ensure a one dimensional heat flow:

- 3) The individual guard heaters and the back heater should have the same temperature as the main heater (difference $< 0.5\text{ }^{\circ}\text{C}$).

The third condition for a steady state was added as one must be sure that the temperature difference, and the resulting heat flow between the main heater and the guard heaters is absent. Otherwise, the heat dissipated by the main heater (Q) is incorrectly calculated.

Only during the moments when the system was in steady state, the thermal conductivity coefficient (k) was calculated. The k -values within these moments were averaged and this final k -value was assigned to the measured sample.

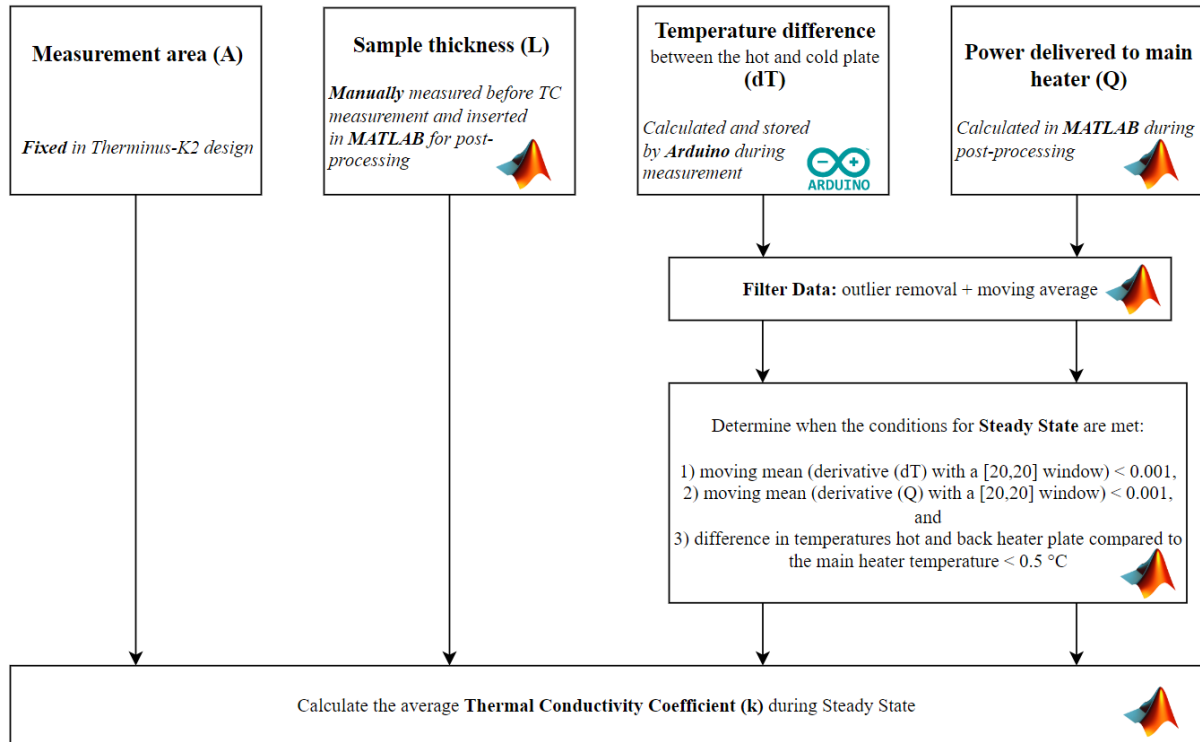


Figure 22. Flowchart of the calculation of the thermal conductivity coefficient (k) of a textile sample by Therminus-K2.

5.2.4 Specifications

The general specifications of Therminus-K2 were listed in **Table 5**.

The guard heater width should at least be 30 mm for a 60 x 60 mm main heater (section 4.1), but again heaters with a width of 40 mm were the smallest available. The air gap width was 1 mm, as it was the smallest possible with the laser cutting machine. However, some connections between the main heater plate and guard heater area were still present, as it was needed for construction. These connections could still conduct some heat between main and guard heaters. Temperature sensors were calibrated and validated from 18 $^{\circ}\text{C}$ to 40 $^{\circ}\text{C}$. If temperature exceed this range, no reliable TC measurements can be guaranteed.

The dimensions of the heating assembly were determined by the minimal dimensions of the available heater foils. The used heater sizes for main (60x60 mm) and guard (100x40 mm) heaters were the smallest available. As discussed in section 4.1, using a 60x60 main heater would require a guard heater width of at least $0.5 \times 60\text{ mm}$. Again, 40x100 mm guard heaters were the smallest available and were therefore used.

Therefore, to perform TC measurements cut samples with dimensions of 120x120 mm² to 140x140 mm² should be inserted in the Terminus-K2 prototype. This conflicts with the user's wish to keep textile intact or use smaller samples (**Requirement 5**). However, this was inevitable with the available heater sizes and the need for rapid prototyping.

The samples that Terminus-K2 can theoretically measure can have maximum 60 mm thickness (section 4.1 and 5.2.1). Furthermore, the device is designed to test samples with k-values ranging from 0.02 to 0.7 W/mK. Exceeding this range could result in incorrect measurements or damage to the device. The device should be used at ambient temperatures ranging between 18 °C – 30 °C, when setting the temperature difference between the plates to a maximum of 10 °C.

Heat generated in the main heater and guard heaters will flow downward in vertical direction towards the cold plate. There, heat generated by the Peltier elements is dissipated by the heat sinks and the fans.

	Minimum	Maximum
Heating assembly size	160 x 144 x 14 mm	
Main heater area	60 x 60 x 2 mm	
Guard heater width	40 mm	
Air gap width	1 mm	
Temperature	18 °C	40 °C
Cooling assembly size	160 x 144 x 28 mm	
Number of Peltier elements	9	
TC measurements		
Sample material size	120 x 120 mm	140 x 140 mm
Sample thickness	0.1 mm	60 mm
Thermal conductivity of the sample	0.02 W/mK	0.7 W/mK
Environment temperature	18 °C	30 °C
Direction of heat flow from the main heater	Vertical Downward	

Table 5. Specifications of Terminus-K2

6. THERMINUS-K2 TESTS

Four tests were carried out to test the working of Therminus-K2. The first test served to validate the configuration of Therminus-K2 with guard heaters and a back heater to eliminate parasitic heat flows. In the second test, the device's performance was assessed in terms of accuracy, precision and measurement time. Besides this, the device's sensitivity to errors in input parameters was mathematically tested. Eventually, a case study demonstrated whether the effects of moisture content and fabric compression on the calculated k-values of samples measured by Therminus-K2 correspond with the literature.

The general measurement workflow used in the tests is visualized in **Figure 23**. Appendix H specifies the measurement protocol that was followed for TC measurements. In Appendix I contains details about the tested textile samples.

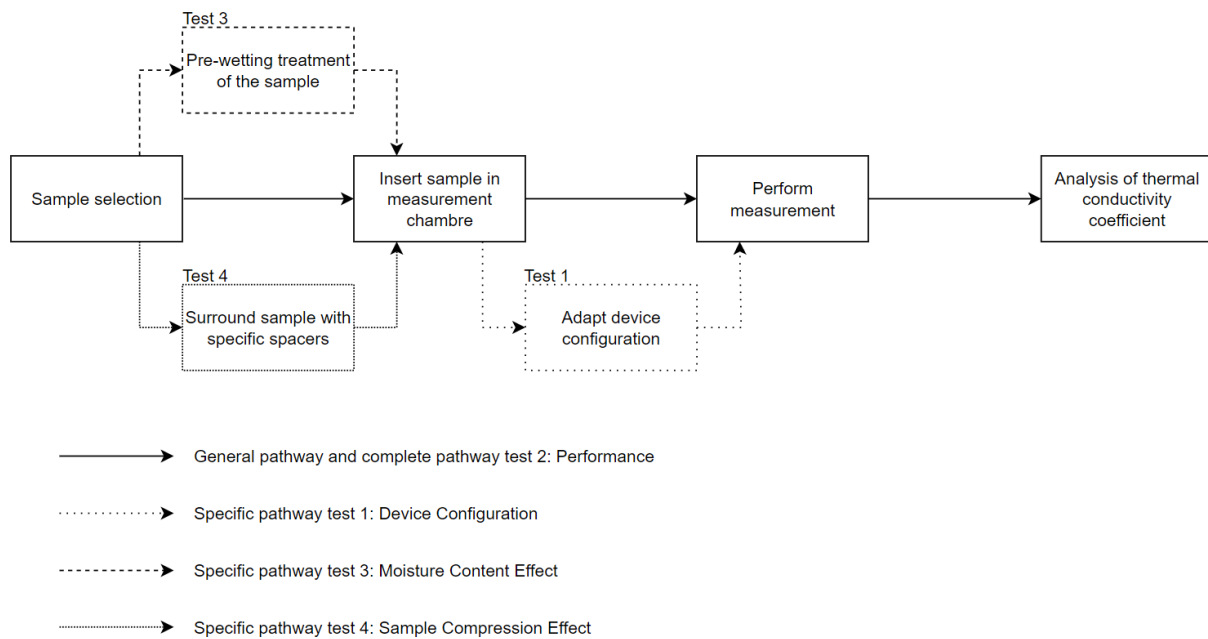


Figure 23. General measurement workflow for the performed tests 1 – 4.

6.1 Therminus-K2 Validation and Performance

6.1.1 Device Configuration Test

Introduction

The Device Configuration Test was performed to validate the chosen configuration of Therminus-K2.

In the GHP method, TC can only be determined when a steady-state one dimensional heat flow through the sample is achieved. Consequently, the purpose of the device's components is to ensure that the heat generated by the main heater only flows through the sample towards the cold plate across a constant temperature difference. To validate this, this test aimed to evaluate the effect of the device's components on the heat flow and the obtained k-value. The tested components were: aerogel insulation, guard heaters, extra Peltier elements and a back heater.

Method

A flat polycarbonate (PC) sample (size: 140x140x2.69 mm) was used for testing six different device configurations (**Figure 24**). Each device configuration measurement was repeated three times with a measurement time of 15 minutes. The temperature difference between the plates was set to 10 °C.

Calculated k-values and power to the main heater per device configuration were visualized in scatterplots using SPSS IBM Statistics 26.

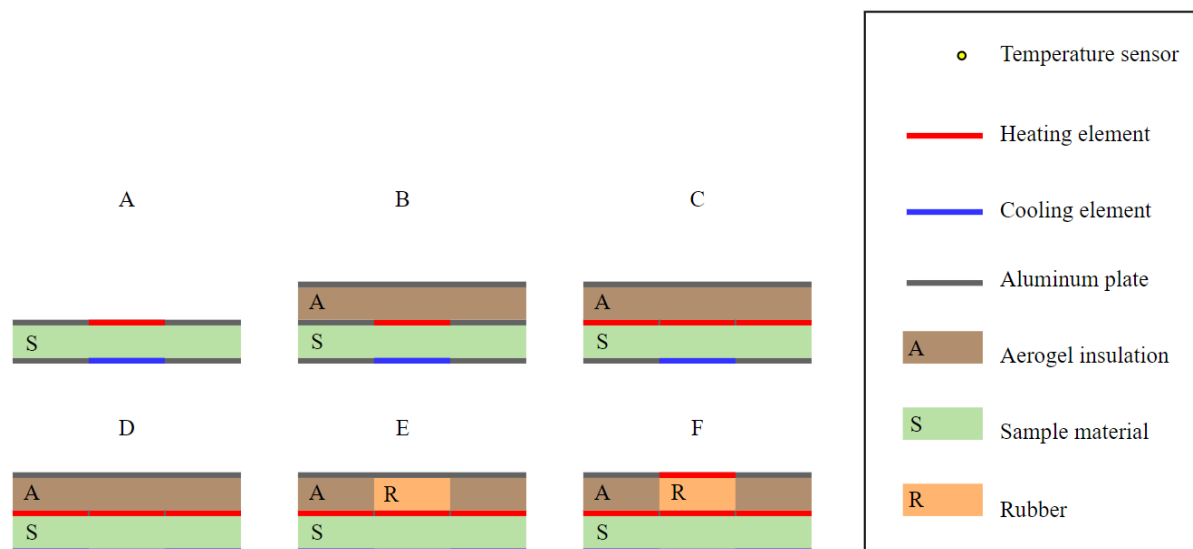


Figure 24. Tested device configurations:

- A) Air – Main heater – Sample – Peltier n = 1);
 B) Aluminum plate – Aerogel – Main heater – Sample – Peltier (n = 1);
 C) Aluminum plate – Aerogel – Guard heater: Main heater: Guard heater – Sample – Peltier (n = 1);
 D) Aluminum plate – Aerogel – Guard heater: Main heater: Guard heater – Sample – Peltier (n = 9);
 E) Aluminum plate – Rubber – Guard heater: Main heater: Guard heater – Sample – Peltier (n = 9);
 F) Back heater – Rubber – Guard heater: Main heater: Guard heater – Sample – Peltier (n = 9);

Results

Figure 25 shows the calculated power delivered to the main heater to achieve the set hot plate temperature for the six tested configurations (A – F). **Figure 26** shows the measured k-values of the PC sample determined by using the different device configurations. In both figures, the largest difference in measured power to the main heater and k-value is observed when guard heaters are added to the configuration.

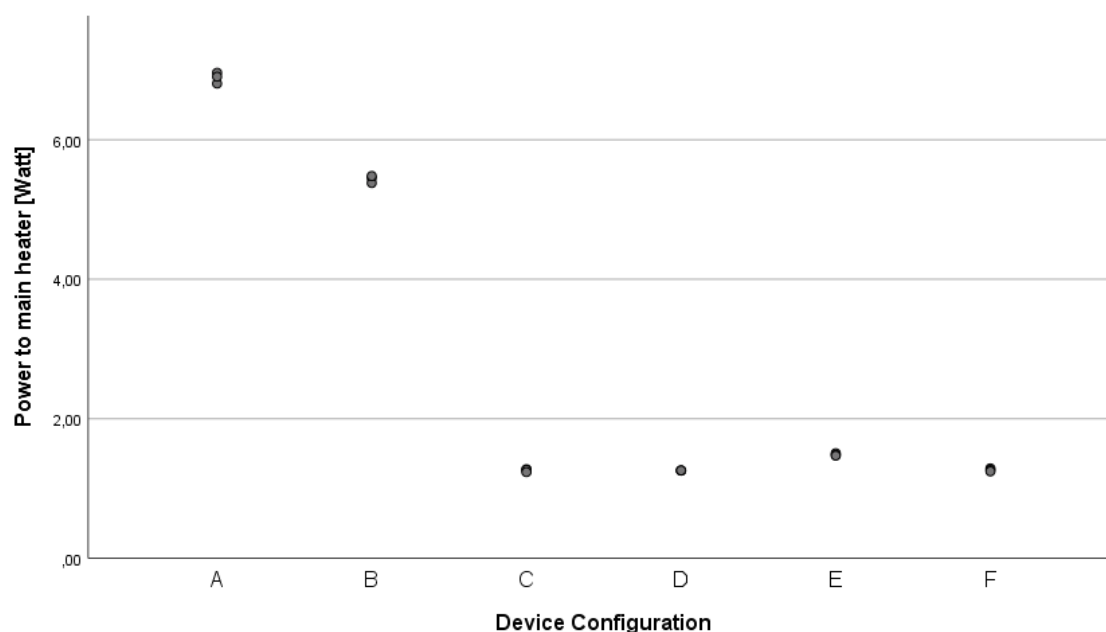


Figure 25. Scatterplot of the determined power to the main heater for the 6 tested device configurations, as specified in Figure 21. Per configuration, 3 repetitions were performed and inserted in this scatterplot.

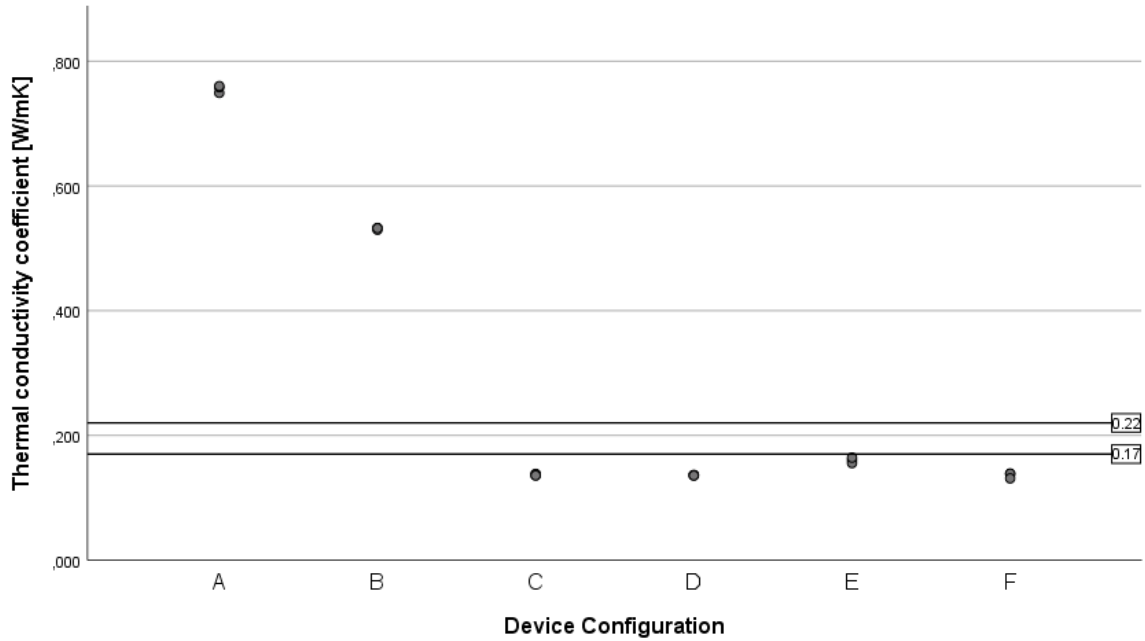


Figure 26. Scatterplot of the measured thermal conductivity coefficients for the 6 tested device configurations, as specified in Figure 24. Per configuration, 3 repetitions were performed and inserted in this scatterplot. The dotted line indicates the range of reference (0.17 – 0.22 W/mK) between which the thermal conductivity coefficient of Polycarbonate usually lies at 23 °C [70-72].

The high power delivered to the main heater in configurations A and B indicates a high generation of heat by the main heater dissipating in multiple directions (**Figure 25**). In configuration A, only a heating and cooling element were used without any measures to eliminate parasitic heat flows. Resultingly, heat was free to flow in all 6 directions (**Figure 27**). In configuration B, the heat flow in the upper direction is minimized due to the addition of insulation on top of the assembly. This is confirmed by the results shown in **Figure 25**, in which the heat flow decreases in similar proportions ($\sim 1/6^{\text{th}}$). Adding guard heaters to configuration B results in a large decrease in power delivered to the main heater (**Figure 25**). This decrease in power consumption theoretically results in a decrease in heat generation and could explain that the major heat flow in configurations using guard heaters, and either back insulation or a back heater is towards the cold plate (**Figure 27**).

Configurations C to F, all using guard heaters, show comparable results in power to the main heater and calculated k-values. In configuration E a higher power consumption by the main heater was observed than in configuration C, D and F due to the partial replacement of aerogel ($\sim 0.01\text{-}0.02$ W/mK) by rubber (~ 0.5 W/mK).

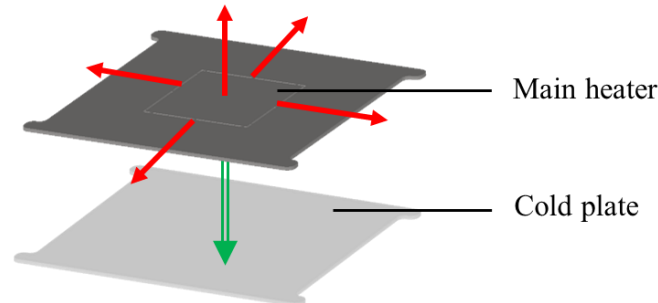


Figure 27. Heat flow directions (arrows) from the generated heat in the main heater Area. In the used configuration F, the major heat flow (green, - -) is directed towards the cold plate and the other heat flow directions (red) are negligible.

Configuration F, which was used in the final Terminus-K2 prototype, can indeed measure samples with lower k-values by using a back heater instead of back insulation. Using back insulation (aerogel ($\sim 0.01\text{-}0.02$ W/mK)) would limit the range of k-values that can be measured, as the k-values of textile

samples could get close to the k-value of aerogel and again backward heat flow could take serious sizes. Therefore, configuration F using a back heater and guard heaters is indeed suitable for TC measurements of textile samples.

6.1.2 Performance Test

The Performance Test aimed to assess the accuracy and precision of Therminus-K2 together with the time needed to achieve steady-state measurements, in order to evaluate **Requirements 3, 4 and 7**.

Method

Five flat samples (140x140 mm) of different materials were used to perform TC measurements on. Two samples were cut from homogeneous isotropic materials (PC and NY6) and three samples were cut out pieces of clothing (undershirt, long sleeve and joggers). **Figure 28** schematically visualizes the tested samples. Five measurements were performed per sample, taking 30 minutes each.

Result analysis included calculation and evaluation of the accuracy, precision and measurement time of the Therminus-K2 device. Accuracy was assessed by comparing calculated k-values of a sample by reference k-values as determined by other studies. Precision was defined as the standard deviation of the calculated k-values of a sample (five repetitions) divided by the average calculated k-value of a sample. Time to steady state was defined as the first moment in time in which a steady state (as described in Chapter 5) was reached. SPSS IBM Statistics 26 was used to calculate the average and the standard deviation of calculated k-values and the time to and time in steady state. MATLAB was used to plot the calculated k-values in relation to the k-values as determined by other studies.

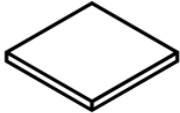
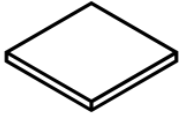



Polycarbonate (PC) slab	Nylon 6 (NY6) slab	Cotton (100% CO) undershirt	Polyester (100% PES) long sleeve	Polyester/Cotton (65/35 % PES/CO) joggers
2.69 mm thick	2 mm thick	0.6 mm thick	2 mm thick	1.4 mm thick
				

Figure 28. Sample materials used for the Performance Test.

Results

Table 6 shows the determined k-values of the tested samples. The precision of the measurements ranged from 2 to 5 % and the time needed to achieve the first moment of steady state ranged from 2.81 to 6.94 minutes. The time in which the system was in steady state, according to the definition in section 5.2.3, ranged from 5.25 – 15.65 minutes.

Table 6. Descriptive results about the determined thermal conductivities of the tested samples. Std = standard deviation.

* Precision: Standard Deviation k-value / Mean k-value. Min – Max: the minimum and maximum values.

	Thermal Conductivity Coefficient k (W/mK)		Precision*	Time to Steady State (minutes)	Time in Steady State (minutes)
	Mean	Std	%	Min - Max	Min - Max
PC	0,129	0,005	4	4,53 – 6,94	5,25 – 7,40
NY 6	0,132	0,002	2	3,88 – 5,65	5,28 – 13,09
CO	0,042	0,001	2	4,07 – 5,75	6,27 – 8,97
PES	0,033	0,002	5	2,81 – 4,91	8,35 – 15,65
PES/CO 65%/35%	0,036	0,001	3	3,21 – 4,08	6,05 – 11,37

It is not possible to assess the measurement's absolute accuracy without using either standard reference materials or performing a control measurement by a well (ISO) classified TC measurement device. Therefore, the measured TCs were compared with TCs of the same materials as found in other studies (see **Figure 29**) [63, 64, 70-79]. The TCs as determined by Therminus-K2 always were either lower than the reference values or within the referencing range.

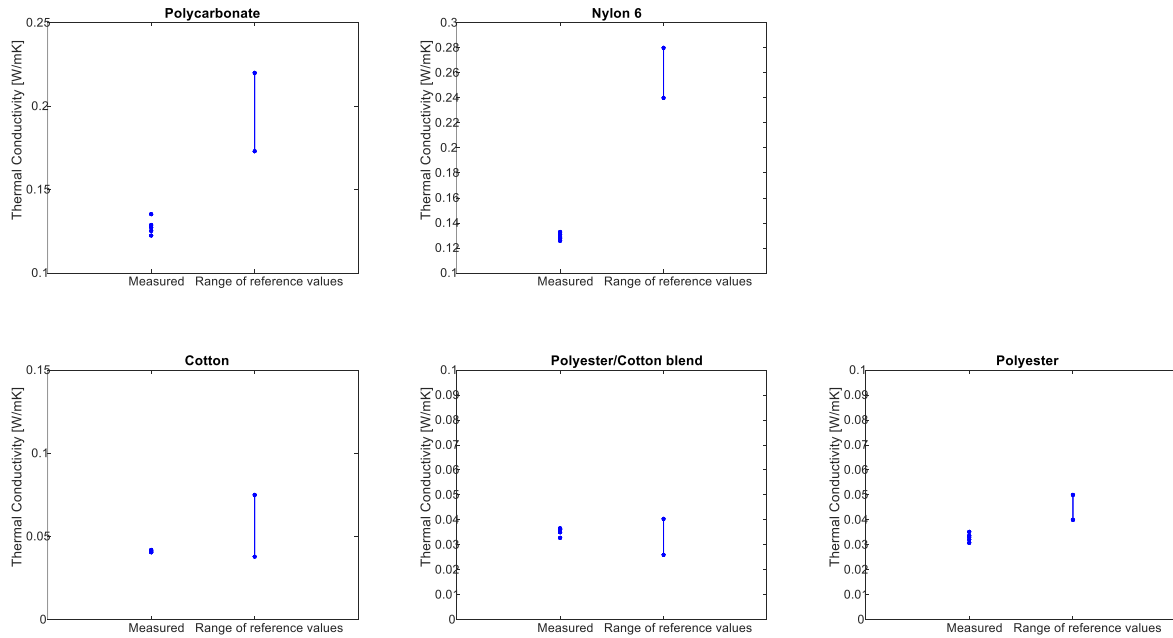


Figure 29. Five plots comparing measured thermal conductivity coefficients with some thermal conductivity coefficients of the same materials by different studies [63, 64, 70-79].

6.2 Error Sensitivity Test

The sensitivity of Thermanus-K2 to errors in its input parameters was mathematically tested. The error sensitivity test was performed to discover the main factors causing variation in *k-value* calculation by Thermanus-K2. It investigated how changes in input parameters affect the measured *k-value*, as calculated based on Equation 1.

Table 7 shows the parameters needed in TC calculation. Based on the resolution of the measurement method with which the parameters are measured, the uncertainty in a single measurement is calculated [80]:

$$\text{Uncertainty in a single measurement} = \frac{\text{resolution of the measurement}}{2} \quad (3)$$

Subsequently, the uncertainty in the total measurement is calculated per parameter [80]. The ranges of the parameters as measured in the samples in the Performance Test (section 6.1.2) are displayed and the resulting change (%) of the determined *k-value* due to the parameter's uncertainty over the boundaries of these ranges is determined. As all parameters linearly correlate with the *k-value* (Equation 1 in section 2.1), the effect of a parameter's uncertainty on the parameter itself is similar as its effect on the *k-value*.

Table 7. Uncertainty of input parameters in TC calculation by Thermanus-K2 with their effect on the calculated *k-value* (%).

Parameter	Unit	Measurement method or instrument	Uncertainty in a single measurement	Total uncertainty	Range as calculated in Performance Test	Resulting change of <i>k-value</i> (%)
Power \dot{Q}	Watt	PWM bits to power conversion	± 0.095	± 0.0212	Min: 0.457 Max: 1.576	4.6 % 1.4 %
Sample thickness L	meter	Digital caliper	$\pm 0.005 * 10^{-3}$	$\pm 0.1 * 10^{-3}$	Min: $0.6 * 10^{-3}$ Max: $2.69 * 10^{-3}$	16.7 % 3.7 %
Measuring Area A	squared meter	Digital caliper	$\pm 0.005 * 10^{-3}$	$\pm 0.85 * 10^{-6}$	$3618.02 * 10^{-6}$	0.024 %
Temperature difference ΔT	° Celsius	Thermistors	± 0.4	± 0.089	Min: 5.91 Max: 8.61	1.5 % 0.7 %

Power \dot{Q}

The resolution for the power measurement delivered to the main heater is determined on the resolution of the bits to power conversion (48 Watt divided by 256 (8-bit) is 0.19 Watt). The resulting uncertainty in a single measurement would be 0.095 Watt (see Equation 3). However, the total uncertainty of the power is lower, as a result of averaging which takes place after data acquisition. A moving average with a [10,10] window is applied to the data. Therefore, the total uncertainty becomes [80]:

$$\text{uncertainty in the mean} = \frac{\text{resolution}}{2 * \sqrt{\text{window size}}} = \frac{0.19}{2 * \sqrt{20}} = 0.0212 \text{ Watt} \quad (4)$$

Applying this uncertainty to the minimum and maximum values as determined in the Performance Test, the resulting effect on the calculated *k-value* varies from 1.4 % to 4.6 % (**Table 7**).

Sample thickness L

The resolution of the digital caliper with which the sample thickness is measured was $0.01 * 10^{-3}$ mm. Resultingly, the uncertainty in a single measurement would be $0.005 * 10^{-3}$ mm. However, the total uncertainty in the measurement is estimated to be higher ($0.1 * 10^{-3}$ mm) due to the possibility for incorrect hot and cold plate positioning.

The effect of sample thickness uncertainty on the *k-value* is lower for thicker samples (2.69 mm – 3.7%) than for thinner samples (0.6 mm – 16.7 %). The effect is high, as the sample thickness is only

measured once and that single value is used in TC calculation, without being subjected to any averaging or other post-processing.

Measuring Area A

The measuring area is an intrinsic property of Thermanus-K2 and is not changed between measurements. The effect of the measurement uncertainty in this parameter on the k-value is therefore the same in all measurements.

After the rapid production process (laser cutting) the measuring area became 60.1 mm by 60.2 mm ($3618.02 \cdot 10^{-6} \text{ mm}^2$), as measured with a digital caliper. Resultingly, the total uncertainty resultingly is $0.85 \cdot 10^{-3}$, estimated using the rule for uncertainty propagation by multiplication (Equation 5) [80]. In all measurements the k-value could have been affected by an uncertainty in measurement area, although this effect appears to be extremely small (0.024%).

$$Uncertainty = |xy| \cdot \sqrt{\left(\frac{\Delta x}{x}\right)^2 + \left(\frac{\Delta y}{y}\right)^2} = |60.1 \cdot 60.2| \cdot \sqrt{\left(\frac{0.01}{60.1}\right)^2 + \left(\frac{0.01}{60.2}\right)^2} = 0.8506 \text{ mm}^2 \quad (5)$$

Temperature difference ΔT

During validation of the used thermistors, it appeared that the individual temperature sensors all had a Root Mean Squared Error (RMSE) $< 0.2 \text{ }^\circ\text{C}$ in relation to the reference temperature sensor for a temperature range from $18 - 42 \text{ }^\circ\text{C}$. When determining the temperature difference, this results in a possible deviation of $0.4 \text{ }^\circ\text{C}$ from the actual temperature difference in a single measurement. As a moving average with a window of 20 data points is applied to the measured temperature differences, the uncertainty of the total measurement becomes $0.089 \text{ }^\circ\text{C}$ ($0.4/\sqrt{20}$), as determined via Equation 4.

This could result in an error up to 1.5% for a minimum ΔT of $5.91 \text{ }^\circ\text{C}$ on the determined k-value. Using a larger ΔT between the hot and cold plate would result in a smaller effect of temperature sensor uncertainty on TC.

The effect of uncertainty in sample thickness on the calculated k-value is the highest (3.7 - 16.7%) of all input parameters. Especially for thin samples (0.6 mm thick), an incorrectly measured sample thickness ($\pm 0.1 \text{ mm}$) could have an extreme effect (16.7%) on the calculated k-value.

Thermal Contact Resistance

Beside these input parameters, the contact resistance between the sample and the surface plates also affects the calculated k-value. Thermal contact resistance arises due to insufficient contact between two bodies, in this case surface plate and sample surface. Due to irregularities in the surfaces, the actual contacting area on micro-level available for thermal conduction is small. The areas of improper contact are filled by air which generally acts as an extra insulation (thermal resistor) layer. Even if no irregularities are noticed by eye, still irregularities exist on microscopic level (microcontact resistance).

The thermal contact resistance is affected by multiple parameters, such as geometry of the contacting surfaces, gap thickness, type and k-value of ambient gas/fluid, k-values of the surfaces, elastic modulus of the surfaces and (ambient) temperatures. In order to investigate the effect of contact resistance in measurements with Thermanus-K2, some simplifications are necessary.

Thermal resistance is the inverse of TC multiplied by the material's thickness (Equation 6). Heat flowing from the hot plate through the sample towards the cold plate is schematically visualized by three thermal resistances in series (**Figure 30**). Two thermal resistances (R_{c1} and R_{c2}) are caused by the thermal contact resistance between the surface plates and the sample material surface. The middle thermal resistance (R_s) is the inverse of TC of the sample material.

$$R = \frac{L}{k} \left[\frac{\text{m}^2\text{K}}{\text{W}} \right] \quad (6)$$

The effect of thermal contact resistance on the determined k-value can be estimated. The thermal resistance of a 2.69 mm thick PC sample with an actual k-value of 0.2 W/mK would be:

$$R_s = \frac{L}{k} = \frac{2.69 \times 10^{-3}}{0.2} = 0.01345 \left[\frac{m^2 K}{W} \right] \quad (7)$$

When a small air ($k \sim 0.002$ W/mK) layer of 0.1 mm is present between the hot plate and the sample, the thermal resistance in the upper contact (R_{c1}) would be:

$$R_{c1} = \frac{L}{k} = \frac{0.1 \times 10^{-3}}{0.02} = 0.005 \left[\frac{m^2 K}{W} \right] \quad (8)$$

Assuming the air layer between the cold plate and the sample is also 0.1 mm,

$$R_{c1} = R_{c2} \quad (9)$$

which results in a total thermal resistance of

$$R_{total} = 2 * R_{c1} + R_s = 0.02345 \left[\frac{m^2 K}{W} \right] \quad (10)$$

Translating this back to thermal conductivity results in an apparent k-value of

$$k = \frac{L_{total}}{R_{total}} = \frac{(2.69 + 2 \times 0.1) \times 10^{-3}}{0.02345} = 0.123 \left[\frac{W}{mK} \right] \quad (11)$$

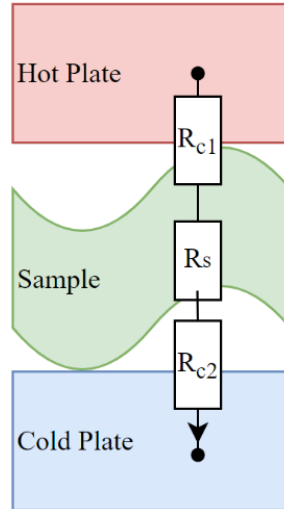


Figure 30. Representation of the thermal resistances through which the heat generated in the hot plate flows towards the cold plate. R_{c1} : contact resistance between the hot plate and the sample, R_s : thermal resistance of the sample, and R_{c2} : contact resistance between the sample and the cold plate.

As determined through a simplified estimation in Equations 7 to 11, it seems that the k-value of PC (with a reference k-value of 0.2 W/mK) is calculated to be 0.123 W/mK when incorporating the presence of two small (0.1 mm thick) air layers between the surface plates and the sample in the calculation. Even these small air layers could thus result in a decrease in the estimated k-value of 38.5%. This is comparable to the results of the Performance Test, in which an average k-value of PC of 0.129 W/mK is determined whereas literature values range between 0.17 and 0.22 W/mK.

6.3 Thermanus-K2 Case Study

In this case study, Thermanus-K2 was used to investigate the effects of some of the previously determined factors affecting TC of textile (section 2.2) [7]. Moisture content of the sample and sample compression had the largest effects on the calculated k-value of textile as found by multiple studies [7, 26-48]. These effects easily result in a 100% in- or decrease in determined k-value. When using Thermanus-K2 in forensic practice, wetted and compressed textile samples will have to be measured. Therefore, this case study was performed.

6.3.1 Moisture Content Effect Test

In this test the effect of moisture content of the sample on the calculated k-value was investigated, assuming Thermanus-K2 works properly. The research question of this test was: Do the TC measurements results of samples with different moisture contents correspond with the effect of moisture on TC as seen in literature [7, 26-48]?

Method

Figure 31 shows the materials from which samples (each 140 x 140 mm) were cut to perform TC measurements on. The samples were tested in two different states of moisture content: air dried and wetted. A sample was categorized as air dried after leaving the materials in a room (± 21 °C; 40 – 60% relative humidity) for seven days prior to testing. Wetted samples were created by fully soaking a sample in water, then squeezing most water out and letting it dry for 1,5 hours.

Three measurements of 30 minutes were performed per sample and per moisture state. SPSS IBM Statistics 26 was used to visualize the calculated k-values per sample and moisture state in a scatterplot, and to calculate the average and standard deviation of these k-values. Results should be analyzed qualitatively, as the final achieved moisture content during measurement is likely to differ amongst wetted samples, due to the preparation method used.

Denim (CO) skirt	Polyester/Cotton (65/35 % PES/CO) joggers	Acrylic/polyester (PAN/PES) fur coat
0.8 mm thick	0.96 mm thick	8 mm thick
		

Figure 31. Sample materials used in the Moisture Content Effect Test.

Results

All measurements performed on wetted samples showed an increase in calculated k-value compared to the same samples in dried states (see **Table 8** and **Figure 32**). The increase was highest in the PAN/PES coat (415%) and was in all cases above 200%. Furthermore, standard deviations within the wetted samples were higher than in the corresponding dried samples.

Table 8. Determined mean thermal conductivity coefficients of samples in two different states of moisture content. Std = standard deviation. ‘Wetted : Dried State’: the mean k-value of a wetted sample as a percentage of the mean k-value of the corresponding dried sample.

Calculated Thermal Conductivity Coefficient k [W/mK]					
	Dried State		Wetted State		Wetted : Dried State*
	Mean	Std	Mean	Std	
DENIM (CO) skirt	0,0516	0,0052	0,1058	0,1058	205%
PAN/PES coat	0,0696	0,0160	0,2888	0,2888	415%
PES/CO 65%/35% joggers	0,0360	0,0006	0,0879	0,0879	244%

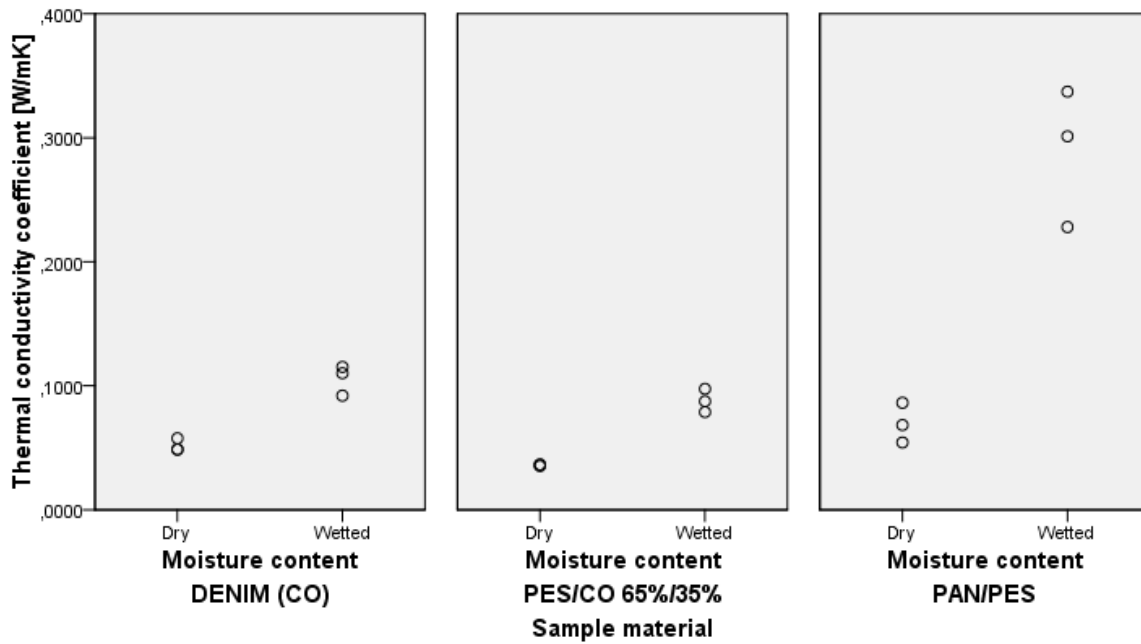


Figure 32. Scatterplot of the effect of moisture content on measured thermal conductivity coefficients of three different textile samples. Per sample and per state three repetitions were measurement and visualized.

6.3.2 Sample Compression Effect Test

In this test the effect of compression of the sample on the calculated k-value was investigated. The research question of this test was: Do the TC measurement results of samples with different states of compression correspond with the expected effect of sample compression on TC in literature [7, 26-48]?

Method

Three different textile samples were investigated in this test in three different states of compression (standard compression, 25% compression and 50% compression) (**Figure 34**). Prior to performing the TC measurements of the samples, their initial thicknesses in state of standard compression were measured with a digital caliper (see Appendix H for definition of standard compression). Subsequently, PMMA laser-cut and PLA 3D-printed spacers were fabricated with thicknesses needed to achieve 25 % and 50 % compression (**Figure 33** and **Figure 34**). However, the realized spacer thicknesses deviated slightly from the desired thicknesses due to rapid production processes. The realized thicknesses were measured and used in TC calculations.

When inserting the sample in the measurement area for testing, the samples were surrounded by their corresponding spacers. Weights (3 x 500 gram) were added on top of the back heater plate to achieve adequate compression. Furthermore, four spring clamps were used to clamp the edges of the hot and cold plate towards each other.

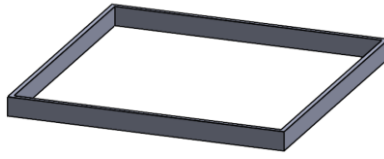


Figure 33. SolidWorks drawing of the spacer used to obtain specific states of sample compression. During measurement, the textile sample was placed within this frame.

Three measurements of 30 minutes were performed on each sample and for each state of compression. SPSS IBM Statistics 26 was used to calculate the average and standard deviation of the calculated k-values per sample and for each compression state. Furthermore, scatterplots were made to visualize the calculated k-values and the calculated power towards the main heater per sample, split by compression state.




Sample	Polyester (PES) long sleeve 2 mm thick		Nylon/polyester (NY/PES) padded jacket 3 mm thick		Acrylic/polyester (PAN/PES) fur coat 8 mm thick	
Standard thickness						
	Desired thickness	Realized thickness	Desired thickness	Realized thickness	Desired thickness	Realized thickness
25% compression	1.5 mm	1.61 mm	2 mm	2.18 mm	6 mm	6.15 mm
50% compression	1 mm	1.19 mm	1.5 mm	1.61 mm	4 mm	4.16 mm

Figure 34. Samples materials used for the Fabric Compression Test with the heights of spacers needed to achieve 25% and 50% compression. The thicknesses of the spacers deviated from the desired thicknesses due to production tolerances. The realized thicknesses were used in TC calculation.

Results

Figure 35 and **Figure 36** show the measured k-values and heat flows for samples in different states of compression. It appears that in the measurement of Thermanus-K2, the calculated k-value of the 50% compressed materials is lower than k-values of 25% compressed materials. Besides this, the standard deviation in k-values determined in states of standard compression is much higher (0.010 – 0.016) than the standard deviation in k-values in compressed states (25 % and 50 % range resp 0.001 and 0.001 – 0.004) (**Table 9**).

Table 9. Mean thermal conductivity coefficients of samples in three different states of compression measured with Thermanus-K2.

	Calculated Thermal Conductivity Coefficient k [W/mK]					
	Standard compression		25 % compression		50 % compression	
	Mean	Std	Mean	Std	Mean	Std
NY/PES padded jacket	0,040	0,010	0,041	0,001	0,033	0,001
PAN/PES coat	0,070	0,016	0,066	0,001	0,062	0,004
PES shirt	0,041	0,012	0,047	0,001	0,039	0,001

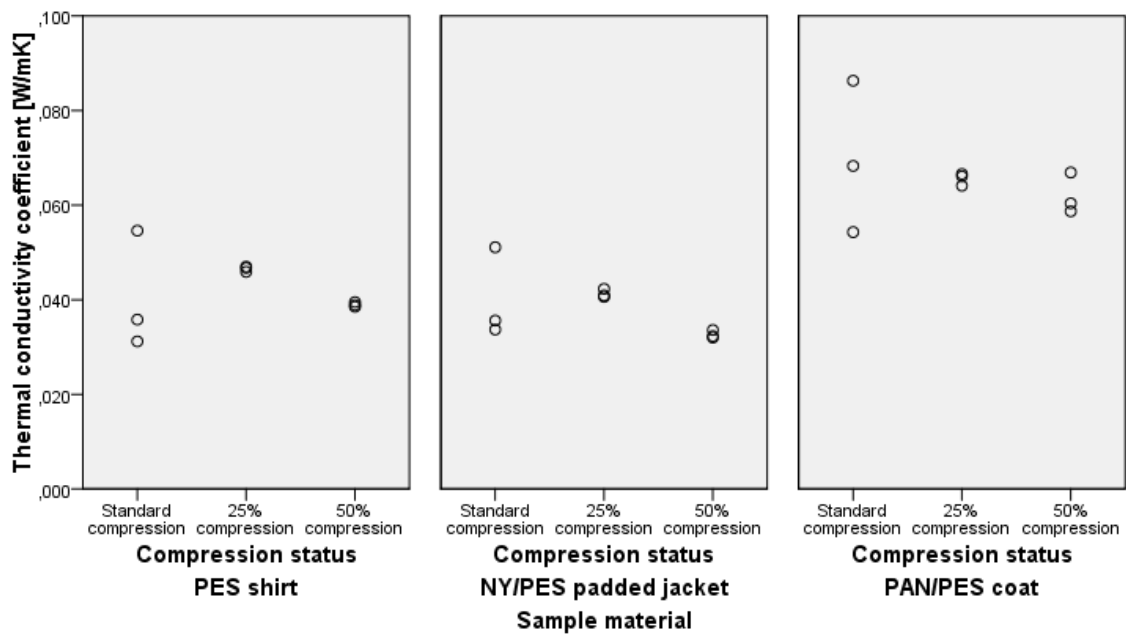


Figure 35. Scatterplot of thermal conductivities of three samples split by their state of compression, with three repetitions.

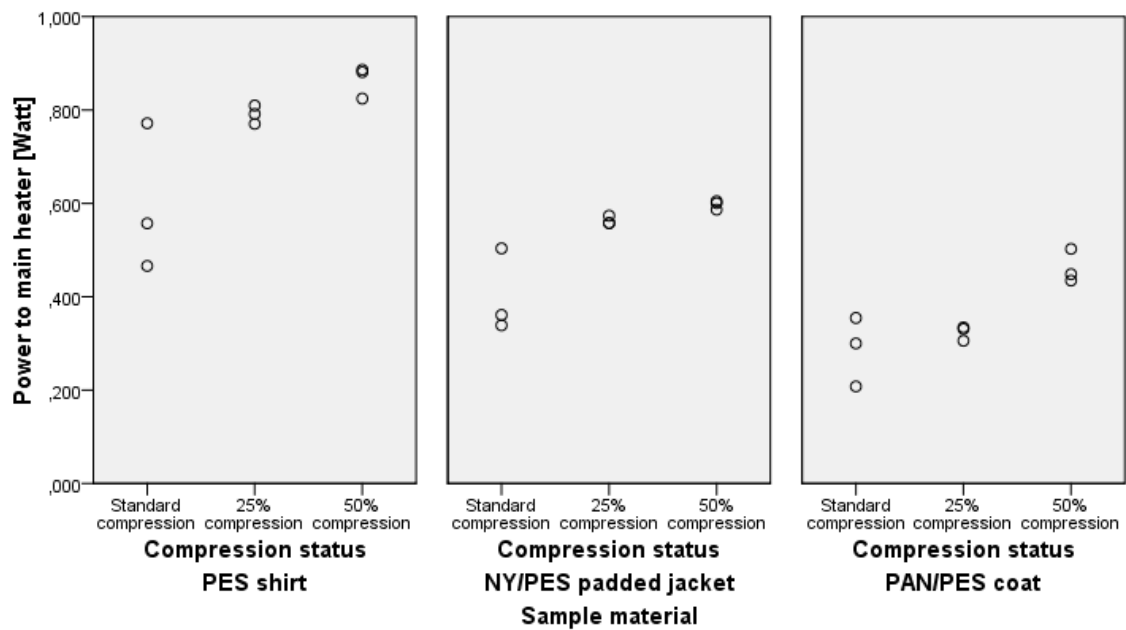


Figure 36. Scatterplot of the power delivered to the main heater for three samples split by their state of compression, with three repetitions.

7. DISCUSSION

In this study, a device for measuring TC of textile samples for forensic purposes was designed, developed and tested: the Thermanus-K2 prototype. Its device configuration was validated and its performance was investigated. Besides this, an error sensitivity test was performed and a case study was done.

7.1 Interpretation of the Experimental Results

Validation and Performance Tests

These tests showed that the chosen GHP configuration using a back heater and guard heaters resulted in precise results ($\leq 5\%$) within 30 minutes of measurement. A steady state, as currently defined in the used post-processing method (section 5.2.3 and **Figure 22**), was already achieved within a maximum of 6.94 minutes. The time within the 30-minute measurement in which the system was in steady state ranged from 5.25 to 15.65 minutes. Hence, Thermanus-K2 still has difficulties with keeping the system in steady state once it has been reached. This might be subscribed to errors in temperature sensor readouts which are proceeded in the PID controlled heating and cooling of the plates, due to which temperatures might fluctuate over time.

In the performance test, most determined k-values were below the range of reference k-values (**Figure 26** and **Figure 29**). As discussed in the error sensitivity test in section 6.2, this can likely be attributed to the contact resistance between the hot and cold plate surfaces and the sample surfaces. This effect is also present in the textile layer surrounding a deceased body.

The difference between the calculated k-values of PC and NY6 samples and their reference k-values was larger than for the other tested materials (CO, PES and CO/PES) (**Figure 29**). This could be attributed to the contact resistance having a bigger effect on PC and NY6 slabs due to their rigidity. Besides this, PC and NY6 (range 0.18 – 0.28 W/mK) are supposed to have much higher k-values than CO, PES and CO/PES (0.03 – 0.14 W/mK). Therefore, the effect of an air layer (0.02 W/mK) as a result of insufficient contact is higher for PC and NY6 than in the other samples, which agrees with the results as shown in **Figure 29**.

Moisture Effect Test

In the moisture effect test, it appeared that wetting textile resulted in an increased k-value (205 – 415 %) in all tested samples (**Table 8**). This agrees with physics and literature, as multiple other studies report an increase in k-value (105 – 755%) due to an increased moisture content of the sample [7, 26-48]. The moisture (e.g. water) that is added to the sample substitutes the air in the fabric pores. Resultingly, the calculated k-value of the sample increases, as water ($k \sim 0.598$ W/mK at 20 °C) is a better conductor than air ($k \sim 0.025$ W/mK at 20°C) [81, 82].

The standard deviation in measured k-values of wetted fabrics was higher than in the measured k-values of dried fabrics. This is likely due to differences in achieved moisture content within the samples, as a result of slight differences in the process of squeezing and drying the samples, after being fully wetted.

The effect of moisture content on the calculated k-value differed per fabric and was highest for the 8 mm thick PAN/PES coat (390% increase). This could be explained as it is likely that more air is present within the fibers of this thick furry coat compared to the other tested samples. This enabled more water absorption, resulting in a higher increase in k-value after wetting.

The observations in the moisture content effect test correspond with literature and support the importance of measuring k-values of textile layers at a crime scene. Addition of water to a textile sample increases its k-value. This most likely also applies to addition of blood or urine to textile, which is often encountered at crime scenes. In practice, this would add a requirement to a new TC measurement device; The measurement area should withstand repeated measurements of wetted samples.

Fabric Compression Test

In literature, it is proven that the k-value of a sample increases with an increase in sample compression [7, 26-48]. During sample compression, air that was present between textile pores gets pressed out. As the k-value of air is smaller ($k \sim 0.025 \text{ W/mK}$ at 20°C) than the k-values of most textiles ($0.057 - 0.52 \text{ W/mK}$, **Requirement 1**), removing air from the sample increases the measured k-value.

In this study, at 25% compression state the calculated k-values in most samples were indeed higher than the k-values at standard compression (see Appendix H for the definition of standard compression). However, a decrease in the calculated k-value was observed between 25% and 50% compression, which differs from the correlation found in literature (**Figure 35**) [7, 26-48]. This may have been caused by an incorrectly determined sample compression. The contact surfaces (hot and cold plate to sample) may have had small irregularities or a small curvature as a result of which the sample thickness wasn't equal over the full sample. Besides this, an uncertainty in sample thickness measurement (section 6.2) may have affected the determined k-value, as a result of which the expected fabric compression effect was not visible. For example, measuring the k-value of a 1 mm thick sample with a sample thickness measurement uncertainty of 0.1 mm could have resulted in an uncertainty in k-value of 10%. However, the k-values of the padded jacket, coat and shirt at 50% compression respectively vary 19%, 6% and 17% to the k-values at 25% compression. Therefore, the sample thickness measurement uncertainty might even be underestimated.

It is unlikely that the extra connection from the hot plate via the spacers to the cold plate may have affected the measurements. This is, because the spacers are made of materials (PLA and PMMA) with relatively low k-values ($\sim 0.13 - 0.25 \text{ W/mK}$) compared to the k-value (130 W/mK) of the plates' material (Al7075). Besides this, the spacers are situated outside of the measuring zone.

Furthermore, the fabric compression test showed a higher standard deviation in calculated k-values at standard compression ($0.009 - 0.016$) than in 25% and 50% compression states (resp. $0.002 - 0.004$ and $0.001 - 0.005$) (**Figure 35** and **Table 9**). Increased compression seems to lead to more precise results, likely due to an increase in contact area between the hot and cold plates and the sample surface, which decreases the contact resistance.

7.2 Evaluation of the Design Requirements

Therminus-K2 was evaluated against the design requirements (Section 1.2.2). The evaluation is presented in **Table 10**, and the assessment of each requirement is briefly discussed below.

Regarding the performance parameters of a TC measurement device, three of the minimal requirements were already fully met, three were partly met, one was unmet and one is still to be tested.

Requirement 1

Therminus-K2 was tested only over a range of k-values from $0.031 - 0.330 \text{ W/mK}$, as textile samples with k-values over a broader range were not available. Based on the design configuration of Therminus-K2, it is however very likely that k-values over the minimal and target requirement range can be measured (**Requirement 1**): The use of a back heater to eliminate backward heat flow would enable measuring lower k-values compared to using aerogel. The upper k-value of 0.7 W/mK is also expected to be achievable, although the higher k-value could require more power to maintain a temperature difference over the sample. However, decreasing the temperature difference over the plate would facilitate measuring higher k-values.

Requirement 2

Heat flow simulations evaluating the ratio of main heater to guard heater dimensions (section 4.1) and the used main heater dimensions ($60 \times 60 \text{ mm}^2$) enabled measurement of textile samples up to 30 mm thick (section 5.2.4). This means that the minimal requirement for sample thickness (**Requirement 2**) was met, even though only samples up to 8 mm thick were measured during the tests.

Requirement 3

This requirement, regarding the accuracy of the TC measurement, was not yet quantified. However, no unexpected results were observed as k-values always were at or below the reference k-values, which is explained by the effect of contact resistance.

Requirement 4 and 5

Therminus-K2 obtained measurements with high precision ($\leq 5\%$), meeting the corresponding minimal **Requirement 4**. **Requirement 5** had to be deviated from in the early design phase, due to the minimum sizes of the available heaters.

Requirement 6, 7 and 8

Therminus-K2 meets the target **Requirements 6** and **7** for respectively setup and measurement time. The time to set up the device prior to measurement took maximum 4 minutes (tested: 5 repetitions) when performed by an expert of Therminus-K2. The total TC measurement took 30 minutes, and a steady state was reached within 6.94 minutes.

Requirement 8, lifetime of the device without recalibration, could not yet be tested. The target of 12 months without recalibration exceeded the duration of the project. Besides this, no recalibration of any of the components was performed, as the device would have to be completely disassembled to do that. However, Therminus-K2 was used for up to 16 measurements a day for up to 5 consequent days over a period of two months. Therefore, it is assumed that Therminus-K2 meets this requirement.

Requirement 9 to 16

Requirement 9, 12, 14 and **15** could not yet be tested on the current prototype, due to the time constraint on the project. However, Therminus-K2 meets the minimal goals for **requirement 10, 11, 13** and **16**. The total costs of the materials and components used in the development of Therminus-K2 were 685.87 euros. In addition, the facilities at TU Delft were used during the prototype's development.

Table 10. Evaluation of Therminus-K2 based on the previously set design requirements. When minimal and target values of a requirement were equal, cells were merged. The column 'Verified' displayed the tested values or qualitative descriptions thereof. The requirements were evaluated based on the performed tests and on the design. Minimal and target requirements were colored light green when partly met, dark green when fully met.

Requirement		Minimal	Target	Verified	Satisfied?
Performance parameters					
1	Range of k-values able to measure	0.057 – 0.52 W/mK	0.022 – 0.7 W/mK	0.031 – 0.330 W/mK	Minimal and target: Test-based: partly; Design-based: yes.
2	Range of sample thicknesses able to measure	0.44 – 28 mm	0.17 – 150 mm	0.6 – 8 mm	Only minimal: Test-based: partly; Design-based: yes.
3	Accuracy error of TC measurement	$\leq 8\%$	$\leq 3\%$	-	Minimal and target: Still to be tested
4	Precision error of TC measurement	$\leq 5\%$	$\leq 1\%$	$\leq 5\%$	Only minimal: Test-based: yes.
5	Sample dimensions needed for measurement	100 x 100 mm ²	Keep textile intact	140 x 140 mm ²	Minimal and target: Design-based: no
6	Setup time	< 5 minutes		< 4 minutes	Test-based: yes;
7	Measurement time	< 90 minutes	< 30 minutes	30 minutes; SS in < 6.94 minutes	Minimal and target: Test-based: yes

	Requirement	Minimal	Target	Verified	Satisfied?
8	Lifetime without recalibration	≥ 3 months	≥ 12 months	-	Minimal: Test-based: expected
Physical parameters					
9	Decontamination	The device should allow frequent (up to 5 times a day) cleaning with agents based on alcohol and with RNA purification products and should otherwise be partly disposable.		-	Still to be tested
10	Shielding	The measurements should be performed in an environment without external influences from wind, water, changing temperatures (max ± 5°C) or thermal radiation.		Measurements were performed in a laboratory environment.	Design-based: yes
11	Power supply	The device should allow powering by a common 230V-16A AC wall outlet.	The device should allow powering by either batteries and/or a 12V-10A DC (car) outlet as well as by a 230 V-16A DC (CS van).	The device was powered through a common wall outlet.	Minimal: Design-based: yes
12	Robustness	The encased device should meet the test for rough handling shocks (NEN-EN-IEC 60069-2-31:2008) and (non)repetitive shocks (NEN-EN-IEC 60068-2-27:2008).		-	Still to be tested
13	Mobility	Dimensions ≤ 330x330x330 mm and weight ≤ 8 kg.	Dimensions ≤ 250x250x250 mm and weight ≤ 2 kg.	320x180x170 mm³ and 1.59 kg**	Minimal: Design-based: yes
User interface					
14	Results communication	The device should deliver both a file with the raw measurement data and a PDF with an description of the measurement and its outcome*.		-	Still to be tested
15	Simplicity	The device should be intuitive and fit to use for forensic investigators and/or forensic investigation Police employees.		-	Still to be tested
Others					
16	Costs per device	≤ €1.945 euros		€685,87 euros	In current prototvpe: satisfied

*: The outcome of the measurement should at least contain determined k-value [W/mK], sample thickness [mm] and time in which a steady state measurement was established [minutes].

* Displayed size and weight is including the electronics and their housing.

7.3 Limitations

The focus of this thesis was to develop a well-performing prototype in terms of accuracy and precision. The requirements for precision are met while the accuracy of Therminus-K2 could not yet be quantified. Due to the focus on performance, the device's major limitation is that it currently is not yet applicable for use in forensic practice. The user interface still needs major improvements prior to using it during CSI processes.

Limitations of the performance of Therminus-K2 are:

In the current prototype, the measurement uncertainty of sample thickness is the highest of all input parameters. An uncertainty in sample thickness might result in up to 16.7% error in k-value. This highly affects the accuracy of Therminus-K2. However, the actual accuracy of Therminus-K2 could not be quantified as the actual k-value of the measured samples was not known. As the performed sample compression test in section 6.3.2 could not differentiate the expected effect of sample

compression on calculated k-value, this uncertainty might even be an underestimation (section 6.3.2 Sample Compression Test).

In the current Therminus-K2 configuration, the cold plate always exceeded the environment temperature by about 2 °C and slightly fluctuated over time. As a consequence, the target temperature difference over the sample was never reached and the temperature difference fluctuated over time. This resulted the measurements being only a short time (5.25 – 15.65 minutes) of the total measurement (30 minutes) in steady state.

The reason for the unstable heating of the Peltier elements was that these elements couldn't cool hard enough: the heat produced by the Peltier element was not enough dissipated to the environment. Another cause of the short period in which the system was in steady state might be due to the noise in sensor data. This resulted in need for filtering sensor and PWM output data. Especially as noise in sensor data translates to noise in PWM output data, this might have affected the steady state period.

Furthermore, the resolution of PWM signals that can be outputted is quite small (8 bits). This limits the resolution in which the heaters and Peltier elements can be controlled.

In general, it should be considered that only three or five repetitions per sample and per tested variable were performed.

7.4 Recommendations

Accuracy

The accuracy of Therminus-K2 should be determined by measuring samples both with Therminus-K2 and with an ISO classified TC measurement device as reference (**Requirement 3**). However, it is recommended to investigate the effect of the calculated k-value of a real textile sample that surrounded a deceased on the achieved PMI by inputting it in the PHOEBE model. Then, these PMI outcomes could be compared to those achieved without using Therminus-K2 to determine the k-value of the textile samples. These results may show the impact of using Therminus-K2 on the achieved PMI, which will hopefully substantiate the need for a TC measurement device in the PHOEBE model. However, this validation could not be performed within the available time for this thesis.

It is recommended to improve the sample thickness measurement, having the highest measurement uncertainty, in order to increase the accuracy and precision of Therminus-K2. An automatized method to measure the thickness of the tested sample should be used. Automatic distance or displacement sensors between the plates (**Table 2**) would remove inter- and intra-observer bias that is created when using a digital caliper and improve the ease of use of the device (**Requirement 15**). However, this feature was not yet implemented due to the time constraint of the project.

It is recommended to repeat the fabric compression test when using automatic methods to determine sample thickness. Furthermore, it should be elucidated which state of sample compression should be used during measurements. This should ideally correspond with the compression state in which the textile layers surrounded the deceased. In practice, adding a possibility for adjustable fabric compression may be an additional new requirement for an improved prototype.

Furthermore, the assumption about the conversion from the PWM signal (based on a PID control) to the power outputted by the main heater should be validated. If this assumption is invalid, a INA260 current-voltage-power sensor or another method to determine the power should be used in the TC calculation [83].

Besides this, it is recommended to aim for a larger temperature difference between the hot and the cold plate, which would result in a smaller effect of the temperature sensor uncertainty (**section 6.2**). This should however be carefully considered, as a larger temperature difference would need a longer time to be reached, which would increase the total measurement time (**Requirement 7**). Therefore, temperature sensors with higher accuracies might be used, when small temperature difference are tested.

Precision

With a precision of $\leq 5\%$, Terminus-K2 is close to the 2% overall measurement uncertainty that can be obtained with GHP measurements according to the ASTM (section 2.1) [60]. In order to reach the target precision of $\leq 1\%$ as set in **Requirement 4**, multiple improvements may be applied:

At first, the sources of the sharp transients in temperature data should be identified and eliminated. During measurement, it seemed likely that the Peltier element configuration affected the high transients in temperature data. Shielded Twisted Pair (STP) cabling may reduce electromagnetic radiation from the pair and crosstalk between neighboring pairs. Furthermore, STP cabling improves rejection of external electromagnetic interference (EMI).

Secondly, the cooling of the Peltier elements may be improved or another cooling solution may be used. To allow the Peltier elements for better and more stable cooling of the cold plate, it must be ensured that the heat produced by the Peltier elements can better dissipate to the environment. This could be achieved by using water-cooled CPU coolers that are used in desktop computers. Then, both a higher precision (**Requirement 4**) and a shorter measurement time (**Requirement 7**) may be achieved.

It is recommended to use an Arduino Due instead of an Arduino Mega, as in the Arduino Due the default 8-bit PWM can be changed to a 12-bit resolution [84]. This would result in a higher output resolution and might result in a higher overall measurement accuracy and precision.

Other performance requirements

More textile samples should be tested to verify the full range of k-values that the Terminus-K2 can measure and identify (**Requirement 1 + 2**). The k-values and thicknesses of these samples should be spread over the full range of allowable values predetermined by the specifications of the Terminus-K2 prototype (section 5.2.4).

To reduce the sample dimensions needed for testing, one may use heaters with smaller, customized dimensions (**Requirement 5**). However, smaller heaters would reduce the allowable sample thicknesses that can be measured (**Requirement 2**). Therefore, a tradeoff should be made in importance of these requirements.

The lifetime of the device without need for recalibration (**Requirement 8**) should still be determined. Preventively, the electronics housing may be improved to ensure shielding of the MOSFETs against static electricity and prolong the devices lifetime. Currently, an anti-electrostatic mat and an anti-electrostatic wristband are used to prevent this, which are not practical for use by forensic investigators at a crime scene.

Requirements for physical parameters, user interface and costs

There is a great deal to be gained in these requirements (**Requirement 9 – 16**) prior to implementing the use of Terminus-K2 during CSI processes. The prototype first needs to be further developed before these requirements are to be tested.

8. CONCLUSION

This study aimed to design, develop and test a fast (< 90 minutes), accurate ($\leq 8\%$) and precise ($\leq 5\%$) measurement device that can determine the thermal conductivity coefficient (k-value) of textile layers at or around a crime scene and deliver measurements fit for use in the PHOEBE cooling model. It was investigated whether this design goal could be achieved with a simple and inexpensive solution.

Through multiple design steps the Terminus-K2 prototype was developed. This device, based on the Guarded Hot Plate technique, uses a back heater and four guard heaters to ensure all heat generated by the main heater only flows one dimensionally through the textile sample. The developed prototype, only using simple and low-cost components, was tested on textile samples (0.6 – 8 mm thick) and identified k-values from 0.031 – 0.257 W/mK, with high precision ($\leq 5\%$) within a short measurement time (30 minutes). Within an even shorter period (≤ 6.94 minutes), the system reaches its first moment of steady state.

All in all, Terminus-K2 gives impressive results in thermal conductivity calculation. It delivers precise, fast and affordable measurements of the thermal conductivity coefficients of textile samples. After a subsequent design phase in which the user friendliness of Terminus-K2 is further improved, the device will show great promise for future implications: using the output of this device in the PHOEBE model to determine the early Post Mortem Interval of a victim at a crime scene.

All supplementary data that is used during this project is combined on a flash drive that is in possession of dr. ir. A.J. Loeve from the 17th of June 2022 onward.

REFERENCES

- [1] CBS. (2021, 18-04-2022). *Overledenen; belangrijke doodsoorzaken (korte lijst), leeftijd, geslacht*. Available: https://opendata.cbs.nl/statline/?ts=1583417518325#/CBS/nl/dataset/7052_95/table
- [2] A. Hendrix *et al.*, *De opsporing verdient sporen*. Politie, 2018.
- [3] R. Shrestha, T. Kanchan, and K. Krishan, "Methods Of Estimation Of Time Since Death," in *StatPearls* Treasure Island (FL), 2021.
- [4] C. Henssge and B. Madea, "Estimation of the time since death in the early post-mortem period," *Forensic Sci Int*, vol. 144, no. 2-3, pp. 167-75, Sep 10 2004.
- [5] C. Henssge, "Death time estimation in case work. I. The rectal temperature time of death nomogram," *Forensic Sci Int*, vol. 38, no. 3-4, pp. 209-36, Sep 1988.
- [6] L. S. Wilk *et al.*, "Reconstructing the time since death using noninvasive thermometry and numerical analysis," *Sci Adv*, vol. 6, no. 22, p. eaba4243, May 2020.
- [7] C. I. Kaanen, "A Systematic Review on Factors Affecting the Thermal Conductivity Measurement of Clothing in a Forensic Context," Delft University of Technology 2021.
- [8] L. Hes, M. Manáková, and O. Paraska, "The effect of long time wears on thermal comfort properties of various parts of denim trousers," *J Textile Sci Eng*, vol. 11, 2021.
- [9] O. I. Kalaoglu-Altan, B. K. Kayaoglu, and L. Trabzon, "Improving thermal conductivities of textile materials by nanohybrid approaches," *iScience*, vol. 25, no. 3, p. 103825, Mar 18 2022.
- [10] H. Shen, A. Yokoyama, and S. Sukigara, "Modelling of heterogeneous heat transfer in fabrics," *Textile Research Journal*, vol. 88, no. 10, pp. 1164 - 1172, 2018.
- [11] M. Azeem, L. Hes, J. Wiener, and M. Noman, "Comfort properties of nano-filament polyester fabrics: Thermo-physiological evaluation," *Industria Textila*, vol. 69, no. 4, pp. 315 - 321, 2018.
- [12] V. Arumugam, R. Mishra, J. Militky, and D. Křemenáková, "Effect of 3-dimensional knitted spacer fabric characteristics on its thermal and compression properties," *Vlakna a Textil*, vol. 23, no. 3, pp. 22 - 29, 2016.
- [13] Y. El-Hage, S. Hind, and F. Robitaille, "Thermal conductivity of textile reinforcements for composites," *Journal of Textiles and Fibrous Materials*, vol. 1, 2018.
- [14] B. Wei, N. Yang, M. Tian, L. Qu, and S. Zhu, "Effect of coating methods on thermal conductivity of graphene-coated fabrics for welding protective clothing," *Materials Letters*, vol. 314, 2022.
- [15] Lambda-Meßtechnik. (17-09-2021). *Design and Function of the Guarded Hot Plate Apparatus*. Available: <https://www.lambda-messtechnik.de/en/thermal-conductivity-test-tool-ep500e/guarded-hot-plate-apparatus-lambda-meter-ep500e-design-and-function>
- [16] Lambda-Meßtechnik. (17-09-2021). *Characteristics and Operations Scope of the Thermal Conductivity Test Tool λ-Meter EP500e*. Available: <https://www.lambda-messtechnik.de/en/thermal-conductivity-test-tool-ep500e/lambda-meter-ep500-characteristics>
- [17] Thermtest. (17-09-2021). *100 SERIES HEAT FLOW METER Thermal Conductivity Measurement System*. Available: <https://thermtest.com/heat-flow-meter>
- [18] HotDisk®. (2021, 08-10-2021). *TPS 3500*. Available: <https://www.hotdiskinstruments.com/products-services/instruments/tps-3500/>
- [19] C-Therm. (2021, 08-10-2021). *TRIDENT: 1 instrument, 3 methods for thermal conductivity*. Available: <https://ctherm.com/thermal-conductivity-instruments/trident/>
- [20] S. Drommel, W. Van den Hoed, Y. Zabel, and H. De Zwart, "Portable Instrument to get One-Sided Measurements of the Heat Flux for Unknown Support Surfaces," Bachelor Thesis, Engineering for Forensics, Delft University of Technology, Delft, 2015.
- [21] O. Dassing, "Surface testing methods to define thermal properties of surfaces at crime scenes," Internship Report, Department of BioMedical Engineering, Delft University of Technology, Delft, 2018.
- [22] M. Stolk, C. Ramsey, B. Tantuo, and J. R. Vijayaragavan, "Improving the ToD estimate by measuring thermal conductivity," Bachelor Thesis, BioMedical Engineering, Delft University of Technology, Delft, 2019.

- [23] M. Cañones Castellano, T. Elzer, D. Jokic, and K. Rijnders, "Determining Thermal Conductivity of Textiles for Forensic Investigations," *BioMedical Engineering*, Delft University of Technology, Delft, 2019.
- [24] I. S. Best, N. S. Noort, S. T. Njio, J. M. Van Schijndel, and F. M. Verhage, "Measuring thermal conductivity of textiles for time of death estimation," Bachelor Thesis, Engineering for Forensics, Delft University of Technology, Delft, 2019.
- [25] M. Van der Helm, "Measuring thermal conductivity of textiles for a more accurate time of death estimation," Internship Report, Engineering for Forensics, Delft University of Technology, Delft, 2021.
- [26] E. Klemenčič, D. Zavec, and M. Slavinec, "Modelling the impact of moisture on the thermal conductivity of cotton jersey," *Fibres and Textiles in Eastern Europe*, Article vol. 29, no. 2, pp. 61-65, 2021.
- [27] F. L. Zhu, "Investigating the effective thermal conductivity of moist fibrous fabric based on Parallel-Series model: A consideration of material's swelling effect," *Materials Research Express*, Article vol. 7, no. 4, 2020, Art. no. 045308.
- [28] W. Wang *et al.*, "A study of thermal conductivity property of socks," in *Materials Science Forum* vol. 1007 MSF, ed, 2020, pp. 118-124.
- [29] E. Akcagun, M. Bogusławska-Bączek, and L. Hes, "Thermal insulation and thermal contact properties of wool and wool/PES fabrics in wet state," *Journal of Natural Fibers*, Article vol. 16, no. 2, pp. 199-208, 2019.
- [30] A. Boughattas, S. Benltoufa, L. Hes, M. Azeem, and F. Fayala, "Thermo-physiological properties of woven structures in wet state," *Industria Textila*, Article vol. 69, no. 4, pp. 298-303, 2018.
- [31] M. Bogusławska-Bączek and L. Hes, "Thermophysiological properties of dry and wet functional sportswear made of synthetic fibres," *Tekstilec*, Article vol. 60, no. 4, pp. 331-338, 2017.
- [32] R. R. Van Amber, C. A. Wilson, R. M. Laing, B. J. Lowe, and B. E. Niven, "Thermal and moisture transfer properties of sock fabrics differing in fiber type, yarn, and fabric structure," *Textile Research Journal*, Article vol. 85, no. 12, pp. 1269-1280, 2015.
- [33] S. Karunamoorthy and A. Das, "Study on thermal resistance of multilayered fabrics under different compressional loads," *Journal of the Textile Institute*, Article vol. 105, no. 5, pp. 538-546, 2014.
- [34] M. Bogusławska-Bączek and L. Hes, "Thermal conductivity and resistance of nomex fabrics exposed to salty water," *Tekstil ve Konfeksiyon*, Article vol. 24, no. 2, pp. 180-185, 2014.
- [35] M. Naebe, N. Robins, X. Wang, and P. Collins, "Assessment of performance properties of wetsuits," *Proceedings of the Institution of Mechanical Engineers, Part P: Journal of Sports Engineering and Technology*, Article vol. 227, no. 4, pp. 255-264, 2013.
- [36] D. Romeli, G. Barigozzi, S. Esposito, G. Rosace, and G. Salesi, "High sensitivity measurements of thermal properties of textile fabrics," *Polymer Testing*, Article vol. 32, no. 6, pp. 1029-1036, 2013.
- [37] R. Zhang, J. Li, J. Xu, and J. Liu, "Dynamic heat conductivity property of fabrics," in *Advanced Materials Research* vol. 332-334, ed, 2011, pp. 845-849.
- [38] N. Nawaz, O. Troynikov, and C. Watson, "Thermal comfort properties of knitted fabrics suitable for skin layer of protective clothing worn in extreme hot conditions," in *Advanced Materials Research* vol. 331, ed, 2011, pp. 184-189.
- [39] N. Oğlakcioğlu and A. Marmarali, "Thermal comfort properties of cotton knitted fabrics in dry and wet states," *Tekstil ve Konfeksiyon*, Article vol. 20, no. 3, pp. 213-217, 2010.
- [40] T. Ramachandran, G. Manonmani, and C. Vigneswaran, "Thermal behaviour of ring- and compact-spun yarn single jersey, rib and interlock knitted fabrics," *Indian Journal of Fibre and Textile Research*, Article vol. 35, no. 3, pp. 250-257, 2010.
- [41] C. Vigneswaran, K. Chandrasekaran, and P. Senthilkumar, "Effect of thermal conductivity behavior of jute/cotton blended knitted fabrics," *Journal of Industrial Textiles*, Article vol. 38, no. 4, pp. 289-307, 2009.

- [42] T. Dias and G. B. Delkumburewatte, "The influence of moisture content on the thermal conductivity of a knitted structure," *Measurement Science and Technology*, Article vol. 18, no. 5, pp. 1304-1314, 2007, Art. no. 016.
- [43] F. Zhu and W. Zhang, "Measuring the thermal conductive property of protective fabrics to radiant heat exposure," *Journal of Industrial Textiles*, Article vol. 37, no. 2, pp. 175-186, 2007.
- [44] L. Hes, M. de Araujo, and V. V. Djulay, "Effect of Mutual Bonding of Textile Layers on Thermal Insulation and Thermal Contact Properties of Fabric Assemblies," *Textile Research Journal*, Article vol. 66, no. 4, pp. 245-250, 1996.
- [45] A. M. Schneider, B. N. Hoschke, and H. J. Goldsmid, "Heat Transfer through Moist Fabrics," *Textile Research Journal*, Article vol. 62, no. 2, pp. 61-66, 1992.
- [46] H. J. Hoge and G. F. Fonseca, "The Thermal Conductivity of a Multilayer Sample of Underwear Material under a Variety of Experimental Conditions," *Textile Research Journal*, Article vol. 34, no. 5, pp. 401-410, 1964.
- [47] J. B. Speakman and N. H. Chamberlain, "The thermal conductivity of textile materials and fabrics," *J Text Inst Trans*, vol. 21, no. 2, pp. 29 - 56, 1930.
- [48] E. S. Rood, "Thermal conductivity of some wearing materials," *Physical Review*, Article vol. 18, no. 5, pp. 356-361, 1921.
- [49] *NEN-EN-IEC 60068-2-31 Environmental testing - Part 2-31: Tests - Test Ec: Rough handling shocks, primarily for equipment-type specimens*, IEC, 2008.
- [50] *NEN-EN-IEC 60068-2-27 Environmental testing - Part 2-27: Tests - Test Ea and guidance: Shock*, IEC, 2008.
- [51] A. A.R.R., Z. Skenderi, B. Kolcavová, and A. A. S. Khalil, "Analysis of Factors Affecting Thermal Comfort Properties of Woven Compression Bandages," *Autex Research Journal*, vol. 20, no. 2, pp. 178 - 185, 2020.
- [52] H. Shen *et al.*, "Analysis of heat transfer characteristics in textiles and factors affecting thermal properties by modeling," *Textile Research Journal*, Article vol. 89, no. 21-22, pp. 4681-4690, 2019.
- [53] M. O. R. Siddiqui and D. Sun, "Thermal analysis of conventional and performance plain woven fabrics by finite element method," *Journal of Industrial Textiles*, Article vol. 48, no. 4, pp. 685-712, 2018.
- [54] M. M. Mangat, L. Hes, and V. Bajzík, "Thermal resistance models of selected fabrics in wet state and their experimental verification," *Textile Research Journal*, Article vol. 85, no. 2, pp. 200-210, 2015.
- [55] Z. E. Kanat, N. Özdil, and A. Marmarali, "Prediction of thermal resistance of the knitted fabrics in wet state by using multiple regression analysis," *Tekstil ve Konfeksiyon*, Article vol. 24, no. 3, pp. 291-297, 2014.
- [56] M. Bogusławska-Baczek and L. Hes, "Determination of heat transfer by radiation in textile fabrics by means of method with known emissivity of plates," *Journal of Industrial Textiles*, Article vol. 44, no. 1, pp. 115-129, 2014.
- [57] D. Gupta, A. Srivastava, and S. Kale, "Thermal properties of single and double layer fabric assemblies," *Indian Journal of Fibre and Textile Research*, Article vol. 38, no. 4, pp. 387-394, 2013.
- [58] *C177-19 Standard Test Method for Steady-State Heat Flux Measurements and Thermal Transmission Properties by Means of the Guarded-Hot-Plate Apparatus*, 2019.
- [59] N. Yüksel, "The Review of Some Commonly Used Methods and Techniques to Measure the Thermal Conductivity of Insulation Materials," in *Insulation Materials in Conext of Sustainability*: INTECH, 2016, pp. 113 - 140.
- [60] S. L. Dubois, F., "Design, Construction and Validation of a Guarded Hot Plate Apparatus for Thermal Conductivity Measurement of High Thickness Crop-Based Specimens," *Mater Struct*, vol. 48, pp. 407 - 421, 2015.
- [61] (2015). *Measuring Temperature Accurately with Semiconductor Sensors*. Available: <https://www.rs-online.com/designspark/measuring-temperature-accurately-with-semiconductor-sensors>

- [62] W. Yang, J. Liu, Y. Wang, and S. Gao, "Experimental study on the thermal conductivity of aerogel-enhanced insulating materials under various hygrothermal environments," *Energy and Buildings*, vol. 206, 2020.
- [63] C. Prakash and R. Govindan, "Effect of Blend Ratio, Loop Length, and Yarn Linear Density on Thermal Comfort Properties of Single Jersey Knitted Fabrics," *Int J Thermophys*, vol. 34, 2013.
- [64] I. Frydrych, G. Dziworska, and J. Biliska, "Comparative Analysis of the Thermal Insulation Properties of Fabrics Made of Natural and Man-Made Cellulose Fibres," *Fibres and Textiles in Eastern Europe*, pp. 40 - 44, 2002.
- [65] S. Krzeminska, A. Greszta, and P. Miskiewicz, "Characterization of heat protective aerogel-enhanced textile packages," *International Journal of Heat and Technology*, Article vol. 38, no. 3, pp. 659-672, 2020.
- [66] (2017, 2022-05-01). 6061 vs 7075. Available: <https://www.clintonaluminum.com/6061-vs-7075/#:~:text=Its%20thermal%20conductivity%20is%20rated%20at%20130%20W%2Fm-K,is%20one%20of%20the%20strongest%20aluminum%20alloys%20available.>
- [67] Y. Q. Li, K. Y. Liang, J. J. Wang, and X. B. Huang, "Research progress of mesoporous silica-based composite phase change materials," *Gongcheng Kexue Xuebao/Chinese Journal of Engineering*, Article vol. 42, no. 10, pp. 1229-1243, 2020.
- [68] M. Ali *et al.*, "Thermal and acoustic characteristics of novel thermal insulating materials made of Eucalyptus Globulus leaves and wheat straw fibers," *Journal of Building Engineering*, Article vol. 32, 2020, Art. no. 101452.
- [69] R. Toulson and T. Wilmshurst, "Chapter 4: Analog Output," in *Fast and Effective Embedded Systems Design* Newnes: Elsevier, 2012, pp. 57 - 75.
- [70] iPolymer. (20-04-2022). POLYCARBONATE. Available: <https://www.ipolymer.com/pdf/Polycarbonate.pdf>
- [71] ProfessionalPlastics. (20-04-2022). *Thermal Properties of Plastic Materials*. Available: <https://www.professionalplastics.com/professionalplastics/ThermalPropertiesofPlasticMaterials.pdf>
- [72] MatWeb. (20-04-2022). *Overview of materials for Polycarbonate, Extruded*. Available: <https://www.matweb.com/search/DataSheet.aspx?MatGUID=501acbb63cbc4f748faa7490884cdbc&ckck=1>
- [73] X. H. Li, M. Z. Chen, and X. Y. Zhou, "Research progress in encapsulation and application of shape-stabilized composite phase-change materials," *Gongcheng Kexue Xuebao/Chinese Journal of Engineering*, Article vol. 42, no. 11, pp. 1422-1432, 2020.
- [74] H. Zhou, S. Zhang, and M. Yang, "The Thermal Conductivity of Nylon 6/Clay Nanocomposites," *Journal of Applied Polymer Science*, vol. 108, no. 6, pp. 3822 - 3827, 2008.
- [75] M. Li, Y. Wan, G. Xiong, X. Wang, C. Wan, and H. Luo, "Preparation and properties of polyamide 6 thermal conductive composites reinforced with fibers," *Materials and Design*, vol. 51, pp. 257 - 261, 2013.
- [76] A. Abbas, Y. Zhao, J. Zhou, X. Wang, and T. Lin, "Improving Thermal Conductivity of Cotton Fabrics Using Composite Coatings Containing Graphene, Multiwall Carbon Nanotube or Boron Nitride Fine Particles " *Fibers and Polymers*, vol. 14, pp. 1641 - 1649, 2013.
- [77] A. Islam, M. Rokonzaman, and Z. Hasan, "Analysis on thermal comfortability of different three thread fleece fabric," *International Journal of Current Engineering and Technology*, vol. 8, pp. 1675 - 1678, 2018.
- [78] S. Alay, F. Gode, and C. Alkan, "Steady-state thermal comfort properties of fabrics incorporated with microencapsulated phase change materials," *Journal of the Textile Institute*, vol. 103, pp. 757 - 765, 2012.
- [79] A. Boughattas, S. Benltoufa, L. Hes, M. Azeem, and F. Fayala, "Thermo-physiological properties of woven structures in wet state," *Industria Textila*, vol. 69, 2018.
- [80] *Managing Errors and Uncertainty*.
- [81] M. Boguslawska-Bączek and L. Hes, "Thermophysiological properties of dry and wet functional sportswear made of synthetic fibers," *Tekstilec*, vol. 60, no. 4, pp. 331 - 338, 2017.
- [82] W. E. Morton and J. W. S. Hearle, "Physical Properties of Textile Fibres, Fourth Edition," *Physical Properties of Textile Fibres, Fourth Edition*, vol. 68, pp. 1 - 776, 2008.

- [83] *INA260 Precision Digital Current and Power Monitor With Low-Drift, Precision Integrated Shunt*, 2016.
- [84] (2022, 2022-05-22). *analogWriteResolution()*. Available:
<https://www.arduino.cc/reference/en/language/functions/zero-due-mkr-family/analogwriteresolution/>

APPENDICES

A. Extension to the Morphologic Chart: sub-solutions to Position Textile Sample



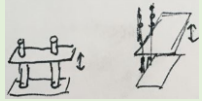
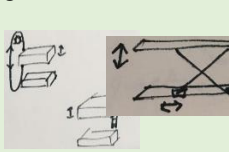
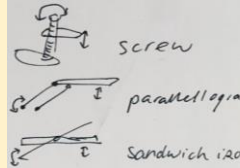



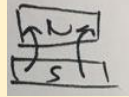

Sub-solutions → Sub-functions ↓		1	2	3	4
Position textile sample	Insert textile sample	Sleeve 	Cut and insert 	Adaptable (both sleeving and cutting possibilities)	
	Clamp sample between measuring plates	Linear with standing guidance 	Linear with moving guidance 	Rotational parallel clamping 	Rotational angular clamping (scissors) 
	Fixate clamping compression	Friction grip (e.g. springs, belts, screw clamp) 	Shape grip (e.g. cable belt, rack & pinion, lead screw) 	Magnetic forces 	Electrostatic forces 

Table 11. Sketch of an extension to the Morphologic Chart in **Table 2**. Solutions on how to position a textile sample within a TC measurement device are suggested.

B. Established Temperature Distributions in Simulation 4.2

Below the results of simulation 4.2 showing the temperature distribution across the Al7075 plate and the cotton sample (which is situated below the Al plate) are displayed. Both Al7075 plate thickness and cotton sample thickness are varied.

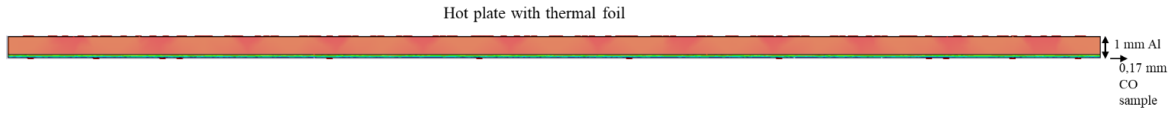


Figure 37. Cross-section of the steady state temperature distribution in a thermal foil – Al7075 plate (1 mm) – cotton sample (0.17 mm) configuration.

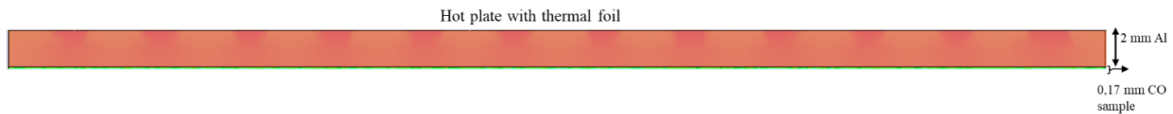


Figure 38. Cross-section of the steady state temperature distribution in a thermal foil – Al7075 plate (2 mm) – cotton sample (0.17 mm) configuration.

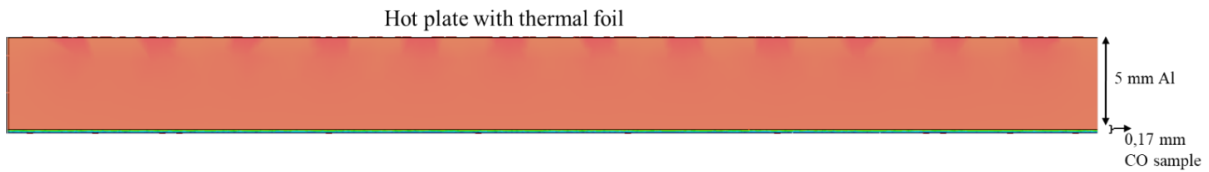


Figure 39. Cross-section of the steady state temperature distribution in a thermal foil – Al7075 plate (5 mm) – cotton sample (0.17 mm) configuration.

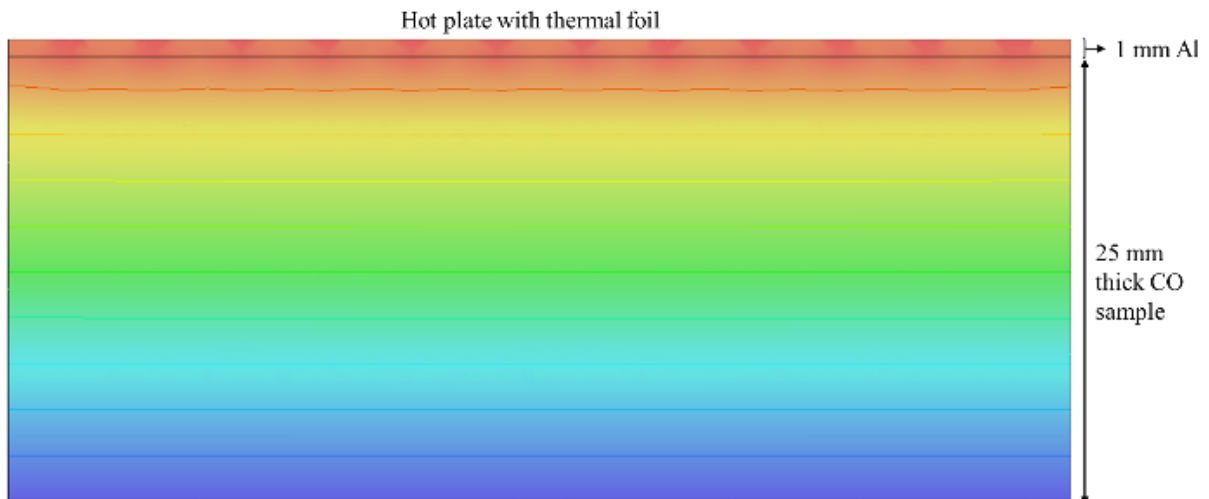


Figure 40. Cross-section of the steady state temperature distribution in a thermal foil – Al7075 plate (1 mm) – cotton sample (25 mm) configuration.

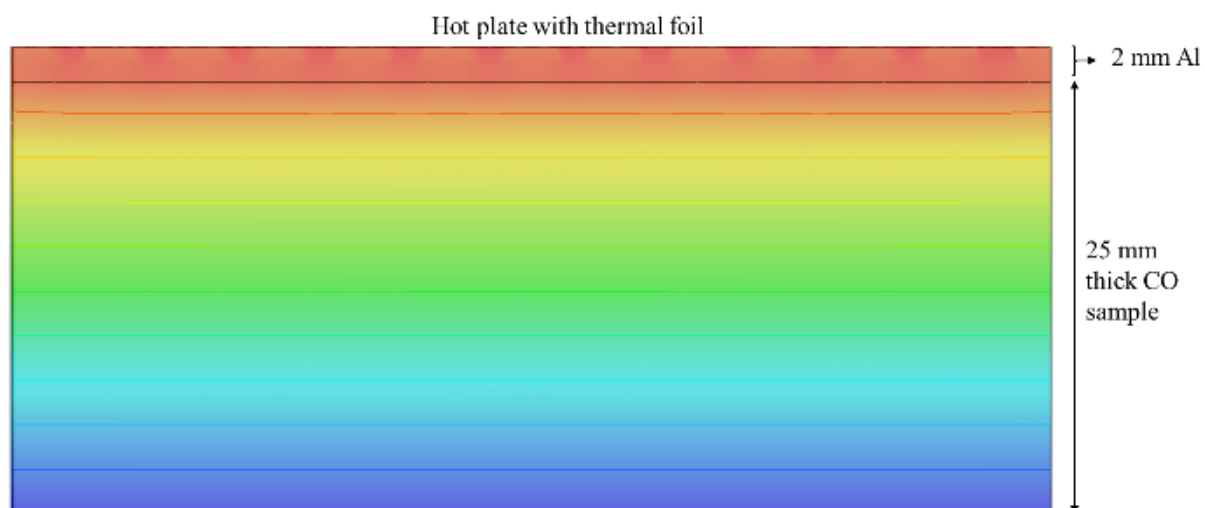


Figure 41. Cross-section of the steady state temperature distribution in a thermal foil – Al7075 plate (2 mm) – cotton sample (25 mm) configuration.

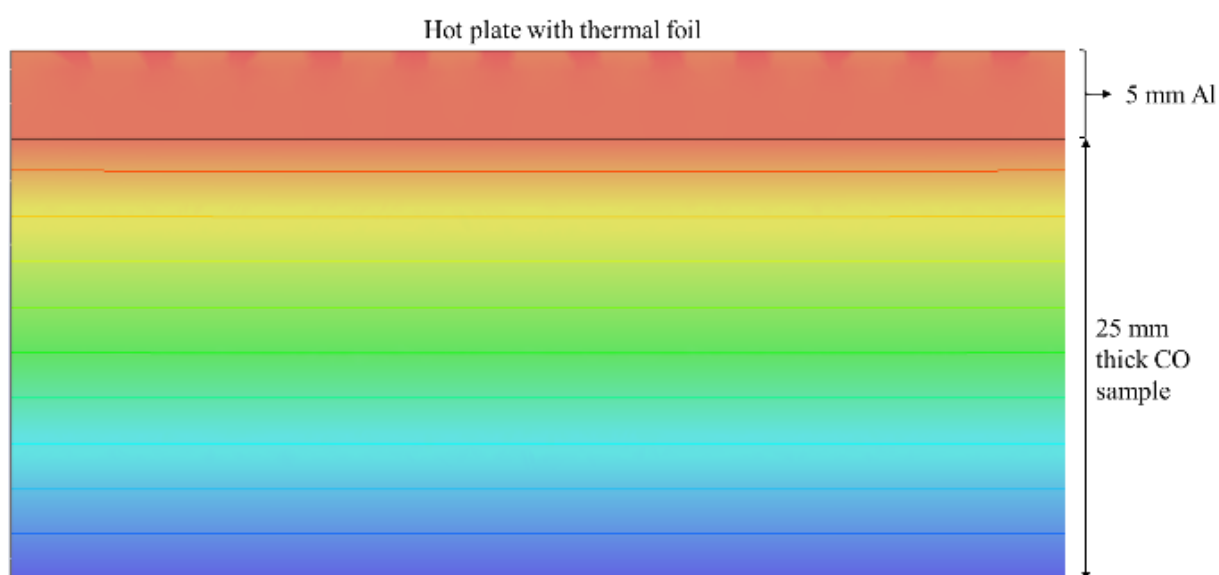


Figure 42. Cross-section of the steady state temperature distribution in a thermal foil – Al7075 plate (5 mm) – cotton sample (25 mm) configuration.

C. Preparation, Calibration and Validation of the Temperature Sensors

Introduction

Thin (film) temperature sensors are needed in the control loop to regulate the temperatures at the hot and cold surface plates near the sample. The resistance of the NTC thermistors decreases with increasing temperature, making them easy and straightforward to use. Prior to using these temperature sensors in the prototype, they should be calibrated. Therefore, the goal of this procedure is to achieve calibrated temperature sensors that can be used in the Thermins-K2 prototype. Furthermore, the calibration of these temperature sensors will be validated.

Method

First, the temperature sensors were prepared to be used in an electronic circuit (see *Procedure Protocol A* below). Then, the prepared sensors were calibrated in water baths with constant temperatures (18 – 40 °C, increment steps of ± 2 °C), see *Procedure Protocol B*. Finally, the calibrated sensors were validated (*Procedure Protocol C*).

Sensor calibration was performed on 12 NTC sensors. In the Therminus-K2 prototype, at least 9 sensors will be needed.

Procedure protocol

A. Sensor preparation

1. Label the NTCs (1 – 12)
2. Solder stranded wires (blue and red, \varnothing 0.5 mm, length 200 mm) to the NTCs (max soldering temperature of 260 °C)
3. Crimp insulating material around the newly made connections
4. Connect the temperature sensors to a soldered circuit board (see **Figure 43**)
5. Connect the soldered circuit board to an Arduino (e.g. Mega 2560)

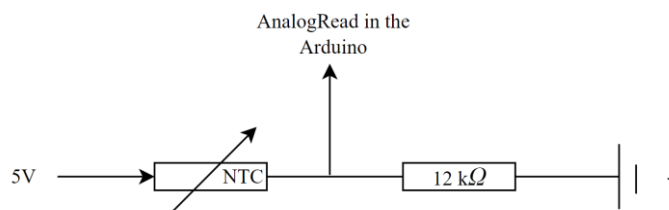


Figure 43. Schematic and Actual Temperature sensor configuration. The 5V (max 500 mA) signal from the Arduino board first crosses the NTC (variable resistor) and then either goes back to the Arduino (AnalogRead to read output voltage) or continues via a constant resistor (12k Ω) to the ground.

B. Sensor calibration

6. Open LabView 2018 (National Instruments)
7. Open temp 3x.vi in LabView
8. Set the reference thermocouples ($n = 3$) at the right environment temperature (cjc value)
9. Make sure all temperature sensors are well connected to the soldered circuit board and the Arduino
10. Connect the Arduino to a laptop and open the Arduino Software
11. Open TemperatureSensor-Calibration.ino
12. Open the Serial Monitor in Arduino Software
13. Set a cup with water (200 mL) on an electric hot stirring plate
14. Put the reference thermocouples ($n = 2$) and the to be calibrated temperature sensors ($n = 12$) in the water. Make sure all are electrically insulated.
15. Report the temperature determined by the reference thermocouples
16. Make sure the Serial Monitor is continuously displaying the output voltages of all individual temperature sensors.

17. Add some hot water to the water bath and let the temperature increase with about 2 °C until a steady temperature is reached (**Figure 44**).
18. Repeat steps 15 – 17 until a final temperature of 40 °C is reached.
19. Save data at temperatures of interest in an Excel file: Calibration_TemperatureSensors_Vout_20220419.xlsx
20. Open the Excel file Calibration_TemperatureSensors_Vout_20220419.xlsx in the MATLAB file Temperature_sensor_calibration_20220419.m
21. The MATLAB file interpolates the determined data points and a formula for the fitted Vout – Temperature polynoma per temperature sensor will be outputted
22. Implement the output formulas in the Arduino code: TemperatureSensor-Validation.ino

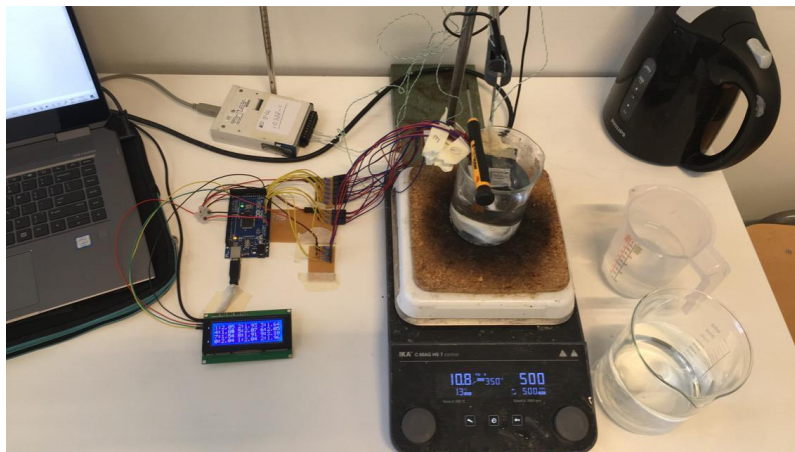


Figure 44. Set up used for calibration of temperature sensors.

C. Sensor validation

23. Repeat steps 6 to 10
24. Open TemperatureSensor-Validation.ino
25. Repeat steps 12 to 17
26. Save data at the temperatures of interest in an Excel file: Validation_TemperatureSensors_20220419.xlsx
27. Open the Excel file Validation_TemperatureSensors_20220419.xlsx in the MATLAB file Temperature_sensor_validation_20220419.m
28. The MATLAB file return the RMSE plots for the temperature sensors and the sensors performing best can be selected to use in the Therminus-K2 prototype.

Results

The results of the preparation, calibration and validation of the 12 temperature sensors is shown in **Figure 45**, **Figure 46**, **Figure 47**, **Figure 48** and **Figure 49**.

Discussion

In temperature sensor validation, the errors of the temperature sensors in relation to temperature sensor 4 were smallest. As it is most important the temperature sensors are accurate in relation to each other, this temperature sensor is used to perform a RMSE plot on for the other sensors.

The 9 sensors having the lowest errors in relation to sensor 4 were used in Therminus-K2. Most of these temperature sensors deviated less than ± 0.2 °C from each other.

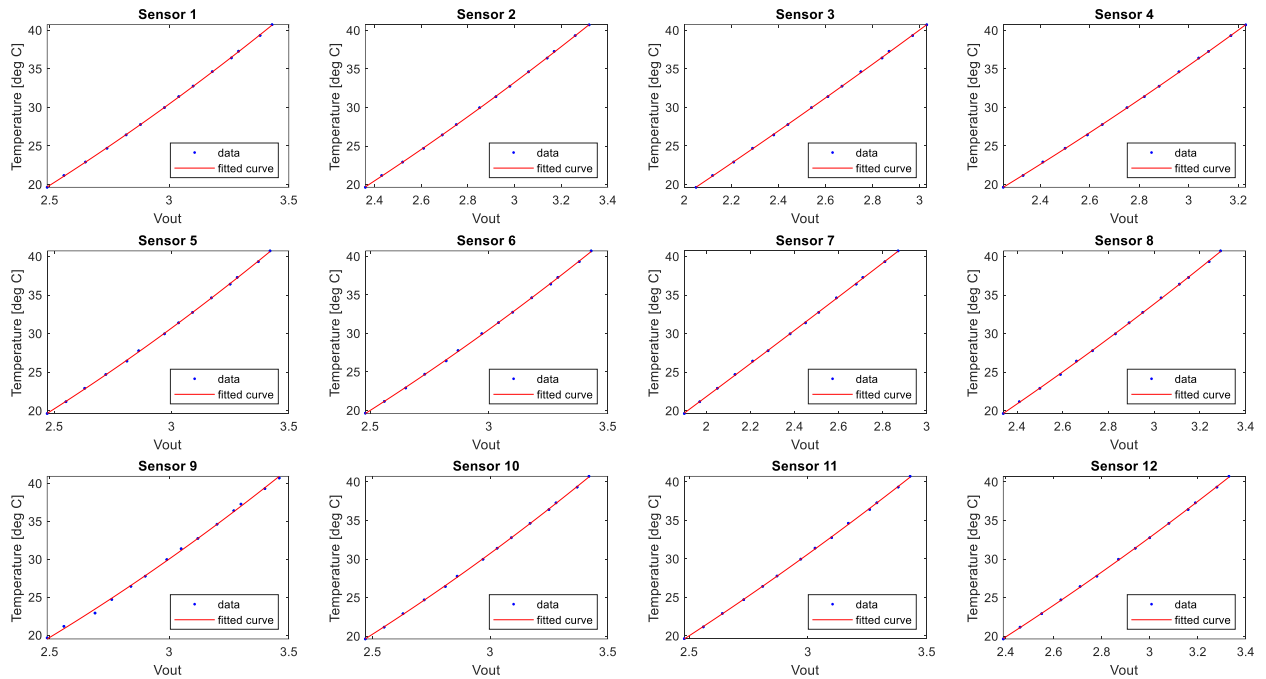


Figure 45. Calibration results: measured data points (Vout to Tref) and their fitted polynomial.

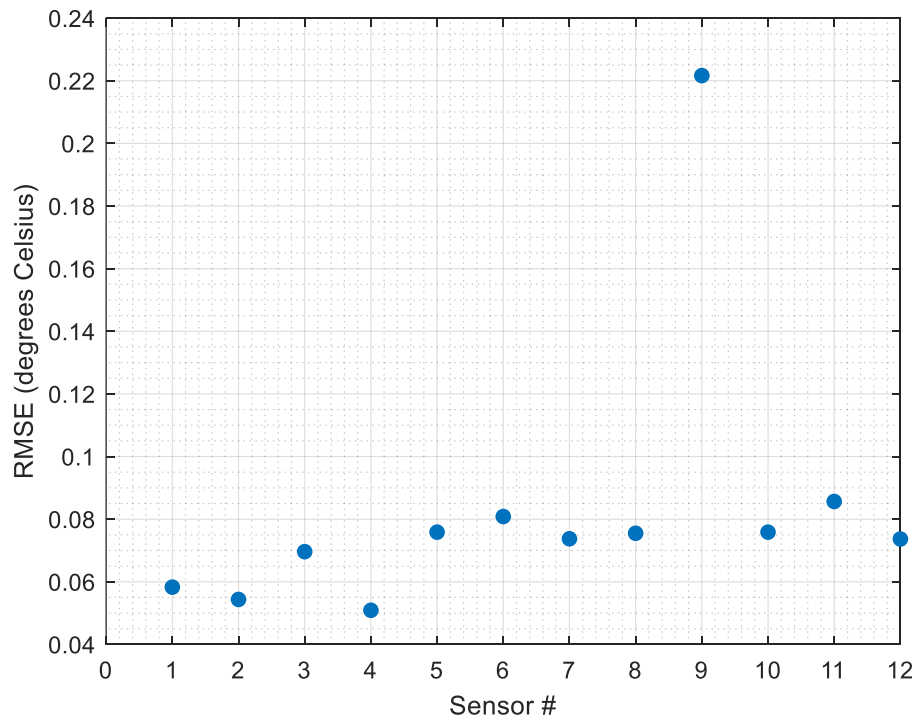


Figure 46. Calibration results: RMSE plot per calibrated temperature sensor.

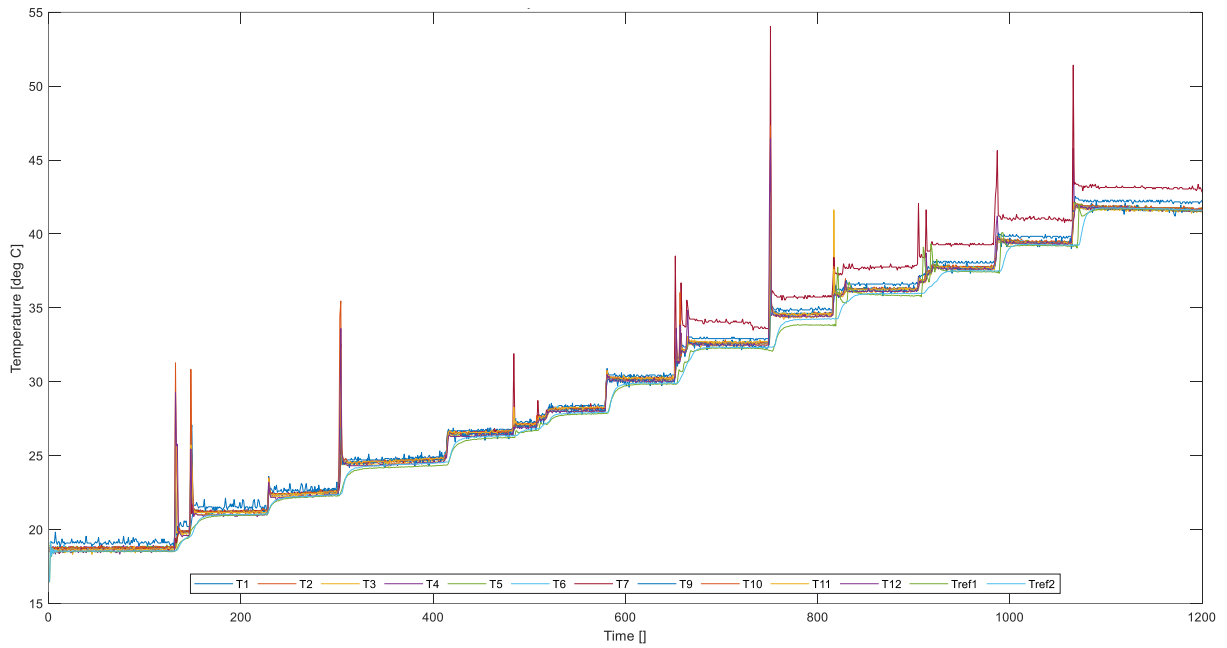
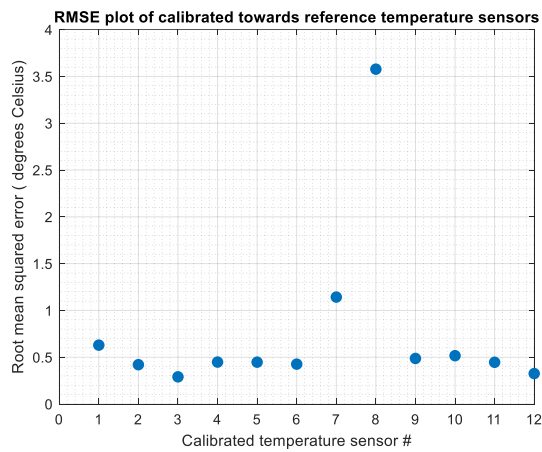
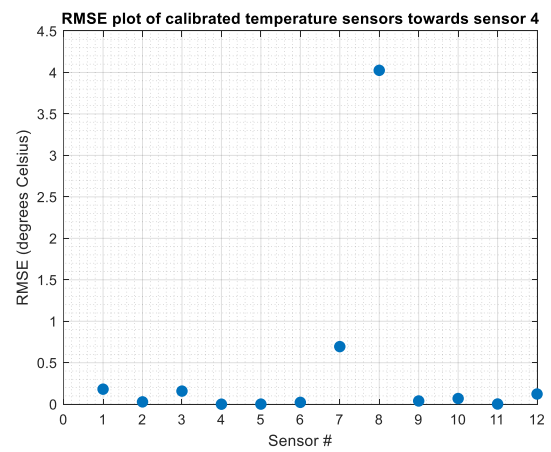


Figure 47. Validation results: response of the calibrated temperature sensors to a step-by-step increase in temperature over time. Temperature sensor 8 is not displayed in this graph as it caused extreme outliers at locations of instant temperature increment.



A



B

Figure 48. Validation results: RMSE plot per calibrated temperature sensor in relation to A) the reference temperature sensors and B) sensor 4.

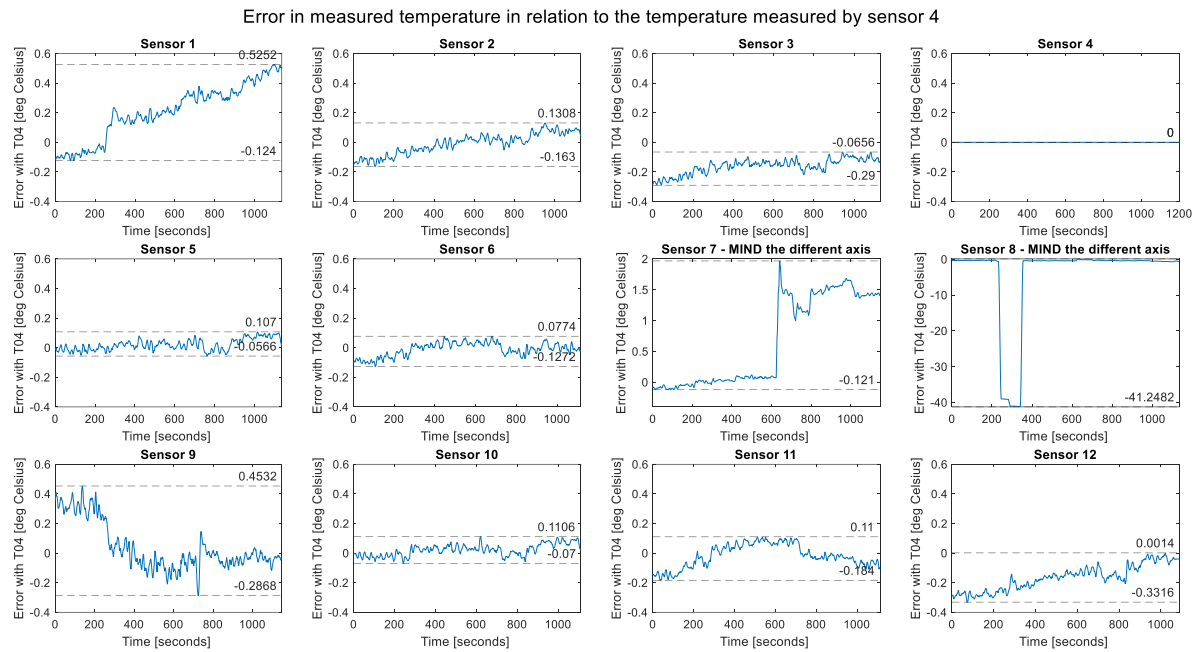


Figure 49. Error in measured temperature over time in relation to temperature measured by sensor 4.

D. Sensor Positioning Cold Plate

Method

The performance of the bought Peltier elements ($n = 9$) was tested using the setup as shown in **Figure 50**. Each Peltier element was tested individually. The Voltage applied to the Peltier element was increased ($0 - 1.03$ V) and the achieved temperatures at the lower side of the aluminum plate were measured. Each Peltier element was tested using the same heat sink and fan on top.

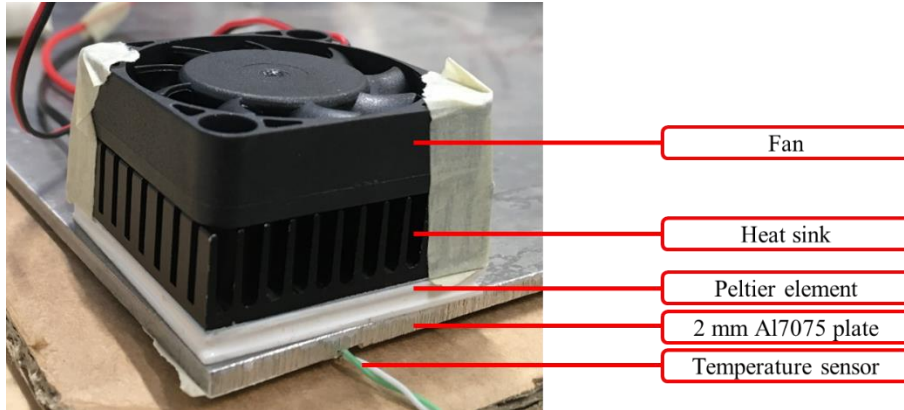


Figure 50. Configuration used for the Peltier element performance test in which a Peltier element was placed on a 2 mm thick aluminum plate, measuring the temperature achieved on the lower side of the aluminum plate. A heat sink and a fan were placed on top of the Peltier element for enhanced cooling.

Results

The response of the tested Peltier elements (1 to 9) to a change in applied voltage is shown in **Figure 51**. As the applied voltage to the Peltier element is increased, a decrease in temperature is observed. The size of this response differs per individual Peltier element. Therefore, a test with a thermal infrared camera is needed to see the combined effect of these nine Peltier elements on an aluminum plate.

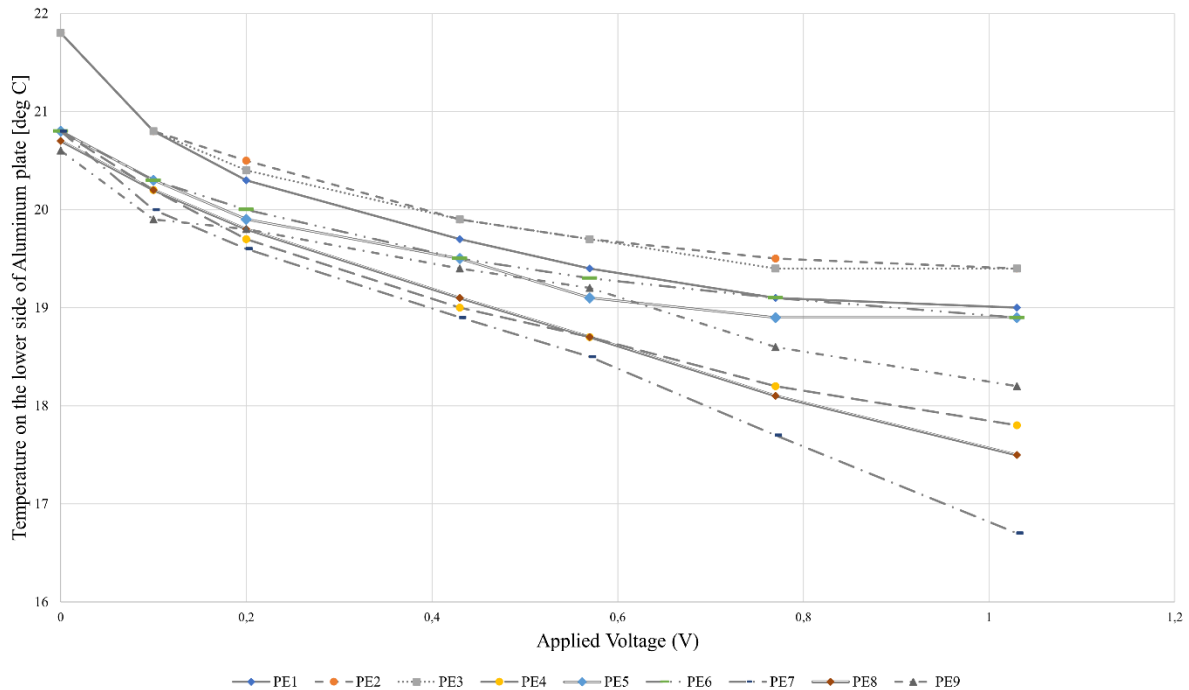


Figure 51. Response of the individual Peltier Elements (PE) to changes in applied voltage, for Peltier element 1 (PE1) to Peltier element 9 (PE9).

Method

The Peltier elements were positioned on the cold plate in the 3x3 configuration that was to be used in the final design. The Peltier elements were connected in a parallel electronic configuration. A thermal infrared camera was positioned in a way to measure the temperature along the cold plate. During thermal measurement, the applied voltages increased from 0 – 5 V.

Results

Figure 52 shows the used setup and the obtained temperature distribution during a single moment in time. **Table 12** illustrates the temperature details of a single moment in time. During the full measurement, temperatures within the red squared CMR did not differ more than 0.1 °C from each other.

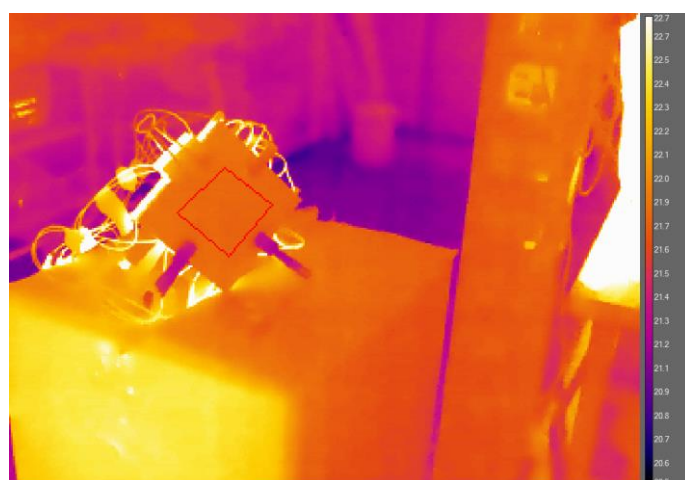
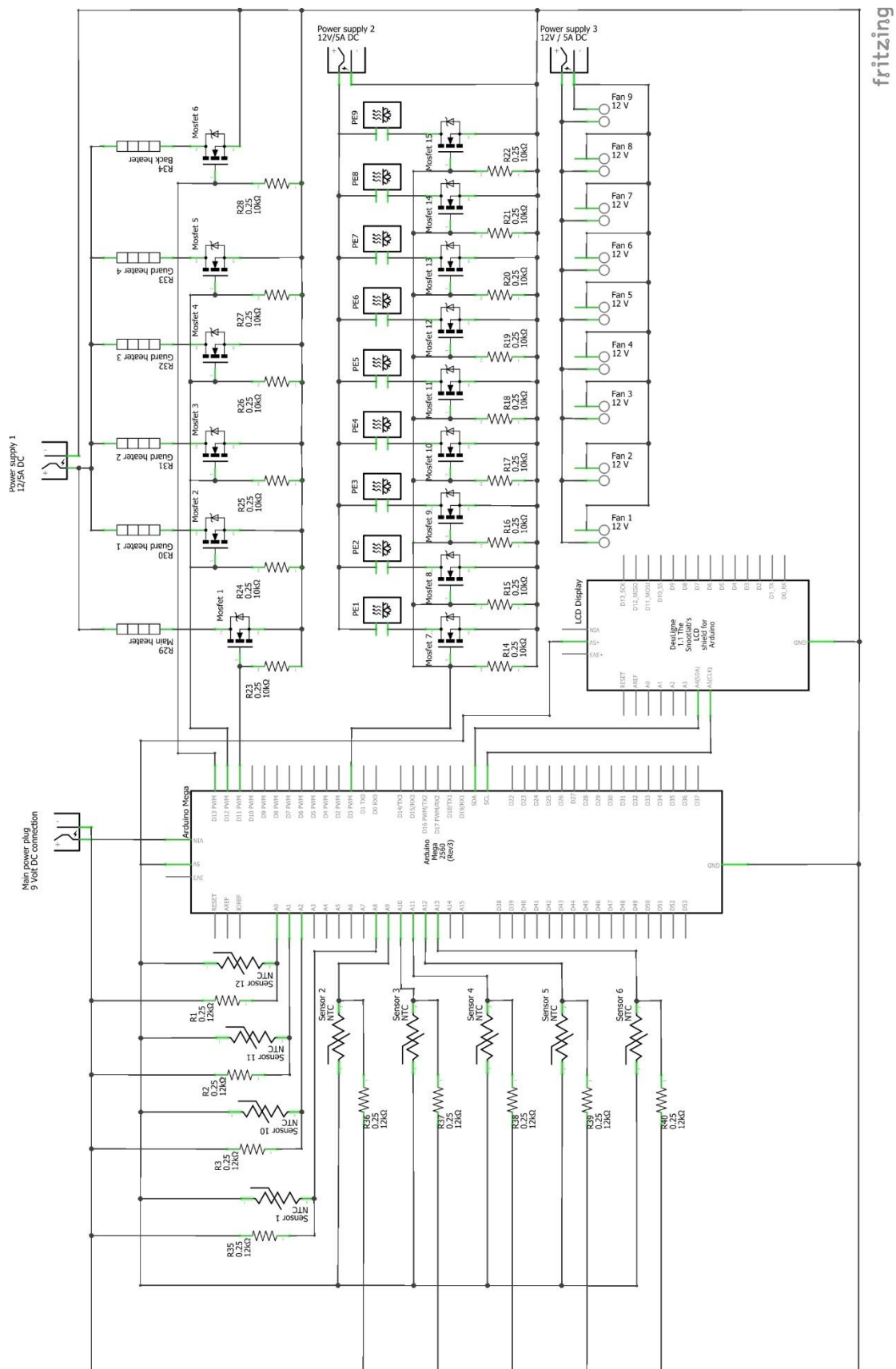


Figure 52. Infrared image of the cold plate setup measured with a thermal camera. Colors indicate the temperature distribution across the image. The red square indicates on the cold plate indicates the CMR (conduction measurement zone) that should be equithermal during TC measurement.

Statistic [units]	Polygon 1
Mean [°C]	21.9
Std. Dev. [°C]	0.0
Center [°C]	(108.0, 99.5) 21.8
Maximum [°C]	(88, 97) 21.9
Minimum [°C]	(111, 94) 21.8
Number of Pixels	1036
Single Pixel Area	N/A
Area [cm²]	N/A
Length [cm]	N/A
u Emissivity	0.95
u Distance [m]	1

Table 12. Details of a single moment during measurement.

E. Full Electronics Scheme



F. Photographs of the Terminus-K2 prototype

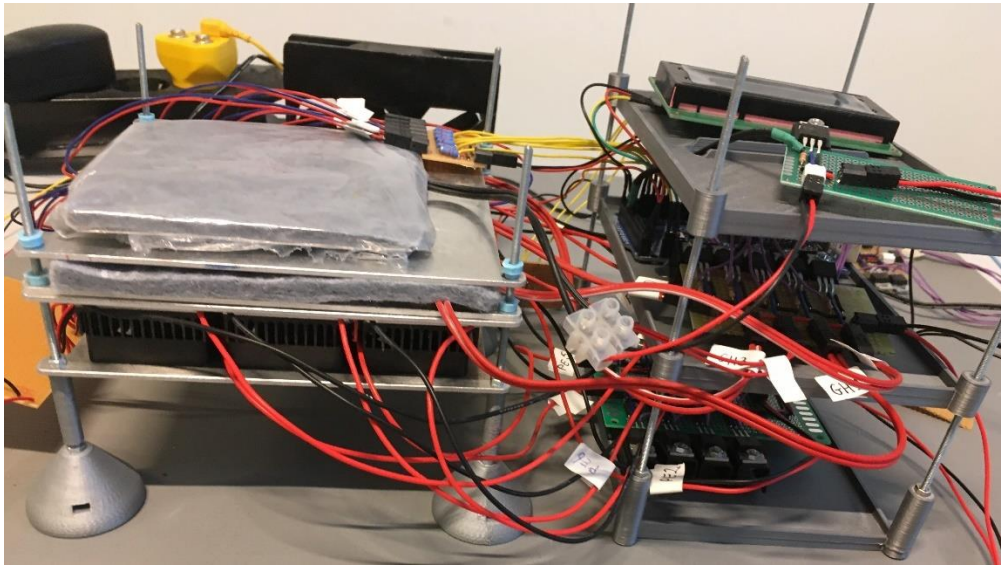
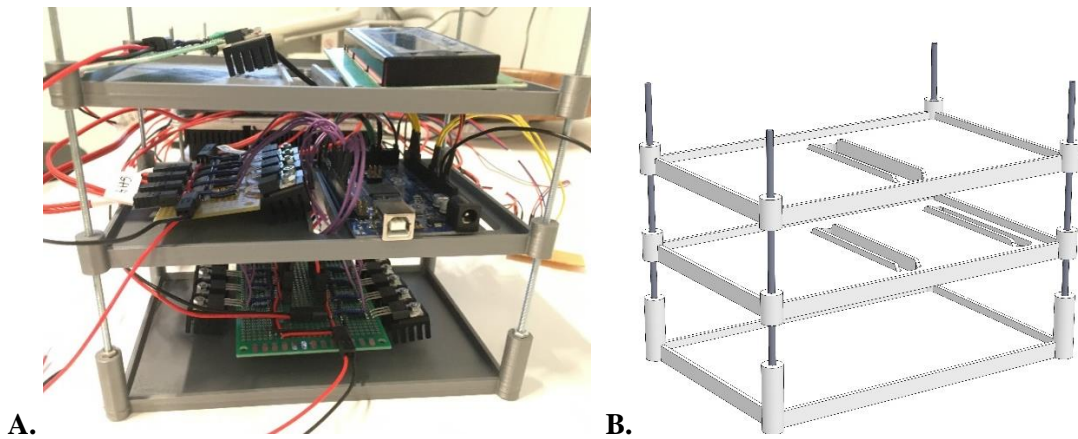


Figure 53. Photograph of Terminus-K2 with the electronics to the right.



A. **B.**
Figure 54. Terminus-K2's electronics housing as photographed (A) and its SolidWorks Assembly

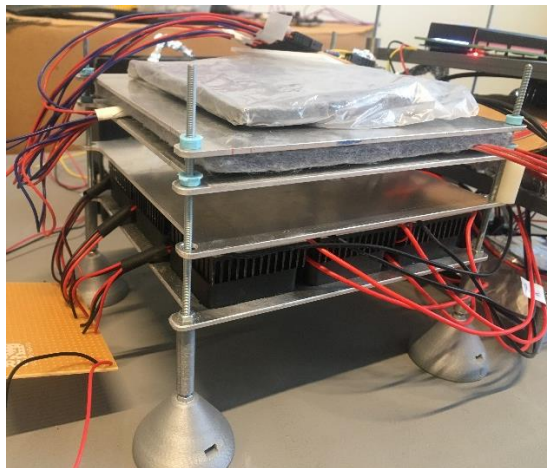


Figure 55. Photograph of Terminus-K2's main measurement part only

G. Visualization of the Terminus-K2 layers and electronics

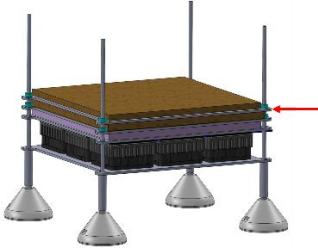

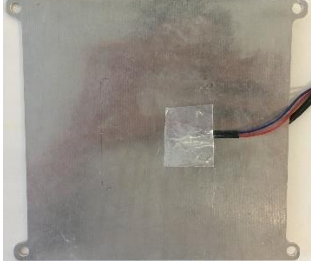
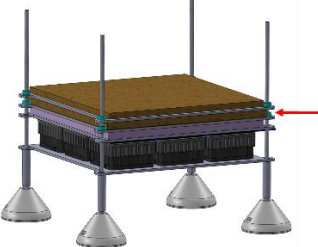

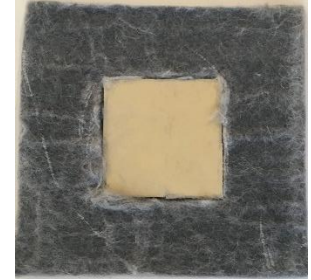
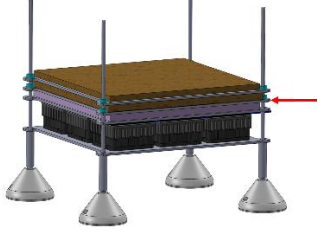
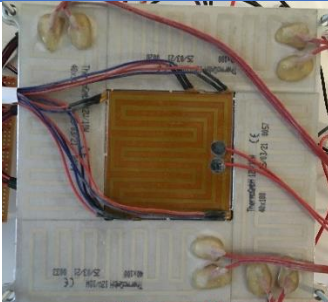
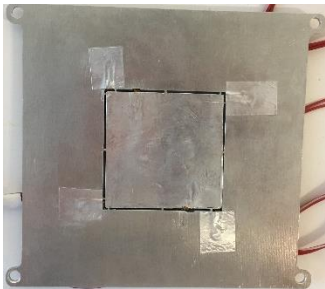
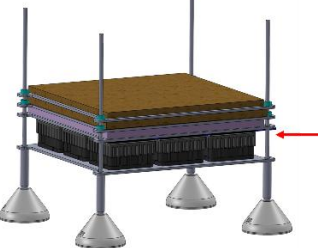
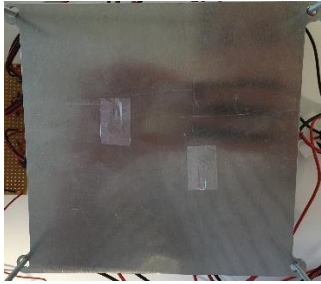
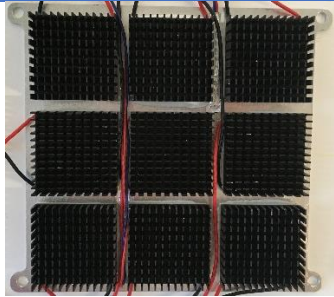
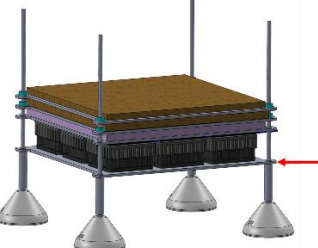


	LAYER	TOP VIEW	BOTTOM VIEW
Heating Assembly	Back Heater Plate 		
	Aerogel – Rubber layer 		
	Hot Plate 		
Cooling Assembly	Cold Plate Assembly 		
	Fan Plate Assembly 		

Table 13. Photographs of the top and bottom view of individual layers within Terminus-K2.

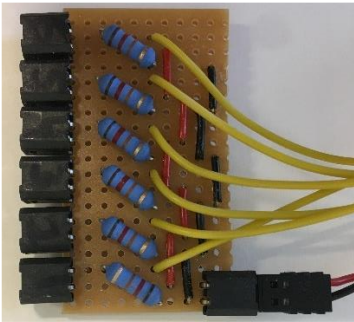
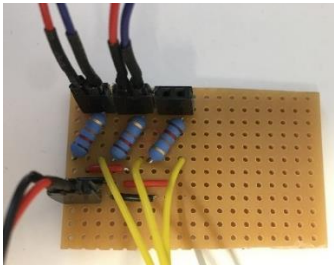
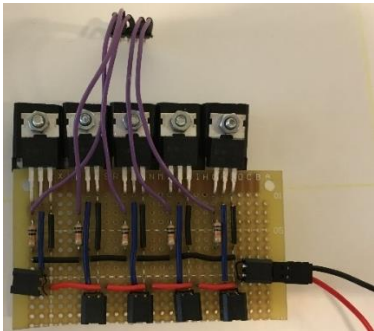
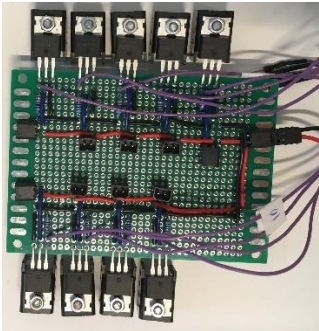
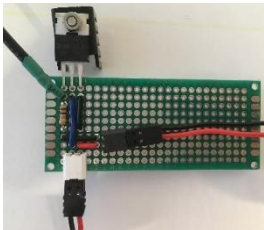
ELECTRONICS FUNCTIONALITY	PHOTO CIRCUIT BOARD
Temperature sensor 1 – 6	
Temperature sensor 10 – 12	
MOSFET plate used for heaters	
MOSFET plate used for Peltier elements	
MOSFET plate used for back heater	

Table 14. Photographs of the electronics used in Terminus-K2.

H. Measurement Protocol

Measurement protocol:

- ☐ 1. Perform measurements in the ‘dark’ room next to the wet lab
- ☐ 2. Place anti-electrostatic mat underneath Terminus-K2
- ☐ 3. Always use the anti-electrostatic wristband when near the device
- ☐ 4. Check if all is well connected in the complete setup: connectors, cables, grounding
- ☐ 5. Place sample material between the hot and the cold plate
 - ☐ E.4: surround the sample by the corresponding spacer, with known thickness
- ☐ 6. Lower the hot plate assembly until touching the sample
- ☐ 7. Make sure the anti-conduction caps are correctly positioned
- ☐ 8.
 - ☐ E.1, E.2 and E.3: Use standard compression: Place five 100 gram weights equally spread on top of the device (back heater plate) to enhance the contact between the sample and the surface plates (to decrease the effect of contact resistance)
 - ☐ E.4: Make sure the hot plate assembly is lowered until sandwiching the spacer between the plates (e.g. ensure compression by adding 4 spring clamps around hot and cold plate and adding extra weights (3 x 500 gram) on top of the device)
- ☐ 9.
 - ☐ E.1, E.2 and E.3: measure the thickness of the sample material by measuring the distance between the hot and the cold plate with a digital capiler and note in Excel file
- ☐ 10. Again, check if all cables are still well connected
- ☐ 11. Report environment temperature
- ☐ 12. Change coding setpoint cold temperature to environment temperature (if temperature > 0.5 set temperature). Both in Arduino and Excel.
- ☐ 13. Turn on the fans
- ☐ 14. Start the measurement (open Serial Monitor Arduino AND turn on the power supplies for the heating and cooling components)
- ☐ 15. Perform measurement for:
 - ☐ E.1, **15** minutes
 - ☐ E.2, E.3 and E.4: **30** minutes
- ☐ 16. Convert data from Serial Monitor Arduino to an Excel file and save as ‘yyymmdd-V0x-DataGHPmeasurement.xlsx’.
- ☐ 17. Turn off the power supplies for the heating and cooling components
- ☐ 18. Leave the power supplies for the fans on
- ☐ 19. Turn on the extra fan (12V DC, 0.26 A, 120x120x25 mm) for enhanced cooling, combined with placing an bowl of ice in front of the fan.
- ☐ 20. Again, report environment temperature
- ☐ 21. The next measurement can start when the temperature sensors of the cold plate have cooled down to at least the ambient temperature + 3 °C.

In this measurement protocol, some abbreviations should be explained:

E.1 = Device Configuration Test

E.2 = Performance Test

E.3 = Moisture Effect Test

E.4 = Sample Compression Effect Test

I. Original Textile Samples used for Measurements



















Sample material	Details	Illustration	Photo of the original	Photo of the sample
Cotton (100% CO) undershirt 0.6 mm thick	ZEEMAN Size L			
Polyester (100% PES) long sleeve 2 mm thick	Love to Lounge Size S			
Polyester/Cotton (65/35 % PES/CO) joggers 1.4 mm thick	Panther Size XL			
Denim (CO) skirt 0.8 mm thick	H&M Size 38			
Acrylic/polyester (PAN/PES) fur coat 8 mm thick	Vroom & Dreesman Size 44			
Nylon/polyester (NY/PES) padded jacket 3 mm thick	ONLY Size XL			

Table 15. Details about the textile pieces used in the tests for TC measurement.

All textile was collected at the thrift store: Kringloop Actief Boxmeer.

J. Extended List of Components used in Thermanus-K2

Number of components	PART NAME	MATERIAL	MANUFACTURING
1	Back heater plate	Al 7075	Lasercutting and filing
1	Hot Plate	Al 7075	Lasercutting, filing and milling
1	Cold plate	Al 7075	Lasercutting, filing and milling
1	Fan plate	Al 7075	Lasercutting, filing, milling and screwtapping
8	Thermally insulating caps	PLA	3D-printing (Multimaker)
4	Lower stand	PLA	3D-printing (Multimaker)
4	Supports	PLA	3D-printing (Multimaker)
2	Spacers	PLA	3D-printing (Multimaker)
3	Spacers	PMMA	Lasercutting and filing
	Housing	PLA	3D-printing (Multimaker)

Table 16. Material and manufacturing method of custom-designed components. Technical drawings made in SolidWorks are visualized in Appendix K.

Number of components	COMPONENT NAME	Link to website supplier (accessed on 02-06-2022)
1	Back heater foil	https://www.conrad.nl/nl/p/thermo-tech-polyester-verwarmingsfolie-zelfklevend-12-v-dc-12-v-ac-15-w-beschermingsgraad-1px4-90-mm-189177.html
1	Main heater foil	https://www.conrad.nl/nl/p/conrad-components-polymide-verwarmingsfolie-12-v-dc-48-w-1-x-b-60-mm-x-60-mm-1484113.html
4	Guard heater foils	https://www.conrad.nl/nl/p/thermo-tech-polyester-verwarmingsfolie-zelfklevend-12-v-dc-12-v-ac-10-w-beschermingsgraad-1px4-1-x-b-100-mm-x-40-mm-1216593.html
9	TTF-103 NTC Thermistor	https://www.conrad.nl/nl/p/tru-components-ttf3a103f34d3ay-temperatuursensor-40-tot-100-c-10-k-3435-k-radiaal-bedraad-1567376.html
4	Thermal grease	https://hackerstore.nl/Artikel/862
1	Thermal Adhesive	https://nl.rs-online.com/web/p/thermal-grease/7259975?cm_mmc=NL-PPC-DS3A--google--DSA_NL_NL_HVAC+%26+Fans+%26+Thermal+Management_Index--Thermal+Grease%7C+Products--DYNAMIC+SEARCH+ADS&matchtype=&aud-827186183886:dsa-1642038826060&gclid=CjwKCAjwv-GUBhAzEiwASUMm4sxfdBiamWNKXqe81QjLjm0trPagxwYyay19vIJt8Hf7Rk67G5-RoCpJwQAvD_BwE&gclid=aw.ds
9	Peltier Elements	https://hackerstore.nl/Artikel/293
9	HeatSinks	https://hackerstore.nl/Artikel/792
9	Fans	https://hackerstore.nl/Artikel/679
1	Arduino Mega 2560	https://hackerstore.nl/Artikel/2
5	Prototyping boards	https://www.conrad.nl/nl/p/tru-components-supcb001-printplaat-vertind-zonder-cu-laag-epoxide-1-x-b-98-mm-x-76-5-mm-rastermaat-2-54-mm-inhoud-1-1572163.html
40	Connectors female	https://www.conrad.nl/nl/p/phoenix-contact-1778832-female-behuizing-kabel-ptsm-totaal-aantal-polen-2-rastermaat-2-50-mm-1-stuk-s-733781.html
40	Connectors male	https://www.conrad.nl/nl/p/phoenix-contact-1778625-male-behuizing-board-ptsm-totaal-aantal-polen-2-rastermaat-2-50-mm-1-stuk-s-733925.html
15	MOSFET IRLZ44NPBF ¹	https://www.conrad.nl/nl/p/infineon-technologies-irlz44npbf-mosfet-1-hexfet-110-w-to-220-162877.html
15	Heat Sink	https://www.conrad.nl/nl/p/assmann-wsw-v7236c1-koellichaam-21-k-w-l-x-b-x-h-19-05-x-13-21-x-12-7-mm-to-220-183931.html
20 meter	Wires 22 AWG (0.35 mm ²)	Aansluitdraden set met solide kern - 6x 7.5M - 22AWG / 0.35mm² (kiwi-electronics.com)

Table 17. Link to the websites the components delivered by external suppliers were retrieved from.

¹ During the design setup, major care was given to the IRLZ44NPBF MOSFETS, which are very sensitive to static electricity.

Number of components	COMPONENT NAME	SPECIFICATIONS
3	Power supply	Delta Elektronika (max 30V, 5 A DC each)
2	Aerogel	Spaceloft (5 x 140 x 140 mm)
1	Rubber	~0.5 W/mK (5 x 60 x 60 mm)
9	Aluminum tape	15 x 15 x 0.2 mm
36	Bolts	Steel, M3, 6 mm length
8	Screwthread	Steel, M3, 150 mm length
9	Resistors for MOSFET circuitries	10 k Ω \pm 5 % uncertainty
15	Resistors for temperature sensor circuitries	12 k Ω \pm 5 % uncertainty

Table 18. List of extra components and materials used in Terminus-K2 with some small specifications.

K. Technical Drawings of Custom-designed Components

Component needed to fabricate prototype:

1. Mold for gluing Peltier elements to cold plate – made from **PLA**

Component needed for Sample Compression Test:

2. Spacers for compression test - made from **PLA**

Components used in prototype:

3. Back heater plate + cold plate – made from **Al7075**
4. Hot plate : main heaters + guards heaters – made from **Al7075**
5. Fan plate – made from **Al7075**
6. Thermally insulating caps - made from **PLA**
7. Housing electronics - made from **PLA**
8. Support - made from **PLA**
9. Lower stand - made from **PLA**

Technical drawing of a mold for glueing PES. The drawing includes an isometric view, a top view, and a side view (SECTION B-B). Dimensions are in millimeters.

Top View Dimensions:

- Overall width: 149,00
- Overall height: 144,00
- Grid dimensions (from left to right): 1,65, 4,35, 4,35, 4,35
- Grid dimensions (from top to bottom): 6,65, 4,65, 4,65, 4,65
- Bottom edge dimensions: 42,00, 4,35

Side View (SECTION B-B) Dimensions:

- Top flange width: 14,80
- Top flange height: 4,85
- Internal width: 13,00
- Internal height: 8,00
- Bottom flange height: 4,95

Section B-B: SECTION B-B

Table:

NAME	SIGNATURE	DATE	TITLE
DRAWN			
CHK'D			
APP'VD			
MFG			
Q.A			

Table:

UNLESS OTHERWISE SPECIFIED: DIMENSIONS ARE IN MILLIMETERS SURFACE FINISH: TOLERANCES: LINEAR: ANGULAR:	FINISH:	DEBURR AND BREAK SHARP EDGES	DO NOT SCALE DRAWING	REVISION

Table:

NAME	SIGNATURE	DATE	TITLE
DRAWN			
CHK'D			
APP'VD			
MFG			
Q.A			

Table:

NAME	SIGNATURE	DATE	TITLE
DRAWN			
CHK'D			
APP'VD			
MFG			
Q.A			

Table:

NAME	SIGNATURE	DATE	TITLE
DRAWN			
CHK'D			
APP'VD			
MFG			
Q.A			

Table:

NAME	SIGNATURE	DATE	TITLE
DRAWN			
CHK'D			
APP'VD			
MFG			
Q.A			

Table:

NAME	SIGNATURE	DATE	TITLE
DRAWN			
CHK'D			
APP'VD			
MFG			
Q.A			

Table:

NAME	SIGNATURE	DATE	TITLE
DRAWN			
CHK'D			
APP'VD			
MFG			
Q.A			

Table:

NAME	SIGNATURE	DATE	TITLE
DRAWN			
CHK'D			
APP'VD			
MFG			
Q.A			

Table:

NAME	SIGNATURE	DATE	TITLE
DRAWN			
CHK'D			
APP'VD			
MFG			
Q.A			

Table:

NAME	SIGNATURE	DATE	TITLE
DRAWN			
CHK'D			
APP'VD			
MFG			
Q.A			

Table:

NAME	SIGNATURE	DATE	TITLE
DRAWN			
CHK'D			
APP'VD			
MFG			
Q.A			

Table:

NAME	SIGNATURE	DATE	TITLE
DRAWN			
CHK'D			
APP'VD			
MFG			
Q.A			

Table:

NAME	SIGNATURE	DATE	TITLE
DRAWN			
CHK'D			
APP'VD			
MFG			
Q.A			

Table:

NAME	SIGNATURE	DATE	TITLE
DRAWN			
CHK'D			
APP'VD			
MFG			
Q.A			

Table:

NAME	SIGNATURE	DATE	TITLE
DRAWN			
CHK'D			
APP'VD			
MFG			
Q.A			

Table:

NAME	SIGNATURE	DATE	TITLE
DRAWN			
CHK'D			
APP'VD			
MFG			
Q.A			

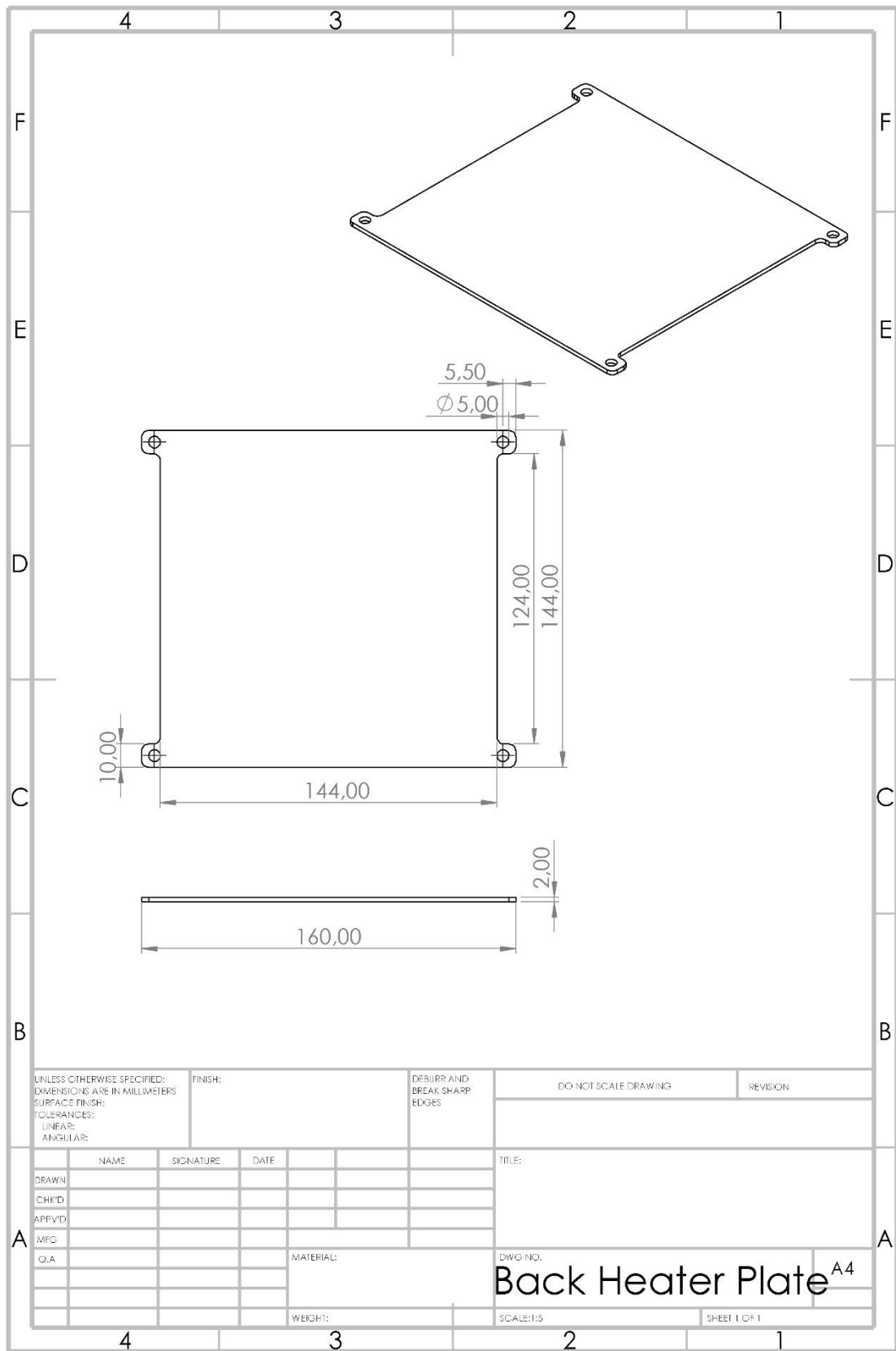
Table:

NAME	SIGNATURE	DATE	TITLE
DRAWN			
CHK'D			
APP'VD			
MFG			

Fabricated at thicknesses: 1, 1.5, 2, 4 and 6 mm.



3. Back heater plate



Technical drawing of a Hot Plate, showing dimensions and specifications.

Top View:

- Overall dimensions: 160,00 (width) x 144,00 (depth).
- Inner dimensions: 60,00 (width) x 43,00 (depth).
- Corner radius: R2,00.
- Dimensions for mounting holes: 4,00 (width), 1,00 (depth), 13,50 (width), 124,00 (depth).
- Mounting holes: 4 holes, Ø 5,00, spaced 5,50 apart.

Front View:

- Overall width: 160,00.
- Overall height: 102,00.
- Dimensions for mounting holes: 2,00 (width), 1,00 (depth), 1,40 (width), 27,13 (depth), 41,00 (depth).

Section B-B (Scale 1:2):

- Overall width: 160,00.
- Overall height: 102,00.
- Dimensions for mounting holes: 2,00 (width), 1,00 (depth), 1,40 (width), 27,13 (depth), 41,00 (depth).

Table:

NAME	SIGNATURE	DATE
DRAWN		
CHK'D		
APP'D		
MFG		
Q.A		

Table:

NAME	SIGNATURE	DATE
DRAWN		
CHK'D		
APP'D		
MFG		
Q.A		

Table:

NAME	SIGNATURE	DATE
DRAWN		
CHK'D		
APP'D		
MFG		
Q.A		

Table:

NAME	SIGNATURE	DATE
DRAWN		
CHK'D		
APP'D		
MFG		
Q.A		

Table:

NAME	SIGNATURE	DATE
DRAWN		
CHK'D		
APP'D		
MFG		
Q.A		

Table:

NAME	SIGNATURE	DATE
DRAWN		
CHK'D		
APP'D		
MFG		
Q.A		

Table:

NAME	SIGNATURE	DATE
DRAWN		
CHK'D		
APP'D		
MFG		
Q.A		

Table:

NAME	SIGNATURE	DATE
DRAWN		
CHK'D		
APP'D		
MFG		
Q.A		

Table:

NAME	SIGNATURE	DATE
DRAWN		
CHK'D		
APP'D		
MFG		
Q.A		

Table:

NAME	SIGNATURE	DATE
DRAWN		
CHK'D		
APP'D		
MFG		
Q.A		

Table:

NAME	SIGNATURE	DATE
DRAWN		
CHK'D		
APP'D		
MFG		
Q.A		

Table:

NAME	SIGNATURE	DATE
DRAWN		
CHK'D		
APP'D		
MFG		
Q.A		

Table:

NAME	SIGNATURE	DATE
DRAWN		
CHK'D		
APP'D		
MFG		
Q.A		

Table:

NAME	SIGNATURE	DATE
DRAWN		
CHK'D		
APP'D		
MFG		
Q.A		

Table:

NAME	SIGNATURE	DATE
DRAWN		
CHK'D		
APP'D		
MFG		
Q.A		

Table:

NAME	SIGNATURE	DATE
DRAWN		
CHK'D		
APP'D		
MFG		
Q.A		

Table:

NAME	SIGNATURE	DATE
DRAWN		
CHK'D		
APP'D		
MFG		
Q.A		

Table:

NAME	SIGNATURE	DATE
DRAWN		
CHK'D		
APP'D		
MFG		
Q.A		

Table:

NAME	SIGNATURE	DATE
DRAWN		
CHK'D		
APP'D		
MFG		
Q.A		

Table:

NAME	SIGNATURE	DATE
DRAWN		
CHK'D		
APP'D		
MFG		
Q.A		

Table:

NAME	SIGNATURE	DATE
DRAWN		
CHK'D		
APP'D		
MFG		
Q.A		

Table:

NAME	SIGNATURE	DATE
DRAWN		
CHK'D		
APP'D		
MFG		
Q.A		

Table:

NAME	SIGNATURE	DATE
DRAWN		
CHK'D		
APP'D		
MFG		
Q.A		

Table:

NAME	SIGNATURE	DATE
DRAWN		
CHK'D		
APP'D		
MFG		
Q.A		

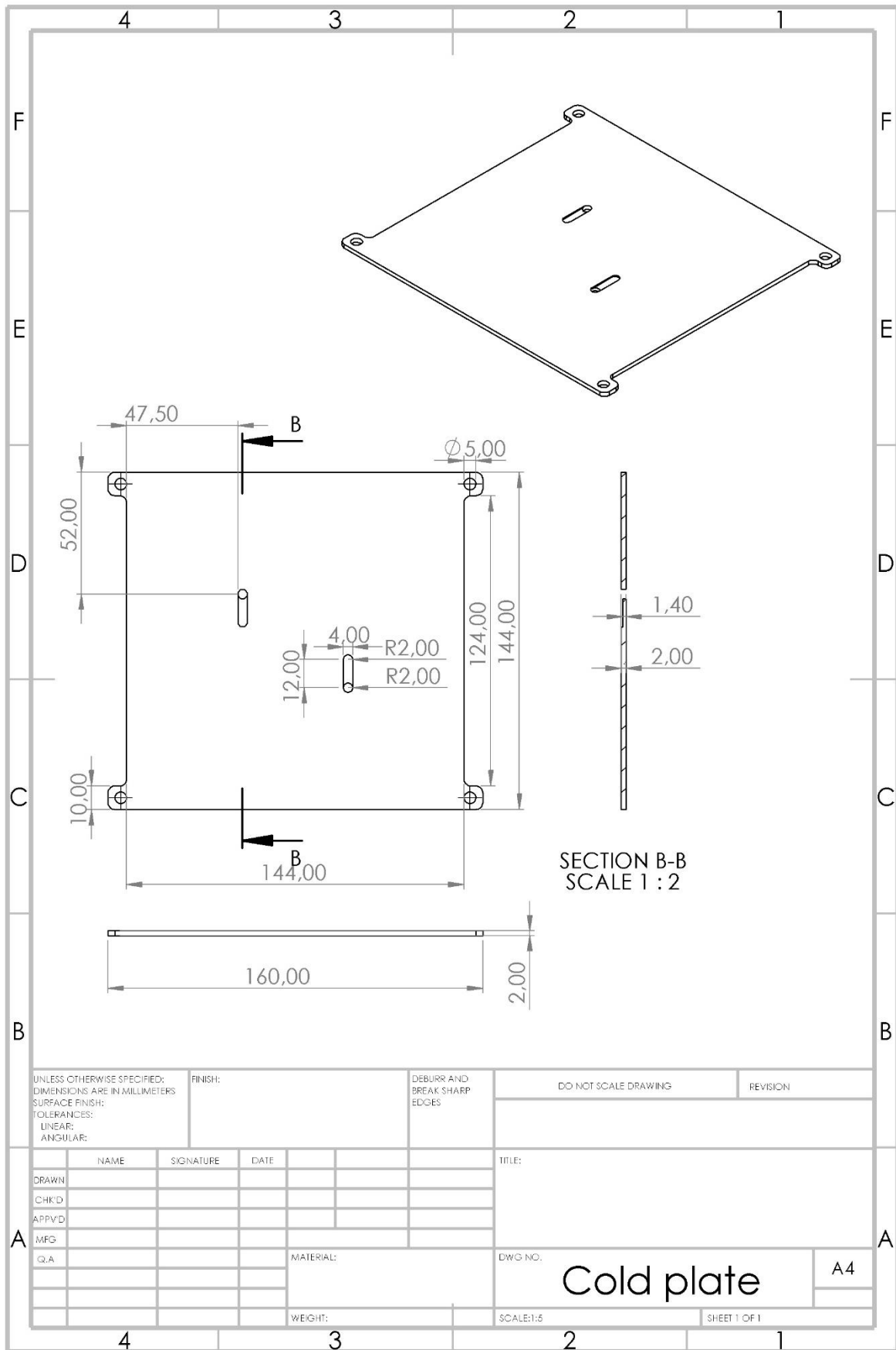
Table:

NAME	SIGNATURE	DATE
DRAWN		
CHK'D		
APP'D		
MFG		
Q.A		

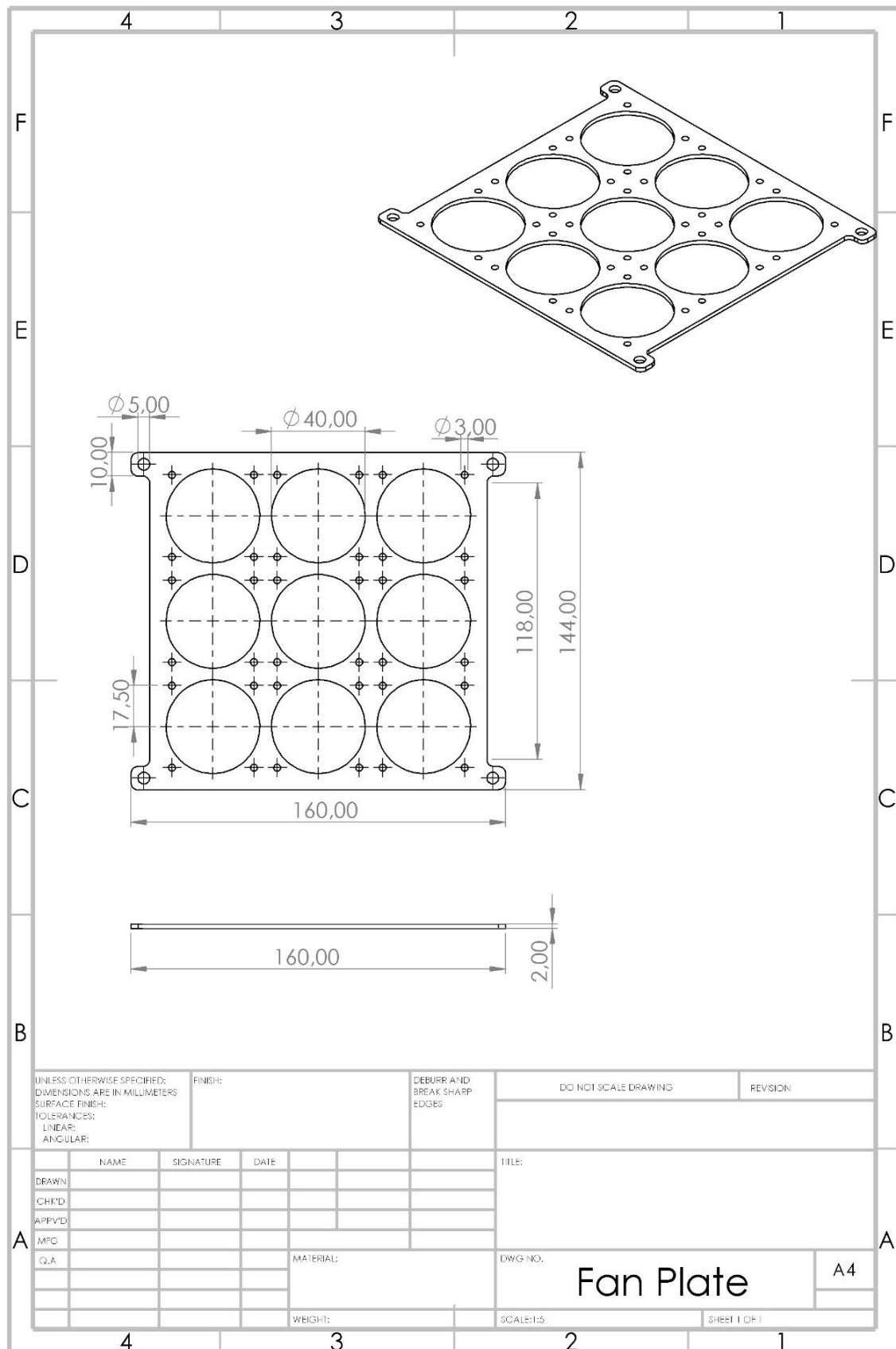
Table:

NAME	SIGNATURE	DATE
DRAWN		
CHK'D		
APP'D		
MFG		
Q.A</		

5. Cold plate



6. Fan plate



In $\varnothing 3$ mm holes screw thread is tapped.

[illegible]

Technical drawing of a rectangular housing assembly, showing dimensions and section A-A.

Top View Dimensions:

- Overall Width: 110,00
- Overall Height: 170,00
- Internal Width: 75,87
- Internal Height: 165,60
- Corner Fillet: R4,00
- Fastener Hole Diameter: $\varnothing 10,00$
- Fastener Hole Spacing: 105,60
- Fastener Hole Diameter: $\varnothing 3,50$
- Fastener Hole Spacing: 101,02
- Fastener Hole Diameter: $\varnothing 10,00$

Side View Dimensions:

- Overall Depth: 14,00
- Internal Depth: 7,00
- Fastener Hole Diameter: $\varnothing 10,00$

Section A-A Dimensions:

- Section A-A: SCALE 1:2
- Section A-A: 14,00
- Section A-A: 7,00
- Section A-A: 4,00
- Section A-A: 2,20

Fastener Detail Dimensions:

- Fastener Detail: 101,02
- Fastener Detail: 120,00
- Fastener Detail: 8,00
- Fastener Detail: 14,00

Notes:

- UNLESS OTHERWISE SPECIFIED: DIMENSIONS ARE IN MILLIMETERS
- SURFACE FINISH: TOLERANCES: LINEAR: ANGULAR:
- DEBURR AND BREAK SHARP EDGES
- DO NOT SCALE DRAWING
- REVISION:

Table:

NAME	SIGNATURE	DATE	TITLE:
DRAWN			Housing - mid
CHK'D			
APP'VD			
MFG			
Q.A			
MATERIAL:			DWG NO.
WEIGHT:			SCALE:1:5
			SHEET 1 OF 1

Technical drawing of a housing top plate. The drawing includes three views: a front view, a top view, and a section view labeled A-A.

Front View Dimensions:

- Overall width: 170,00
- Overall height: 165,60
- Top flange thickness: 8,00
- Top flange width: 4,00
- Top flange hole diameter: $\phi 10,00$
- Top flange hole offset from top edge: 2,20
- Top flange hole offset from side edge: 2,00
- Top flange hole diameter: $\phi 3,50$
- Top flange hole offset from bottom edge: 2,00
- Top flange hole offset from side edge: 2,00
- Top flange hole diameter: $\phi 10,00$
- Top flange hole offset from bottom edge: 2,00
- Top flange hole offset from side edge: 2,00
- Top flange hole diameter: $\phi 10,00$
- Top flange hole offset from bottom edge: 2,00
- Top flange hole offset from side edge: 2,00

Top View Dimensions:

- Overall width: 120,00
- Overall height: 8,00
- Top flange thickness: 14,00
- Top flange width: 8,00
- Top flange hole diameter: $\phi 10,00$
- Top flange hole offset from top edge: 2,20
- Top flange hole offset from side edge: 2,00
- Top flange hole diameter: $\phi 3,50$
- Top flange hole offset from top edge: 2,00
- Top flange hole offset from side edge: 2,00
- Top flange hole diameter: $\phi 10,00$
- Top flange hole offset from top edge: 2,00
- Top flange hole offset from side edge: 2,00

Section A-A Dimensions:

- Overall width: 120,00
- Overall height: 8,00
- Top flange thickness: 14,00
- Top flange width: 8,00
- Top flange hole diameter: $\phi 10,00$
- Top flange hole offset from top edge: 2,20
- Top flange hole offset from side edge: 2,00
- Top flange hole diameter: $\phi 3,50$
- Top flange hole offset from top edge: 2,00
- Top flange hole offset from side edge: 2,00
- Top flange hole diameter: $\phi 10,00$
- Top flange hole offset from top edge: 2,00
- Top flange hole offset from side edge: 2,00

Section A-A Scale: 1 : 2

Notes:

- UNLESS OTHERWISE SPECIFIED: FINISH: DEBURR AND BREAK SHARP EDGES.
- SURFACE FINISH: DO NOT SCALE DRAWING.
- TOLERANCES: REVISION:
- LINEAR: TITLE:
- ANGULAR: MATERIAL:
- SCALE: 1:5
- SHEET 1 OF 1

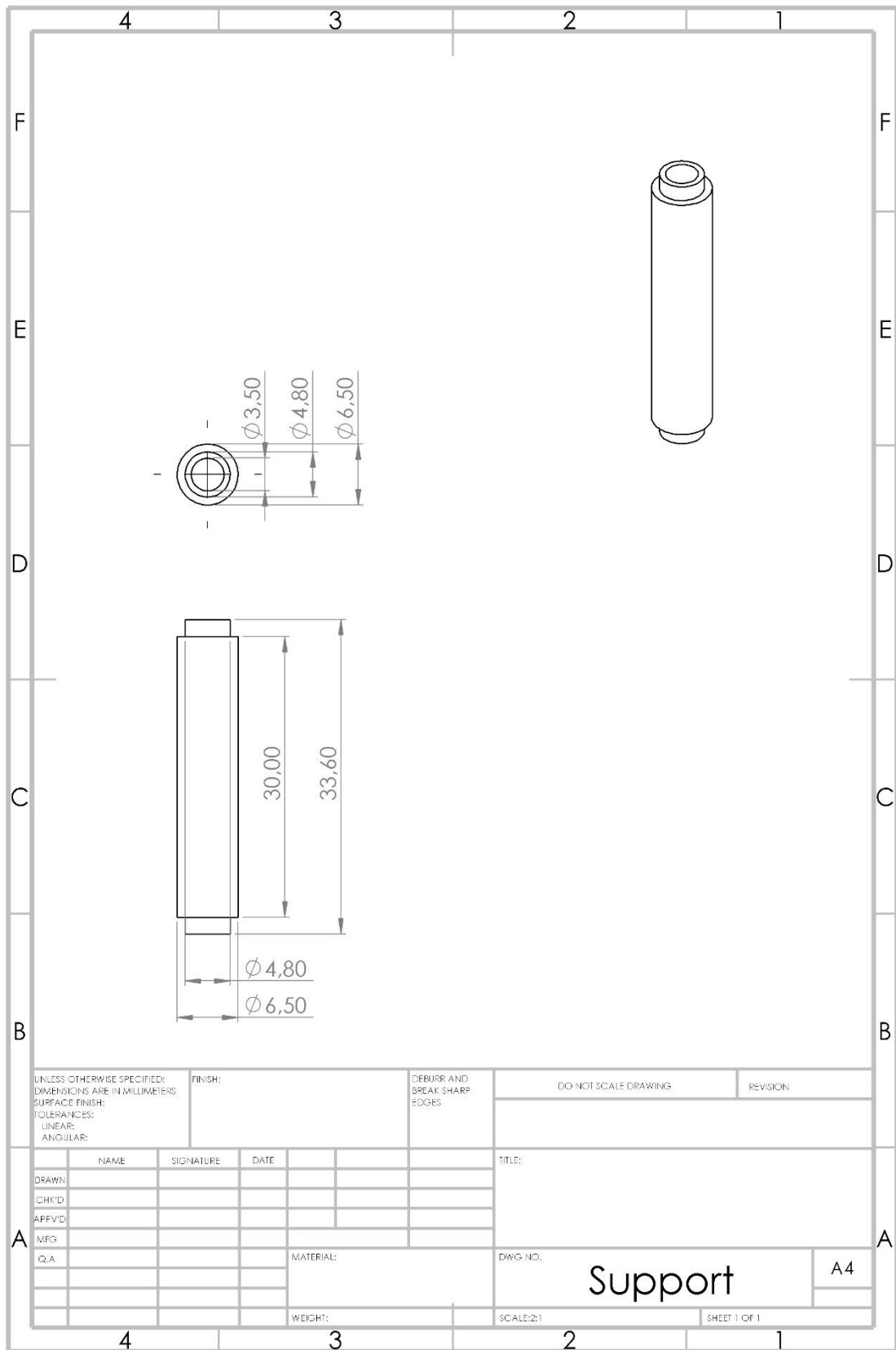
Table:

NAME	SIGNATURE	DATE
DRAWN		
CHK'D		
APP'D		
MFG		
Q/A		

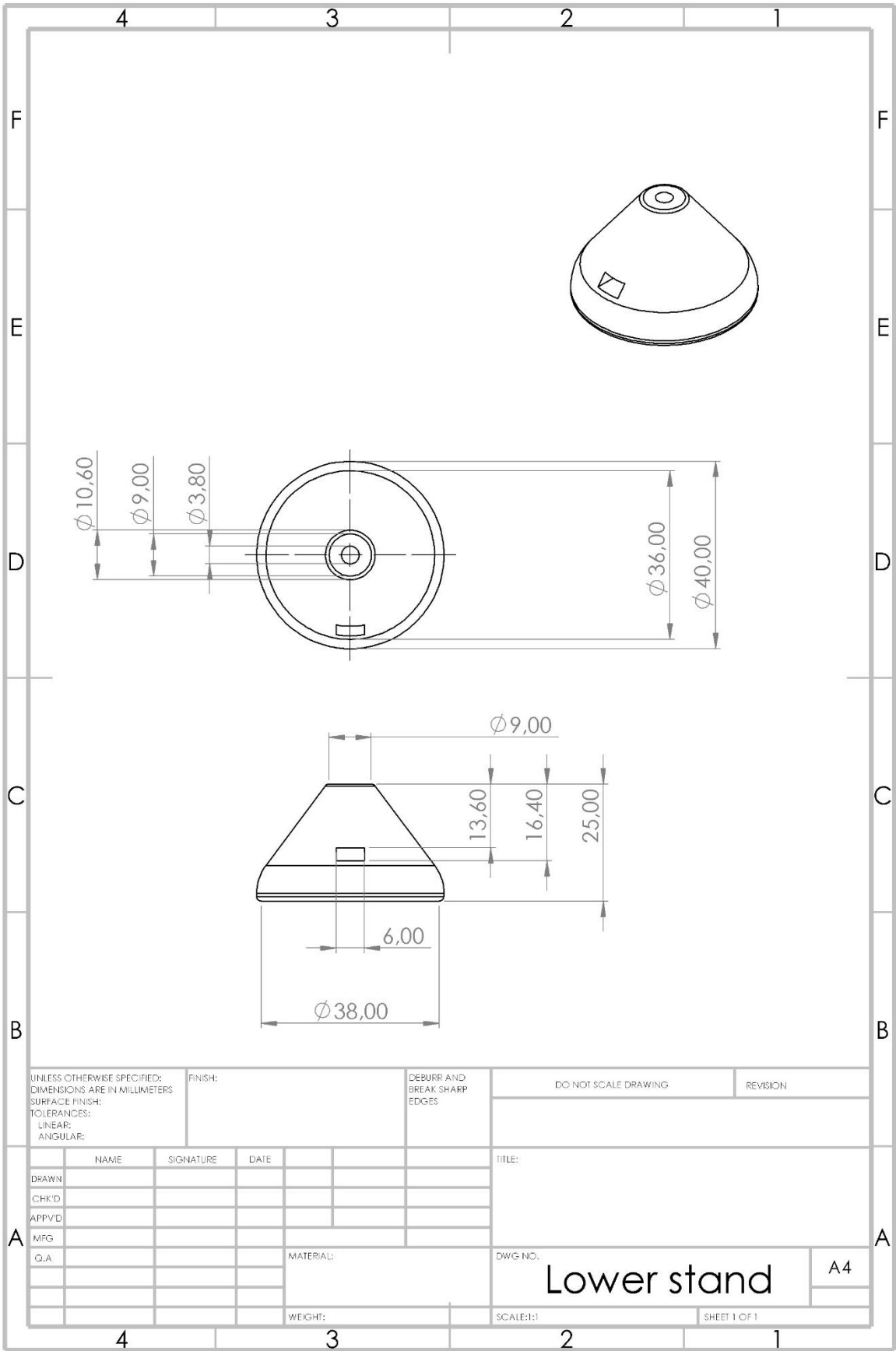
Table:

DWG. NO.	SCALE	SHEET
Housing - top	1:5	1 OF 1

9. Support



10. Lower stand



L. Data Sheets of some (electronic) components

Data sheets are shown for the following components:

- Heaters: main, guard and back
- Temperature sensors
- MOSFETs
- Thermal adhesive glue

Peltier elements were ordered via Hackterstore.nl. Unfortunately, this company does not accompany their products with datasheets.

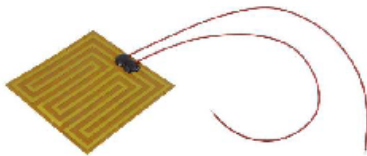
Main heater



DATASHEET

Thermal Foil, 60 * 60 mm
BN 1484113

Version 12/16



Size: 60*60mm
Voltage: 12V
Power: 48W
Material: Polyimide (PI)
Thickness: 0.3mm +/- 0.02mm (including adhesive)
Operation Temp: -20C~100C
Operation Humidity: 10%~100%
Storage Temp: -20C~100C
Storage Humidity: 10%~100%
Max surface temperature: 250C
Element resistance: 2.7-3.3Ω
Watt density chart: 48W
Max. Power/CM2: 0.5W/CM2
Polyimide : 50*70*0.05mm (2PCS)
Alloy Heating wire: 50*70*0.04mm (1PCS)
Cable: UL1332# 24AWG Black L=200mm (2PCS)
3M467 adhesive(1PCS)

This is a publication by Conrad Electronic SE, Klaus-Conrad-Str. 1, D-92240 Hirschau (www.conrad.com).
All rights including translation reserved. Reproduction by any method, e.g. photocopy, microfilming, or the capture in electronic data processing systems require the prior written approval by the editor. Reprinting, also in part, is prohibited. This publication represents the technical status at the time of printing.
© Copyright 2016 by Conrad Electronic SE.

Datenblatt Datasheet

Heizfolie heater

Nennspannung: <i>Nominal Voltage:</i>	12 V (AC oder DC)
Nennleistung: <i>Effective Output:</i>	10 W +/-10%
Abmessungen: <i>Dimensions:</i>	40 x 100 mm 1,57" x 3,94"
Oberflächentemperatur*: <i>Surface temperature**:</i>	ca. 115 °C approx. 239 °F
Sicherheitsthermostat: <i>Safety Thermostat:</i>	nicht vorhanden is not installed
Regelthermostat: <i>Thermostat:</i>	nicht vorhanden is not installed
Dicke: <i>Thickness:</i>	ca. 0,40 mm approx. 0,02"
Träger: <i>Carrier:</i>	Polyesterfolie 125 µm 125 microns polyester foil
Klebeband: <i>Adhesive Tape:</i>	Flammhemmendes Polyesterklebeband mit Schutzpapier Flame-retardant polyester tape with protective paper
Klebstofftyp: <i>Adhesive:</i>	Modifiziertes Acrylat Modified acrylate
Versiegelung: <i>Sealing:</i>	Hochtemperaturbeständiger Dichtstoff High-temperature resistant sealant
Elektro-Anschluss: <i>Electrical Connection:</i>	Kabel FL 2x 0.38 mm ² , Länge ca. 250 mm cable FL 2x 0.38 mm ² , length approx. 250 mm
Temperaturbereich: <i>Temperature Range:</i>	-40 °C bis + 95 °C (Dauerbelastung) Long term loading -40 °F up to max. +203 °F
RoHS konform: <i>RoHS compliant:</i>	Ja yes
Schutzrad: <i>Degree of Protection:</i>	IP X4
Bemerkung:	Achtung: Aufgrund hoher Heizleistung, bezogen auf die Fläche, kann die Heizfolie je nach Einbausituation, ohne ausreichende Kühlung oder Temperaturregelung, überhitzen und dadurch zerstört werden!
Comment:	Attention: Overheating and the resulting destruction, as a consequence of high heating power of the heating foil, can be prevented by providing enough cooling or temperature control, depending on the positioning of the high power heating foil. * Heizfolie frei in der Luft hängend, die Wärmeabgabe erfolgt nur an die Umgebungsluft ** Temperature was measured with the heater suspended freely in the air, the heat was only given off to the ambient air

Datenblatt Heizfolie

Datasheet heater

Nennspannung: <i>Nominal Voltage:</i>	12 V
Nennleistung: <i>Effective Output:</i>	15 W +/-10%
Abmessungen [mm/Zoll]: <i>Dimensions [mm/inch]:</i>	Durchmesser = 90 mm / 3.54" <i>Diameter = 90 mm / 3.54"</i>
Oberflächentemperatur*: <i>Surface temperature**:</i>	ca. 95 °C <i>approx. 203 °F</i>
Regelthermostat: <i>Thermostat:</i>	ohne <i>without</i>
Sicherheitsthermostat: <i>Safety Thermostat:</i>	ohne <i>without</i>
Dicke: <i>Thickness:</i>	ca. 0,4 mm (0.016") <i>approx. 0.4 mm (0.016")</i>
Träger: <i>Carrier:</i>	125 µm Polyesterfolie <i>125 microns polyester foil</i>
Klebeband: <i>Adhesive Tape:</i>	Flammhemmendes Polyesterklebeband m. Silikon-Schutzpapier <i>Flame-retardant polyester foil with silicon protective paper</i>
Klebstoff: <i>Adhesive:</i>	Modifiziertes Acrylat <i>Modified Acrylate</i>
Versiegelung: <i>Sealing:</i>	Hochtemperaturbeständiger Dichtstoff <i>High-temperature resistant sealant</i>
Elektro-Anschluss: <i>Electrical Connection:</i>	Zwillingskabel 2x 0,75 mm ² <i>Double cable 2x 0.75 mm²</i>
Temperaturbereich: <i>Temperature Range:</i>	Dauerbelastung -40 °C (-40 °F) bis max. +95 °C (+203 °F) <i>Long term loading -40 °C (-40 °F) up to max. +95 °C (+203 °F)</i>
RoHS konform: <i>RoHS compliant:</i>	Ja <i>yes</i>
Schutzrad: <i>Degree of Protection:</i>	IP X4 <i>IP X4</i>
Bemerkung:	Achtung: Aufgrund hoher Heizleistung, bezogen auf die Fläche, kann die Heizfolie je nach Einbausituation, ohne ausreichende Kühlung oder Temperaturregelung, überhitzen und dadurch zerstört werden!
Comment:	Attention: Overheating and the resulting destruction, as a consequence of high heating power of the heating foil, can be prevented by providing enough cooling or temperature control, depending on the positioning of the high power heating foil. * Heizfolie frei in der Luft hängend, die Wärmeabgabe erfolgt nur an die Umgebungsluft ** Temperature was measured with the heater suspended freely in the air, the heat was only given off to the ambient air



NTC Thermistor : TTF Series

Insulation Film Type for Temperature Sensing/Compensation

■ Features

1. RoHS compliant
2. Halogen-Free (Hf) series are available
3. Radial leaded insulation film coated
4. Operating temperature range: -40°C~+100°C
5. Aging recognition: $\Delta L/\Delta L$

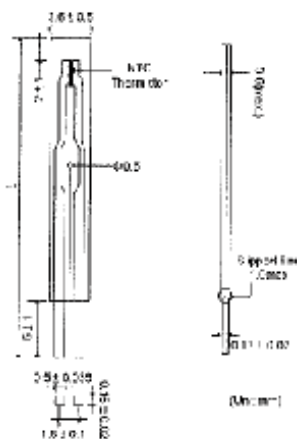
■ Recommended Applications

1. Home appliances
2. Computers
3. Battery packs

■ Part Number Code

1	2	3	4	5	6	7	8	9	10	11	12	13	14	15	16
Product Type	Size	Definition of B Value	Zero Power Resistance (R ₀)	Tolerance of R ₀	B Value	Tolerance of B Value	Optional Suffix								
TTF-ND TTF-NTC TTF Series	3 W3.5mm	A 3mm B 3mm	100 1000 100 10000 470 4700	F ±1% G ±2% H ±3% J ±5% K ±10%	335 3380 343 3430 380 3850 391 3970 432 4320	1 ±1% 2 ±2% 3 ±3%	V RoHS Compliant H RoHS & HF Compliant								
								Appearance							
								A 13.5mm±0.2mm±0.5mm							
								B 13.5mm±0.2mm±0.5mm							

■ Structure and Dimensions



MOSFETS

International
IR Rectifier

PD - 94831

IRLZ44NPbF

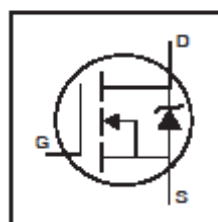
HEXFET® Power MOSFET

- Logic-Level Gate Drive
- Advanced Process Technology
- Dynamic dv/dt Rating
- 175°C Operating Temperature
- Fast Switching
- Fully Avalanche Rated
- Lead-Free

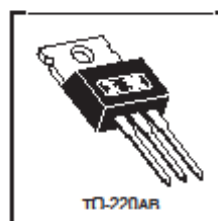
Description

Fifth Generation HEXFETs from International Rectifier utilize advanced processing techniques to achieve the lowest possible on-resistance per silicon area. This benefit, combined with the fast switching speed and ruggedized device design that HEXFET Power MOSFETs are well known for, provides the designer with an extremely efficient device for use in a wide variety of applications.

The TO-220 package is universally preferred for all commercial-industrial applications at power dissipation levels to approximately 50 watts. The low thermal resistance and low package cost of the TO-220 contribute to its wide acceptance throughout the industry.



$V_{DS} = 55V$
$R_{DS(on)} = 0.022\Omega$
$I_D = 47A$



Absolute Maximum Ratings

	Parameter	Max.	Units
$I_D @ T_C = 25^\circ C$	Continuous Drain Current, $V_{GS} @ 10V$	47	A
$I_D @ T_C = 100^\circ C$	Continuous Drain Current, $V_{GS} @ 10V$	33	
I_{DM}	Pulsed Drain Current Φ	160	
$P_D @ T_C = 25^\circ C$	Power Dissipation	110	W
	Linear Derating Factor	0.71	W/°C
V_{GS}	Gate-to-Source Voltage	± 16	V
E_{AS}	Single Pulse Avalanche Energy Φ	210	mJ
I_{AR}	Avalanche Current Φ	25	A
E_{AR}	Repetitive Avalanche Energy Φ	11	mJ
dv/dt	Peak Diode Recovery dv/dt Φ	5.0	V/ns
T_J	Operating Junction and	-55 to +175	°C
T_{STG}	Storage Temperature Range		
	Soldering Temperature, for 10 seconds	300 (1.6mm from case)	
	Mounting torque, 6-32 or M3 screw.	10 lbf-in (1.1N-m)	

Thermal Resistance

	Parameter	Min.	Typ.	Max.	Units
$R_{\theta JC}$	Junction-to-Case	0.02	0.02	1.4	°C/W
$R_{\theta CS}$	Case-to-Sink, Flat, Greased Surface	0.02	0.50		
$R_{\theta JA}$	Junction-to-Ambient	0.02		62	

11/11/03

Thermal Management Solutions Technical Data Sheet

ELECTROLUBE
THE SOLUTIONS PEOPLE

Page 1

TCOR Thermally Conductive RTV (Oxime)

TCOR is a single component, 100% solids, low odour silicone RTV which cures upon exposure to atmospheric moisture. It has been designed to fill the gap between device and heat sink, thus reducing the thermal resistance. It can be applied around components and power resistors to dissipate excess heat to heat sinks, avoiding any potential overheating and subsequent failures. It can also be used as a low bond strength adhesive, sealant or gasketing compound.

- Higher bond strength than standard RTVs; can be used as a sealant or thermal adhesive
- High thermal conductivity; combines adhesive properties with efficiency of heat dissipation
- Very wide operating temperature range; combines properties required for the automotive market
- Single component, non-slump; ideal for applications requiring a higher viscosity product

Approvals	RoHS Compliant (2002/95/EC):	Yes
Typical Properties	Colour: Viscosity @ 1rpm (Pa s): Consistency: Density @ 20°C (g/ml): Shrinkage on Cure Skin Forming Rate*: Cure Time @ 20°C*: *Curing rate and skin forming is dependent upon ambient conditions of temperature and humidity	White 140-150 Non-Slump Paste 2.3 >0.2% 10-15 minutes 24 hours
Cured Properties:	Thermal Conductivity: Temperature Range: Maximum Operating Temperature (30mins): Shore Hardness: Tensile Strength: Peel Strength: Tear Strength: Breaking Strength: Elongation at Break: Dielectric Strength: Electrical Insulation:	1.8 W/m.K -50 to +230°C +250°C A75 2 MPa >4 Kg (aluminium) 1.52 Kg 4.30 Kg 300% >8 kV/mm 1 x 10 ¹⁴ Ohm/cm

<u>Description</u>	<u>Packaging</u>	<u>Order Code</u>	<u>Shelf Life</u>
Thermally Conductive RTV (Oxime)	75ml Syringe	TCOR75S	12 months
Dispensing Gun for 75ml Syringe	1 Unit	TCRGUNB	Not Applicable

Copyright Electrolube 2013

All information is given in good faith but without warranty. Properties are given as a guide only and should not be taken as a specification.

Electrolube cannot be held responsible for the performance of its products within any application determined by the customer, who must satisfy themselves as to the suitability of the product.

Ashby Park, Coalfield Way,
Ashby de la Zouch,
Leicestershire LE65 1JF
T +44 (0)1530 419 500
F +44 (0)1530 416 540
BS EN ISO 9001:2008
Certificate No. FM 32082

M. Arduino Code used for Data Acquisition

Libraries to determine VtoT and PID are available at the flash drive that is to be possessed by dr. ir. A.J. Loeve.

```
/*
   Coding used to regulate the measurements with Therminus-K2, a thermal conductivity measurement device, with.
   By CI Kaanen and AJ Loeve.
   2022-05-01
*/

// Libraries for LCD
#include <Wire.h>
#include <LiquidCrystal_I2C.h>
LiquidCrystal_I2C lcd(0x27, 20, 4);

// Library for temperature sensor
#include <VtoT.h>

// Library for PID controller
#include <PID.h>

float Time;
float Tenv = 22.5;

// *****
// Temperature sensor pins, variables and constants
// *****

double Tmeas = 0.0;
int intPinMax = 1023; //max value an analog read pin can have
double Vmax = 5; //working voltage used for temperature sensors
byte calType = 1; //calibration curve type used for calibration. 1 = polynomial, 2 =steinhart-hart

// Temperature sensor pins
int pinT01 = A8; // Analog IN pin of sensor 01
int pinT02 = A9;
int pinT03 = A10;
int pinT04 = A11;
int pinT05 = A12;
int pinT06 = A13;
int pinT07 = A7;
int pinT08 = A6;
int pinT09 = A5;
int pinT10 = A2;
int pinT11 = A1;
int pinT12 = A0;

// Temperature measurement variables
double Tmeas01; // Temperature measurement of sensor 01
double Tmeas02;
double Tmeas03;
double Tmeas04;
double Tmeas05;
double Tmeas06;
double Tmeas07;
double Tmeas08;
double Tmeas09;
double Tmeas10;
double Tmeas11;
double Tmeas12;

double Tmainheat; // average T-main-hot sensors
double Tcold; // average T-cold-plate sensors

// Temperature measurement coefficients
double calCoefsT01[3] = { -11.4007, 5.3484, 2.8661}; //coefficients for an n-th order polynomial, starting from 0-th
double calCoefsT02[3] = { -13.8369, 8.7169, 2.3267};
```

```

double calCoefsT03[3] = { -17.8685, 16.1408, 1.0563};
double calCoefsT04[3] = { -14.5849, 10.7963, 1.9612};
double calCoefsT05[3] = { -10.1565, 4.8368, 2.9288};
double calCoefsT06[3] = { -12.6369, 6.3822, 2.6672};
double calCoefsT07[3] = { -19.2046, 19.7075, 0.4042};
double calCoefsT08[3] = { -16.5307, 10.7552, 2.0131};
double calCoefsT09[3] = { -8.5646, 3.4738, 3.1317};
double calCoefsT10[3] = { -10.1565, 4.8368, 2.9288};
double calCoefsT11[3] = { -16.7033, 9.2389, 2.1784};
double calCoefsT12[3] = { -14.6098, 8.6946, 2.3689};

byte calCoefsNR = sizeof(calCoefsT01) / sizeof(calCoefsT01[0]); //number of calibration coefficients provided
//Serial.println("calCoefsNR = " + String(calCoefsNR)); // For debugging

// *****
// PID variables and constants
// *****

float setpointcold = -Tenv; //degrees setpoint temperature
float delta_T = 10; // Temperature difference between the plates
float setpointhot = -setpointcold + delta_T; //degrees setpoint temperature
float setpointg = setpointhot; // setpoint guard and back heaters

//PID constants main heater
double Kp_1 = 30;
double Ki_1 = 0.01;
double Kd_1 = 10;
double PWMmaxH = 64; // Maximum PWM value for safety reasons

//PID constants guard heaters
double Kp_2 = 50;
double Ki_2 = 0.05;
double Kd_2 = 100;
double PWMmaxGH = 90;

//PID constants peltier elements
double Kp_6 = 4;
double Ki_6 = 0.001;
double Kd_6 = 10;
double PWMmaxC = 10;

//PID constants back heater
double Kp_7 = 80;
double Ki_7 = 0.1;
double Kd_7 = 10;
double PWMmaxBH = 220;

// *****
// Output (heating) pins, variables and constants
// *****

int gateHPmain = 4; // The pin the digital output PWM for the main HP is connected to
int gateHPg1 = 5; // The pin the digital output PWM for the guard heater 1 is connected to
int gateHPg2 = 2;
int gateHPg3 = 3;
int gateHPg4 = 6;
int gatePE1 = 13;
int gatePE2 = 9;
int gatePE3 = 8;
int gatePE4 = 12;

```



```

int gatePE5 = 45;
int gatePE6 = 7;
int gatePE7 = 11;
int gatePE8 = 10;
int gatePE9 = 44;
int gateBH = 46;

//Make a class for each T sensor so you only have to put in variables once, here at the start of the file
VtoT v2t01(pinT01, intPinMax, Vmax, calType, calCoefsNR, calCoefsT01); //Make class for T01 handling
VtoT v2t02(pinT02, intPinMax, Vmax, calType, calCoefsNR, calCoefsT02);
VtoT v2t03(pinT03, intPinMax, Vmax, calType, calCoefsNR, calCoefsT03);
VtoT v2t04(pinT04, intPinMax, Vmax, calType, calCoefsNR, calCoefsT04);
VtoT v2t05(pinT05, intPinMax, Vmax, calType, calCoefsNR, calCoefsT05);
VtoT v2t06(pinT06, intPinMax, Vmax, calType, calCoefsNR, calCoefsT06);
VtoT v2t07(pinT07, intPinMax, Vmax, calType, calCoefsNR, calCoefsT07);
VtoT v2t08(pinT08, intPinMax, Vmax, calType, calCoefsNR, calCoefsT08);
VtoT v2t09(pinT09, intPinMax, Vmax, calType, calCoefsNR, calCoefsT09);
VtoT v2t10(pinT10, intPinMax, Vmax, calType, calCoefsNR, calCoefsT10);
VtoT v2t11(pinT11, intPinMax, Vmax, calType, calCoefsNR, calCoefsT11);
VtoT v2t12(pinT12, intPinMax, Vmax, calType, calCoefsNR, calCoefsT12);

// Make a class for each PID controller
PID pid01(Tmainheat, setpointhot, Kp_1, Ki_1, Kd_1, PWMmaxH); // Make a class for HPmain handling
PID pid02(Tmeas01, setpointg, Kp_2, Ki_2, Kd_2, PWMmaxGH); // Make a class for HPg1 handling
PID pid03(Tmeas03, setpointg, Kp_2, Ki_2, Kd_2, PWMmaxGH); // Make a class for HPg2 handling
PID pid04(Tmeas02, setpointg, Kp_2, Ki_2, Kd_2, PWMmaxGH); // Make a class for HPg3 handling
PID pid05(Tmeas04, setpointg, Kp_2, Ki_2, Kd_2, PWMmaxGH); // Make a class for HPg4 handling
PID pid06(Tcold, setpointcold, Kp_6, Ki_6, Kd_6, PWMmaxC); // Make a class for Cold Plate handling
PID pid07(Tmeas12, setpointg, Kp_7, Ki_7, Kd_7, PWMmaxBH); // Make a class for Back heater handling

// *****
// Setup and display initial screen
// *****

void setup() {
    // The setup code, to run once:
    Serial.begin(9600);
    Serial.println("Hi there, setup done!");
    Serial.println("Time:Tmainheat;Tcold;dT;outputmh;Tbh;Tmh1;Tmh2;Tgh1;Tgh2;Tgh3;Tgh4;Tc1;Tc2;outputgh1;outputgh2;outputgh3;outputgh4;outputpe;outputbh");
    Serial.println();
    lcd.init();
    lcd.backlight();
}

void loop() {
    // The main code, to run repeatedly:
    Time = millis(); // Start Time measurement
    Tmeas01 = v2t01.CalcT(); // Determine the temperature by sensor 01 via the VtoT library.
    Tmeas02 = v2t02.CalcT();
    Tmeas03 = v2t03.CalcT();
    Tmeas04 = v2t04.CalcT();
    Tmeas05 = v2t05.CalcT();
    Tmeas06 = v2t06.CalcT();
    Tmeas07 = v2t07.CalcT();
    Tmeas08 = v2t08.CalcT();
    Tmeas09 = v2t09.CalcT();
    Tmeas10 = v2t10.CalcT();
    Tmeas11 = v2t11.CalcT();
    Tmeas12 = v2t12.CalcT();

    Tmainheat = (Tmeas05 + Tmeas06) / 2; // Average the temperatures of the main heater s determined by its two individual temperature sensors.
    Tcold = (Tmeas10 + Tmeas11) / 2; // Average the temperatures of the cold plate s determined by its two individual temperature sensors.
    double dT = Tmainheat - Tcold; // Determine the temperature difference between the plates

    int outputmh = pid01.CalcPWM(Tmainheat); //Determine the PWM signal based on the PID controller in the library pid for the main heater
    analogWrite(gateHmain, outputmh); // Write the determined PWM signal as output towards the mosfet regulating the power through the main heater
    int outputgh1 = pid02.CalcPWM(Tmeas01);
    analogWrite(gateHPg1, outputgh1);
    int outputgh2 = pid03.CalcPWM(Tmeas03);
    analogWrite(gateHPg2, outputgh2);
    int outputgh3 = pid04.CalcPWM(Tmeas02);
    analogWrite(gateHPg3, outputgh3);
    int outputgh4 = pid05.CalcPWM(Tmeas04);
    analogWrite(gateHPg4, outputgh4);
    int outputpe = pid06.CalcPWM(-Tcold);

    analogWrite(gatePE1, outputpe);
    analogWrite(gatePE2, outputpe);
    analogWrite(gatePE3, outputpe);
    analogWrite(gatePE4, outputpe);
    analogWrite(gatePE5, outputpe);
    analogWrite(gatePE6, outputpe);
    analogWrite(gatePE7, outputpe);
    analogWrite(gatePE8, outputpe);
    analogWrite(gatePE9, outputpe);

    int outputbh = pid07.CalcPWM(Tmeas12);
    analogWrite(gateBH, outputbh);
}

```

```

delay(500);

Serial.print(Time); // Print output values to later use in the post processing
Serial.print(";");
Serial.print(Tmainheat);
Serial.print(";");
Serial.print(Tcold);
Serial.print(";");
Serial.print(dT);
Serial.print(";");
Serial.print(outputmh);
Serial.print(";");
Serial.print(Tmeas12);
Serial.print(";");
Serial.print(Tmeas05);
Serial.print(";");
Serial.print(Tmeas06);
Serial.print(";");
Serial.print(Tmeas01);
Serial.print(";");
Serial.print(Tmeas03);
Serial.print(";");
Serial.print(Tmeas02);
Serial.print(";");
Serial.print(Tmeas04);
Serial.print(";");
Serial.print(Tmeas10);
Serial.print(";");
Serial.print(Tmeas11);
Serial.print(";");
Serial.print(outputgh1);
Serial.print(";");
Serial.print(outputgh2);
Serial.print(";");
Serial.print(outputgh3);
Serial.print(";");
Serial.print(outputgh4);
Serial.print(";");
Serial.print(outputpe);
Serial.print(";");
Serial.println(outputbh);

lcd.setCursor(0, 0); // Print temperatures on LCD screen for real time insight into the measurement.
lcd.print("H:");
lcd.print(Tmainheat, 1);
lcd.print(" 1:");
lcd.print(Tmeas01, 1);
lcd.print(" 2:");
lcd.print(Tmeas03, 1);

lcd.setCursor(0, 1);
lcd.print("Hp:");
lcd.print(outputmh);
lcd.setCursor(7, 1);
lcd.print("3:");
lcd.print(Tmeas02, 1);
lcd.print(" 4:");
lcd.print(Tmeas04, 1);

lcd.setCursor(0, 2);
lcd.print("C1:");
lcd.print(Tmeas10, 1);
lcd.print(" C2:");
lcd.print(Tmeas11, 1);

lcd.setCursor(0, 3);
lcd.print("C:");
lcd.print(outputpe, 1);
lcd.print("  Tbh:");
lcd.print(Tmeas12, 1);

```

N. Full MATLAB Code

```

%% POST-PROCESSING FOR THERMAL CONDUCTIVITY MEASUREMENTS
% Determine the k-value of a sample by Therminus-K2
% By Charlotte Kaanen (4453719) - May 2022
clear all; close all; clc;

%% Specify constants and read data

% Specify measurement specified constants [ADJUST PER SAMPLE AND
% DEVICE CONFIGURATION!
L = 0.6;           % sample thickness in mm
A = 3618.02;       % measuring area (60.1*60.2 mm) -> 3618.02 mm^2
npe = 9;           % number of peltier elements
gh = 1;           % guard heater (1 = ON; 0 = OFF)
bh = 1;           % back heater (1 = ON; 0 = OFF)

% Read data from Excel file
M = readmatrix('20220408-V06-DataGHPmeasurement.xlsx');

%% Import parameters from data matrix for one measurement
Time = M(2:end,1);
Time = Time./60000; % milliseconds to minutes
ind = find(Time > 30, 1, 'first'); % change per measurement time
Time = Time(1:ind);
ind = ind + 1;
% only data in measurement time
Tmh = M(2:ind,2); % Temperature main heater
Tc = M(2:ind,3); % Temperature cold plate
dT = M(2:ind,4); % Temperature difference hotcold
PWM_mh = M(2:ind,5); % delivered PWM to main heater
Tbh = M(2:ind,6); % Temperature back heater
Tmh1 = M(2:ind,7); % Temperature sensor 1 main heater
Tmh2 = M(2:ind,8); % Temperature sensor 2 main heater
Tgh1 = M(2:ind,9); % Temperature sensor 1 guard heater
Tgh2 = M(2:ind,10); % Temperature sensor 2 guard heater
Tgh3 = M(2:ind,11); % Temperature sensor 3 guard heater
Tgh4 = M(2:ind,12); % Temperature sensor 4 guard heater
Tc1 = M(2:ind,13); % Temperature sensor 1 cold plate
Tc2 = M(2:ind,14); % Temperature sensor 2 cold plate
PWM_gh1 = M(2:ind,15); % delivered PWM to guard heater 1
PWM_gh2 = M(2:ind,16); % delivered PWM to guard heater 2
PWM_gh3 = M(2:ind,17); % delivered PWM to guard heater 3
PWM_gh4 = M(2:ind,18); % delivered PWM to guard heater 4
PWM_cold = M(2:ind,19); % delivered PWM to Peltier elements
PWM_bh = M(2:ind,20); % delivered PWM to back heater

% Calculate power delivered to the loads by a 8-bit (resolution 256) PWM
% output signal. Duty cycle = PWM output / total PWM resolution.
bits = 256; % 8-bit resolution is 256
duty_out = PWM_mh./bits; % duty cycle to main heater
duty_gh1 = PWM_gh1./bits; % duty cycle to guard heater 1
duty_gh2 = PWM_gh2./bits; % duty cycle to guard heater 2
duty_gh3 = PWM_gh3./bits; % duty cycle to guard heater 3
duty_gh4 = PWM_gh4./bits; % duty cycle to guard heater 4
duty_cold = PWM_cold./bits; % duty cycle to individual peltier elements
duty_bh = PWM_bh./bits; % duty cycle to back heater
Q = 48*duty_out; % power to the main heater [Watt]
Q_gh1 = 10*duty_gh1*gh; % power to guard heater 1 [Watt]
Q_gh2 = 10*duty_gh2*gh; % power to guard heater 2 [Watt]
Q_gh3 = 10*duty_gh3*gh; % power to guard heater 3 [Watt]
Q_gh4 = 10*duty_gh4*gh; % power to guard heater 4 [Watt]
Q_cold = 50*duty_cold*npe; % power to total peltier elements [Watt]
Q_bh = 15*duty_bh*bh; % power to back heater [Watt]

Qunf = Q; % Save unfiltered power main heater data
dunf = dT; % Save unfiltered temp difference data
%% VISUALIZE DATA: Temperature sensors and PWM output signals to the loads

```

```

% Visualize raw data, prior to any post-processing
figure(1)
sgtitle("Raw data visualisation");
subplot(1,2,1);
plot(Time,Tmh1);
hold on
plot(Time,Tmh2);
plot(Time,Tc1);
plot(Time,Tc2);
plot(Time,Tgh1);
plot(Time,Tgh2);
plot(Time,Tgh3);
plot(Time,Tgh4);
plot(Time,Tbh);
title("Data temperature sensors during measurement");
xlabel('Time [minutes]');
ylabel('Temperature [degrees Celsius]');
legend('mh1','mh2','c1','c2','gh1','gh2','gh3','gh4','bh');
xlim([0 30]);

subplot(1,2,2);
plot(Time,Q);
hold on
plot(Time,Q_gh1);
plot(Time,Q_gh2);
plot(Time,Q_gh3);
plot(Time,Q_gh4);
plot(Time,Q_cold);
plot(Time,Q_bh);
title("Data power outputs during measurement");
xlabel('Time [minutes]');
ylabel('Power [Watt]');
legend('mh','gh1','gh2','gh3','gh4','cold','bh');
xlim([0 30]);

%% Data filtering to remove outliers and smooth data (dT and Qmh).

stepmh = 48/bits;          % resolution for PWM output to main heater (48 Watt)
stepgh = 10/bits;          % to a guard heater (10 Watt)
steppe = npe*50/bits;      % to total peltiers (npe * 50 Watt)
stepbh = 15/bits;          % to the back heater (15 Watt)
stepT = 0.1;               % resolution for temperature sensors

% Outliers removal was only performed after the initialisation of the
% measurement at approximately 1 minute (100th step). When the difference
% between two successive data points was more than x - times the resolution,
% the next four data points adopt the average value of the past four values

%Remove outliers in Qmh: power to main heater
for k = 100:length(Q);
    if k+1 <= length(Q)-10;          % measure to prevent chaos at the end
        if abs(Q(k+1)-Q(k)) >= 6*stepmh; % check if diff is above stepsize
            Q((k+1):(k+4)) = (Q(k)+Q(k-1)+Q(k-2)+Q(k-3))./4; %fill outlier
        end
    end
end

%remove outliers in dT: temperature difference
for k = 100:length(dT);
    if k+1 <= length(dT)-10;
        if abs(dT(k+1)-dT(k)) >= 6*stepT;
            dT((k+1):(k+4)) = (dT(k)+dT(k-1)+dT(k-2)+dT(k-3))./4;
        end
    end
end

%remove outliers in Tmh: temperature of main heater
for k = 100:length(Tmh);
    if k+1 <= length(Tmh)-10;

```

```

        if abs(Tmh(k+1)-Tmh(k)) >= 6*stepT;
        Tmh((k+1):(k+4)) = (Tmh(k)+Tmh(k-1)+Tmh(k-2)+Tmh(k-3))./4;
        end
    end
end

%remove outliers in Tgh1: temperature of guard heater 1
for k = 100:length(Tgh1);
    if k+1 <= length(Tgh1)-10;
        if abs(Tgh1(k+1)-Tgh1(k)) >= 6*stepT;
            Tgh1((k+1):(k+4)) = (Tgh1(k)+Tgh1(k-1)+Tgh1(k-2)+Tgh1(k-3))./4;
            end
        end
    end
end
%remove outliers in Tgh2: temperature of guard heater 2
for k = 100:length(Tgh2);
    if k+1 <= length(Tgh2)-10;
        if abs(Tgh2(k+1)-Tgh2(k)) >= 6*stepT;
            Tgh2((k+1):(k+4)) = (Tgh2(k)+Tgh2(k-1)+Tgh2(k-2)+Tgh2(k-3))./4;
            end
        end
    end
end
%remove outliers in Tgh3: temperature of guard heater 3
for k = 100:length(Tgh3);
    if k+1 <= length(Tgh3)-10;
        if abs(Tgh3(k+1)-Tgh3(k)) >= 6*stepT;
            Tgh3((k+1):(k+4)) = (Tgh3(k)+Tgh3(k-1)+Tgh3(k-2)+Tgh3(k-3))./4;
            end
        end
    end
end
%remove outliers in Tgh4: temperature of guard heater 4
for k = 100:length(Tgh4);
    if k+1 <= length(Tgh4)-10;
        if abs(Tgh4(k+1)-Tgh4(k)) >= 6*stepT;
            Tgh4((k+1):(k+4)) = (Tgh4(k)+Tgh4(k-1)+Tgh4(k-2)+Tgh4(k-3))./4;
            end
        end
    end
end
end

%remove outliers in Tbh: temperature of the back heater
for k = 100:length(Tbh);
    if k+1 <= length(Tbh)-10;
        if abs(Tbh(k+1)-Tbh(k)) >= 6*stepT;
            Tbh((k+1):(k+4)) = (Tbh(k)+Tbh(k-1)+Tbh(k-2)+Tbh(k-3))./4;
            end
        end
    end
end
end

%Calculate the moving mean over time of the data with removed outliers
Qm      = movmean(Q,[10,10],'Endpoints','shrink');
dTm     = movmean(dT,[10,10],'Endpoints','shrink');
Tmhm    = movmean(Tmh,[10,10],'Endpoints','shrink');
Tgh1m   = movmean(Tgh1,[10,10],'Endpoints','shrink');
Tgh2m   = movmean(Tgh2,[10,10],'Endpoints','shrink');
Tgh3m   = movmean(Tgh3,[10,10],'Endpoints','shrink');
Tgh4m   = movmean(Tgh4,[10,10],'Endpoints','shrink');
Tbhm    = movmean(Tbh,[10,10],'Endpoints','shrink');

%% VISUALIZE FILTERED Temperature DATA
figure(2)
sgtitle("Filtered temperature data");
plot(Time,Tmhm,'LineWidth',1);
hold on
plot(Time,Tgh1m,'LineWidth',1);
plot(Time,Tgh2m,'LineWidth',1);
plot(Time,Tgh3m,'LineWidth',1);
plot(Time,Tgh4m,'LineWidth',1);
plot(Time,Tbhm,'LineWidth',1);
xlabel('Time [minutes]');

```

```

ylabel('Temperature [degrees Celsius]');
legend('Tmh','Tgh1','Tgh2','Tgh3','Tgh4','Tbh');
xlim([0 30]);

%% VISUALIZE FILTERED DT and Q data
figure(3)
sgttitle('Raw and filtered Data Visualisation');
subplot(1,2,1)
plot(Time,Qunf,'color','color','0072BD');
hold on
plot(Time,Q,'m');
plot(Time,Qm,'color','color','A2142F','Linewidth',3);
title("Power delivered to the main heater during measurement");
xlabel('Time [minutes]');
ylabel('Power [Watt]');
legend('Raw data','Outliers removed from data','Smoothed data');
xlim([0 30]);
subplot(1,2,2);
plot(Time,dunf,'color','color','0072BD');
hold on
plot(Time,dT,'m');
plot(Time,dTm,'color','color','A2142F','Linewidth',3);
title("Temperature difference between the hot and cold plate during measurement");
xlabel('Time [minutes]');
ylabel('Temperature [degrees Celsius]');
legend('Raw data','Outliers removed from data','Smoothed data');
xlim([0 30]);

%% ANALYSE DATA: Determine k-value during steady state measurement
% use filtered dT and Qmh to Calculate the k-value over time
k = (Qm.*L)./(A.*10^-3).*dTm;

% calculate the moving mean derivatives of dT, k and Q
ddT = movmean(diff(dTm),[20,20]);
dk = movmean(diff(k),[20,20]);
dQ = movmean(diff(Qm),[20,20]);

%%
% Calculate the difference between the guard heaters and back heater, and
% the main heater
egh1 = Tmhm - Tgh1m;
egh2 = Tmhm - Tgh2m;
egh3 = Tmhm - Tgh3m;
egh4 = Tmhm - Tgh4m;
ebh = Tmhm - Tbh;

% Determine the data points at which steady state was reached
SS = find((abs(ddT)<0.001) & (abs(dQ)<0.001) & (abs(egh1(2:end))<0.5) &
(abs(egh2(2:end))<0.5) & (abs(egh3(2:end))<0.5) & (abs(egh4(2:end))<0.5) &
(abs(ebh(2:end))<0.5));
kSS = k(SS); % only include k in steady state for plot
TimeSS = Time(SS); % only include time in steady state for plot

% DETERMINE K, Q AND dT IN STEADY STATE AND TIME TO REACH THAT
k_SS = mean(kSS); % aveage k in steady state
kSS_max = max(kSS); % maximum k in steady state
kSS_min = min(kSS); % minimum k in steady state
kSS_std = std(kSS); % std of k in steady state
dT_SS = mean(dTm(SS)); % average dT in steady state
Q_SS = mean(Qm(SS)); % average Q in steady state

figure(5);
title("Thermal conductivity coefficient (" + k_SS + " W/mK)");
hold on
xlabel('Time [minutes]');
ylabel('Thermal conductivity coefficient [W/mK]');
grid minor
plot(Time,k);

```

```

hold on
xlim([0 30]);
if kSS == 0;
else
    plot(TimeSS, kSS, '.');
end
legend('Transient state', 'Steady state');

%% Overview graphs to explain results
figure(6)
sgtitle('Overview graph to explain results');
subplot(1,2,1)
yyaxis left
plot(Time, k);
ylabel('Thermal conductivity coefficient [W/mK]');
xlabel('Time [minutes]');
yyaxis right
plot(Time, Qm);
ylabel('Power to main heater [Watt]');
subplot(1,2,2)
yyaxis left
plot(Time, k);
ylabel('Thermal conductivity coefficient [W/mK]')
xlabel('Time [minutes]')
yyaxis right
plot(Time, dTm);
ylabel('Temperature difference [degrees Celsius]')

%% OUTPUT
TimeSS1 = TimeSS(1); % First time in steady state
TimeSSlength = length(TimeSS)*0.011; % Total time in steady state

% [k; kmin; kmax; kstd; dT; Q; TimeSS1; TimeSSlength]
OUTPUT = [k_SS kSS_min kSS_max kSS_std dT_SS Q_SS TimeSS1 TimeSSlength]

```

O. Output of post-processing data in MATLAB

This appendix contains an example of output plots generated after post-processing of the measurement data. The Excel data used for this example was saved in 20220428-V04-DataGHPmeasurement.xlsx. The MATLAB code that generated these plots is described in Appendix N. Section 5.2.3 contains further explanation about the post-processing the data was subjected to.

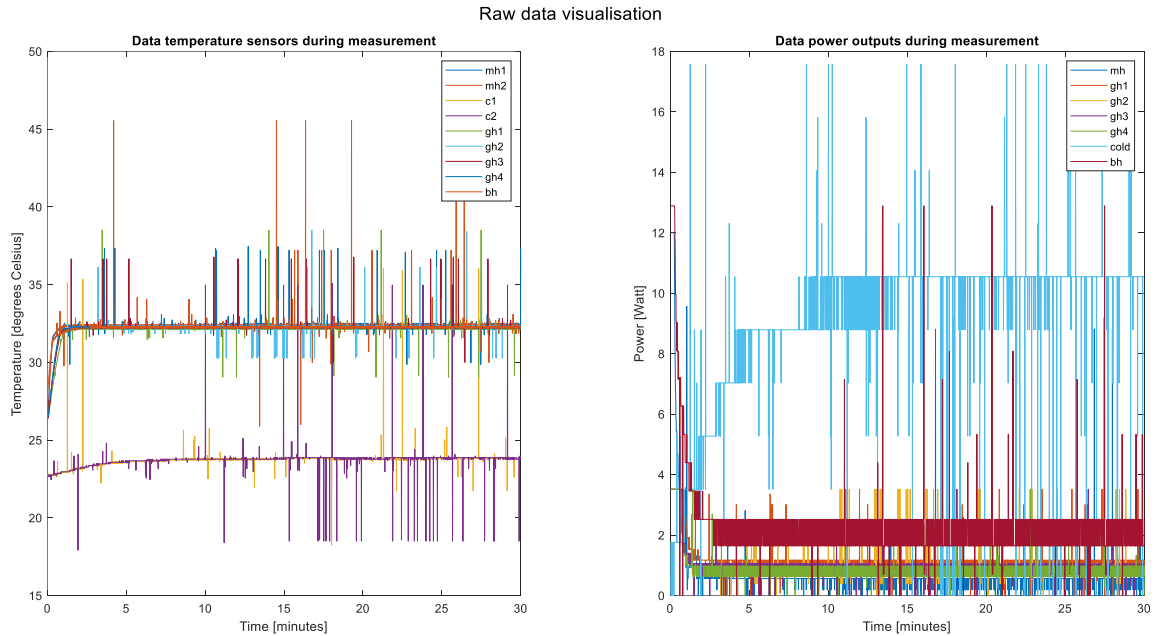


Figure 56. Visualization of the raw data of a measurement by Thermanus-K2: temperature sensor data and PWM output signals over time.

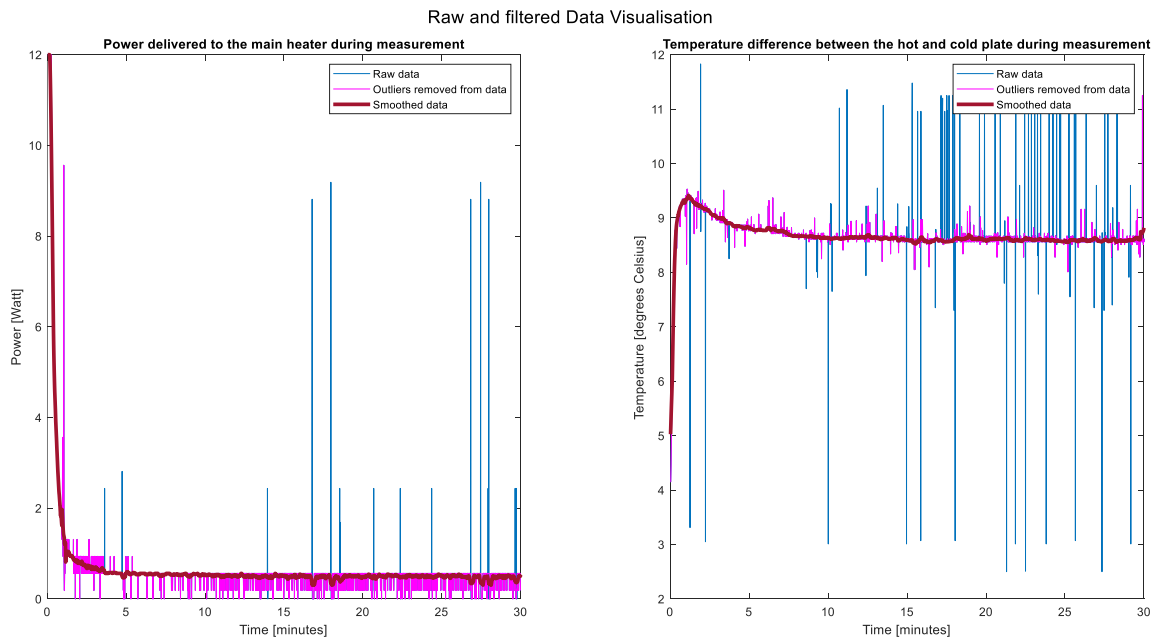


Figure 57. Graphs for both raw and filtered data of the power delivered to the main heater and the temperature difference between hot and cold plate, over time.

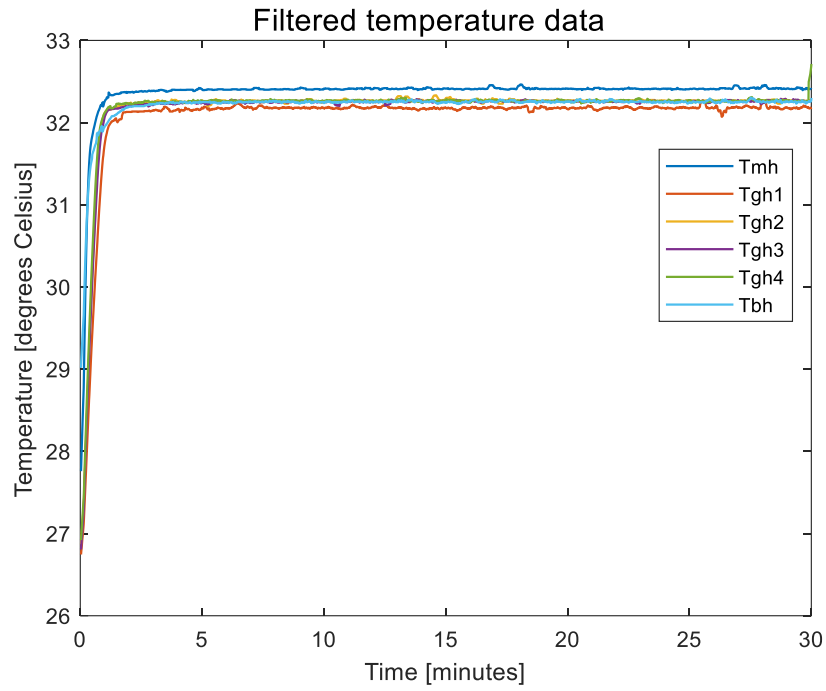


Figure 58. Graph of the filtered temperature sensor data over time.

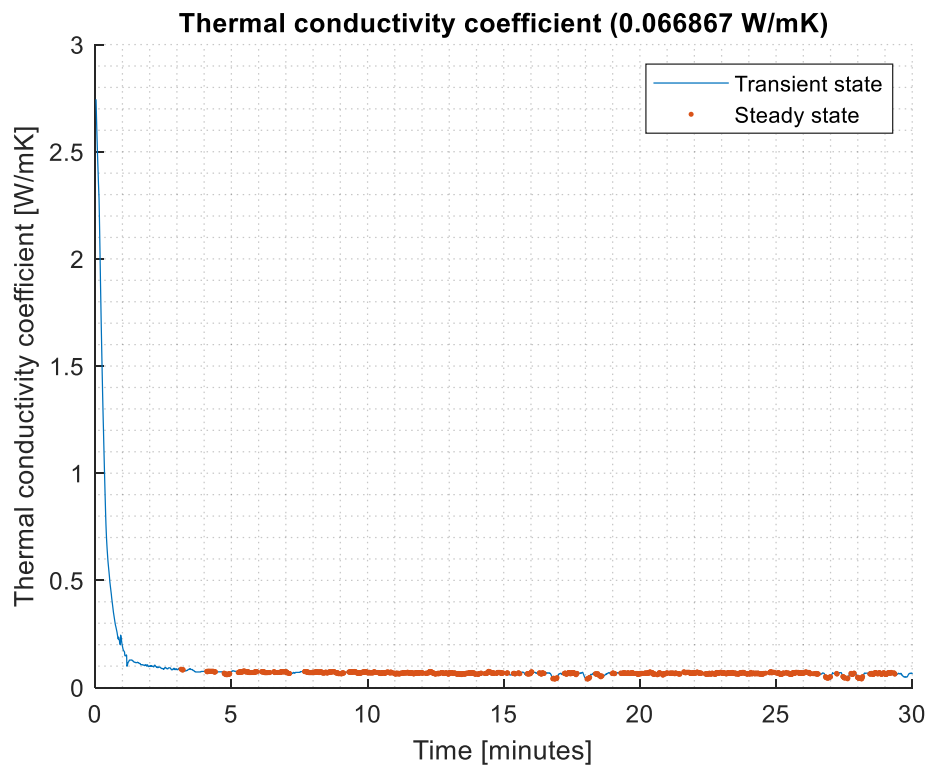


Figure 59. Graph of the calculated thermal conductivity coefficient (k) over time, in which the bold lines indicate the part in which steady state was achieved (as formulated in the customized post-processing: section 5.2.3).

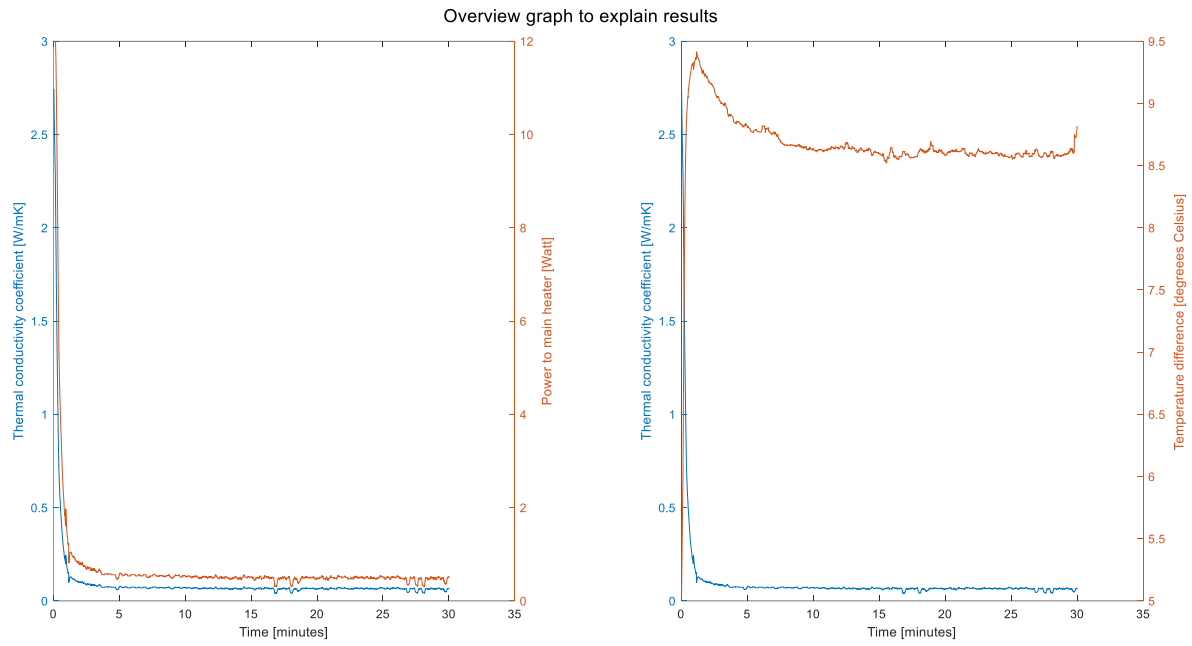


Figure 60. Visualization of the calculated thermal conductivity coefficient (k) over time plotted together with the power delivered to the main heater (left) and the temperature difference between the hot and cold plate (right).

P. Literature Study

A Systematic Review on Factors Affecting Thermal Conductivity Measurement of Clothing in a Forensic Context

Literature study as part of the MSc-Assignment-Therminus-ThermalMeasurement

C.I. Kaanen (4453719)¹

Supervised by drs. C.A.W. Pellemans² and dr. ir. A.J. Loeve³

¹ *MSc programme BioMedical Engineering, Delft University of Technology, 2628 CD Delft, The Netherlands*

² *Forensic Investigation, Politie Nederland, 3709 JA Zeist, The Netherlands*

³ *Department of BioMechanical Engineering, Delft University of Technology, 2628 CD Delft, The Netherlands*

Delft, December 2021

Abstract

Background Determining the postmortem interval (PMI), the time passed shortly (3 – 72 hours) after an individual's death, is often a vital component to evidence in forensics. In order to calculate the PMI utilizing the thermodynamic cooling model, instant determination of the thermal conductivity (TC) of the deceased's clothing is required at the crime scene. However, simple and inexpensive measurement devices for TC determination for forensic purposes are currently lacking. Therefore, a new device must be developed. For this development, factors affecting TC measurement of clothing should be explored.

Purpose A literature review was performed to provide an overview of factors influencing TC measurement of clothing.

Methods Following the PRISMA methodology, a literature search was conducted in Scopus. Data of included studies were extracted and descriptive analysis was executed.

Results and Conclusions A total of 48 studies were included, reporting twelve different factors affecting TC measurement of clothing. For forensic purposes, the most dominant factors (effect size > 100%) were fabric thickness (correlation with TC: –), moisture content (+), air layer thickness (–) and fabric compression (+). Prior to and during measurements, alterations of the clothing sample must be avoided and a direct connection between clothing sample and measurement plates should be established. In the design of a TC measurement device, precise fabric thickness measurement and water tightness of the design should be focused on.

Keywords Thermal conductivity · Thermal resistivity · Textile · Clothing · Measurement · Review

1 Introduction

In 2019, 1.811 people in the Netherlands committed suicide and 125 murders were committed [1, 2]. Besides these, other non-natural deaths like (un)intentional injuries and accidents unfortunately occur regularly, although exact numbers were not available.

When finding human remains, obviously the cause and time of death must be determined. Consequently, the Dutch

Police needs to investigate many bodies throughout the year.

Estimation of the early postmortem interval (PMI), the time passed shortly (3 – 72 hours) after death, is used for several purposes [3]. The PMI estimation can be used to narrow down and test possible scenarios when mortal remains are found by reducing the estimated time frame of the PMI. In forensic investigations, the PMI

could help in temporal reconstructions of the events surrounding the death. Investigations can proceed with more focus, when the estimated range of the PMI is narrower. This allows for faster research, which is crucial in forensic investigations. Forensic information becomes more meaningful when it is obtained at a higher speed [4]. In addition, the increased speed helps to strengthen red-handedness, enables swift adjustments to the investigation if needed, and makes the investigation as efficient as possible [5].

Nomenclature

Abbreviations

TC	Thermal conductivity
TR	Thermal resistance
PMI	Post mortem interval
GHP	Guarded hot plate
SGHP	Sweating guarded hot plate

Materials

AR	Aramid
BA	Bamboo
CA	Hemp
CA	Acetate
CMD	Modal
CO	Cotton
CV	Viscose (Rayon)
EL	Elastane (Lycra or Spandex)
FG	Fiberglass
JU	Jute
KP	Kapok
LI	Linen
MAC	Modacrylic
NY	Nylon
PA	Polyamide
PAN	Acrylic
PC	Polycarbonate
PE	Polyethylene
PES	Polyester
PET	Polyethylene terephthalate
PP	Polypropylene
PTFE	Polytetrafluoroethylene
PUR	Polyurethane
PVC	Polyvinylchloride
SE	Silk
WM	Mohair
WO	Wool

Currently, the PMI is determined using the golden standard: Henssge's method [3, 6]. This method is mainly based on rectal (core) temperature, body weight and ambient temperature and relates these factors to the PMI. It is presented as a nomogram and assumes that the postmortem rectal temperature of any human undergoes double exponential decay. The model, however, includes only one correction factor for cooling conditions deviating from the standard, based on body weight and clothing estimations [6]. For the estimation of this correction factor, personal experience in estimating body weight and clothing parameters is required [7]. However, Henssge's method does not take other non-standard environmental and posture conditions into account, which limits its accuracy.

Therefore, Wilk et al. (2020) developed a new method to estimate the PMI, which uses skin thermometry together with a thermodynamic finite-difference model [8]. This model is extremely promising, as it can reduce the maximum error of the PMI estimation from ± 7 hours (Henssge) to ± 3.2 hours (Wilk), respectively based on data of 53 bodies (maximum true PMI: 75 hours) and 4 bodies (maximum true PMI: 50 hours) [7, 8]. Furthermore, 83.3% of the reconstructed PMIs ($n = 80$; calculated based on the same 4 bodies) by Wilk et al. (2020) deviated no more than ± 1 hour from their corresponding real PMIs [8].

The main input parameters in Wilk's model are initial body temperature, body weight, body fat percentage, thermal conductivity (TC) of clothes, TC of fat tissue and TC of non-fat tissue. According to Wilk et al. (2020), variation in TC of clothes (± 0.01 W/mK) induces the largest variation in the PMI estimation ($\pm 1-2$ hours) [8]. Therefore, it is important that TC of the deceased's clothes are correctly determined. That way, it can be used as input in the cooling model to determine the PMI at a crime scene.

Unfortunately, since TC of clothing depends on many parameters, it cannot

simply be calculated based on the material composition of the clothing indicated in its garment label. In fact, intrinsic fabric construction parameters, like weaving pattern, yarn spacing, (nano)additives and multilayer sequences change TC of a clothing piece [9-12]. When determining a clothing's TC based only on its material composition, crucial impact of these factors might be unjustly ignored.

To settle this difficulty, a reliable and standardized TC measurement method is needed that can measure TC of a piece of the deceased's clothing directly at a crime scene. Existing TC measurement systems are currently unsuitable to use for forensic purposes, especially at crime scenes, due to their limited mobility and high costs. Therefore, a novel TC measurement device is being developed for this purpose.

Insight into factors possibly affecting a TC measurement system is indispensable in developing such a method. Factors influencing TC measurement of construction materials have already been investigated, but a review on TC of clothing has, to the best of our knowledge, not yet been conducted [13].

Therefore, this review aimed to provide an overview of factors influencing apparent TC of textile during TC measurement. The effects of these factors were evaluated, and ways to control them prior to and during measurement were examined.

This knowledge is intended to support the design and use of a TC measurement device. Hence, only factors that can be controlled or accounted for during measurements, without changing the intrinsic material properties, were investigated. This implies that intrinsic fabric parameters, like microstructure, density, (fiber) composition and weaving pattern, were disregarded as the material sample cannot and should not be changed.

The research question therefore was: What factors, besides non-adjustable intrinsic fabric parameters, affect TC measurement of clothing, and how?

1.1. Background

In heat transfer, the first law of thermodynamics (conservation of energy) describes that a change in a system's internal energy ΔU [J] is equal to the difference between heat transferred into the system and heat generated within the system, where \dot{Q} [W] is the rate at which heat transfers into the system and \dot{Q}_v [W] is the rate at which heat is generated within the system [14]. Over a time interval Δt [s], the first law of thermodynamics results in the formula

$$\Delta U = \dot{Q}\Delta t - \dot{Q}_v\Delta t \text{ [J]} \quad (1)$$

Heat transfer, the energy transfer due to temperature gradients, can take place due to conduction (the transfer of heat due to interaction between adjacent particles), convection (the heat transfer between a solid surface and an adjacent moving medium), and radiation (the heat transfer due to the emission of electromagnetic waves) [14]. In the PMI determination model by Wilk et al. (2020), currently only thermal conduction of clothing is used [8].

Heat conduction is generally described using Fourier's law of heat conduction, stating that in a material, the local heat flux is proportional to the negative of the local temperature gradient [14],

$$q = \frac{\dot{Q}}{A} \text{ [W/m}^2\text{]} \quad (2)$$

$$q = -k \frac{dT}{dx} \text{ [W/m}^2\text{]} \quad (3)$$

where q is the heat flux, A [m²] the surface area (area perpendicular to the heat flow) and $T(x)$ [K] the temperature distribution over x [m], the spatial coordinate in the flow direction. When the system reaches a steady state, the temperature distribution through the sample body is linear (Figure 1). The temperature gradient through a body of thickness L [m] due to the temperature difference $T_2 - T_1$ [K] between the face at

$x = 0$ [m] and the face at $x = L$ [m] can be expressed as:

$$\frac{dT}{dx} = \frac{T_2 - T_1}{L} \text{ [K/m]} \quad (4)$$

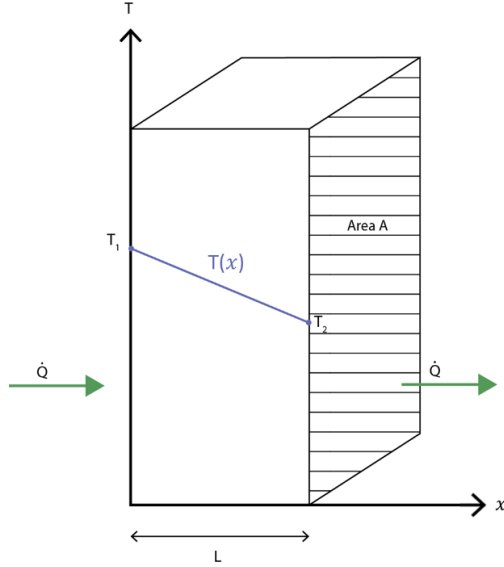


Figure 1. One-dimensional heat transfer across a plane wall by conduction, showing the temperature distribution.

Combining Eq. (3) and (4) results in the Fourier equation for one-dimensional steady state heat flow rate per unit area:

$$\dot{Q} = kA \frac{(T_1 - T_2)}{L} = kA \frac{\Delta T}{L} \text{ [W]} \quad (5)$$

In this study, the main interest is the TC, represented by the symbol k , of the fabric,

indicating the ability of a material to conduct heat. When rearranging Eq. (5), the formula for TC becomes:

$$k = \frac{\dot{Q}L}{A\Delta T} \text{ [W/(mK)]} \quad (6)$$

Results for conduction in unsteady state conditions, in which the temperature within the system varies with time, are typically complicated and difficult to apply due to the high amount of unknown constants and its unknown system behavior. Therefore, where possible, approximations are used via the steady state equations.

1.2 TC measurement methods

TC can be measured using several different methods. In general, these methods are categorized into two classes: steady state methods and transient state methods. Steady state methods measure while the sample material is in complete equilibrium. This primary and most accurate measurement method involves simple signal processing, albeit with a long measurement time [15].

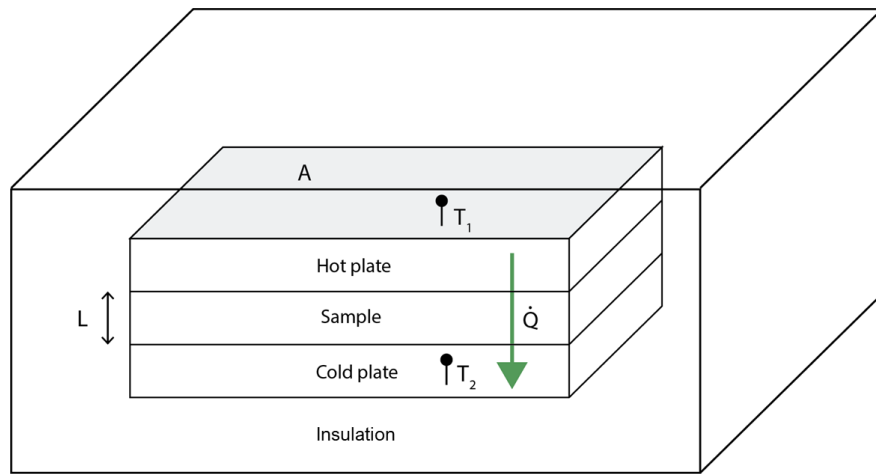


Figure 2. Schematic general guarded hot plate method for TC measurement of flat samples

T_1 and T_2 : indicating temperature measurement; L : sample thickness; \dot{Q} : heat flow per unit area; A : area hot plate = area sample = area cold plate.

Table 1. Search query for database search (Scopus)

<i>Category</i>	<i>Syntax TITLE-ABS-KEY</i>
<i>Influence</i>	(influenc* OR affect* OR {related to} OR impact* OR control* OR (depend* PRE/1 on) OR correlat* OR effect* OR induc*)
	AND
<i>Type of material</i>	(cloth* OR textile OR fabric OR cotton OR synthetic* OR weaves OR knitt* OR garment* OR nylon OR woven OR wool OR polyester OR CV OR silk OR neoprene OR jeans OR cashmere)
	AND
<i>Investigated property</i>	(thermal PRE/0 (conduct* OR resist*))

The transient state methods instantly measure TC during the heating process and are thus much faster than the steady state method. However, the accuracy of transient state methods on dry materials is lower than for steady state methods.

Steady state techniques include the commonly used guarded hot plate (GHP) and heat-flow meter [16]. Generally used transient state techniques are the hot-wire, hot-disk and laser flash method [16].

The American Society for Testing and Materials (ASTM) has denoted the steady state GHP method as the most accurate TC measurement method for materials with low TC [17]. Therefore, this technique is the most frequently used method for measuring TC of insulation materials, including clothing [16]. Accordingly, our novel TC measurement method for forensic applications is being based on the GHP method.

The GHP method involves placing a hot and a cold plate parallel to each other. This creates a steady state heat transfer between the two due to the generated temperature difference. The GHP method is utilized in multiple configurations. In general, it consists of a unidirectionally arranged GHP, acting as a heater (Figure 2) [16]. This hot plate is covered by the sample material on either one or both sides, behind which a cold plate is placed. This system is then fully insulated to ensure the heat produced by the hot plate flows through the sample towards the cold plate, acting as a heat sink.

Temperatures are measured in the hot and cold bodies and are used to determine TC together with the known sample thickness and surface area of the hot plate.

The GHP technique is applicable to a wide range of materials, including both insulators and conductors, and can measure conductivities in the range of 0.0001 – 1.0 W/mK [18, 19]. Its uncertainty is 2.0 - 5.0 % and the method can measure at a wide range of temperatures (80 – 1500 K) [18]. Although the GHP method is recommended to be used in the design of a TC measurement system in forensic applications, in this literature study no preconditions for the investigated measurement systems are set. This is not expected to bias the results as there isn't even a uniform method to compare insulating materials.

2 Methods

A systematic literature search was performed in Scopus (<https://www.scopus.com>) including studies up to May 24, 2021.

2.1 Search strategy

The search string contained three categories: influence, type of material, and investigated property (Table 1). These terms were needed to retrieve articles investigating parameters affecting (specified in the influence term) TC or TR (investigated property) of clothing (type of material).

Table 2. Inclusion and exclusion criteria for study selection

		Criteria
Title	<i>Inclusion</i>	contains terms related to research of thermal conductivity or resistivity OR refers to textiles or other insulating fabrics OR indicates potential relevance in another way.
	<i>Exclusion</i>	explicitly indicates research of only non-clothing materials, such as liquids, concrete, diamonds, soils and rocks OR mainly contains terms related to a completely different research area, like electronics OR indicates the research of only the material's intrinsic parameters, such as fiber orientation and density.
Abstract	<i>Inclusion</i>	indicates investigation of the thermal conductivity or resistivity of fabrics OR shows potential for further investigation in any other way.
	<i>Exclusion</i>	shows that only non-clothing materials were studied OR shows that only the effect of a material's previous treatment, like coating, washing or a specific knitting pattern was investigated OR shows that only intrinsic fabric parameters, such as density and composition, were investigated.
Full-text	<i>Inclusion</i>	reports at least one factor influencing thermal conductivity or resistivity of fabrics.
	<i>Exclusion</i>	investigated materials are not suitable for clothing, e.g. for building insulation purposes or electronic boards OR investigates the effect of a material's previous treatment or the effect of intrinsic fabric parameters on the thermal conductivity OR does not contain sufficient detail to carry out data analysis OR showed the authors did not perform the measurements to study influencing factors themselves OR could not be accessed in any way available to the authors.

Words related to clothing and their synonyms were added to the type-of-material category. Results retrieved were scanned (Title-Abstract) for relevance and if a term did not add relevant studies it was removed from the syntax. A similar approach was conducted for the influence category syntax (Table 1).

In addition to searching for TC, thermal resistance (TR) was also explored; TR is the inverse of TC multiplied by the material's thickness. It is apparent that factors influencing TR also affect TC.

Only papers in English, Dutch, French and German were included.

2.2 Study selection

Study selection was performed using the PRISMA methodology, based on the criteria listed in Table 2. Studies were screened first on title and then on abstract. If selected, a full study review followed and

a final inclusion was determined. Lastly, reference lists of the identified studies were screened for relevant titles (backward snowballing).

2.3 Data extraction

A data extraction table was prepared to extract relevant information from the included studies (see Results). Extracted data included information such as general reference specifications, study aim, material characteristics, TC or TR measurement method, elaboration on parameters with significant influence and conclusions.

2.4 Analysis of results

Because of the heterogeneity of the results, descriptive data synthesis was used. The retrieved factors influencing TC or TR measurement were categorized and qualified as having a positive or negative effect on TC. Effects based on TR

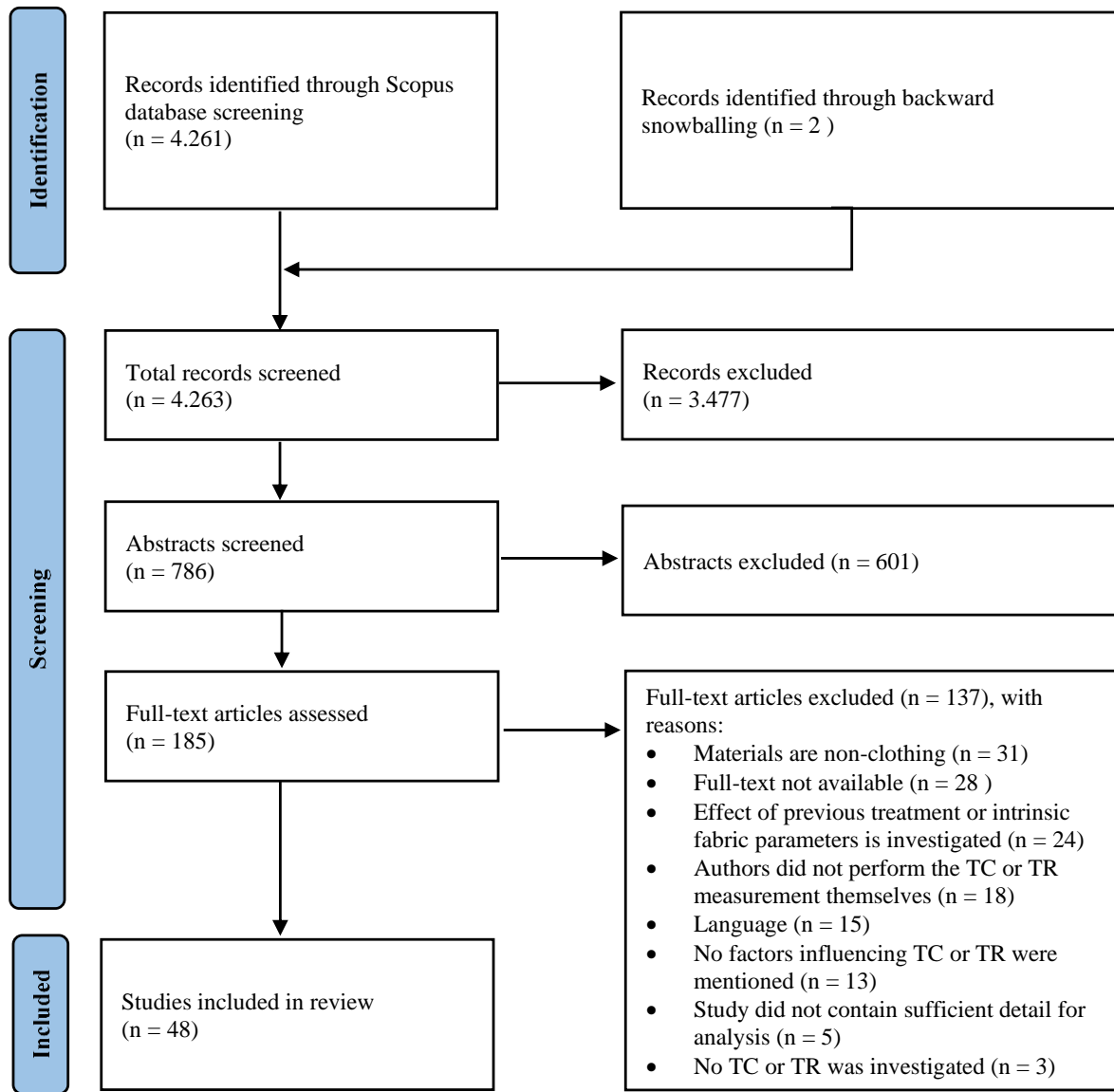


Figure 3. PRISMA Flow Diagram of the literature selection process.

measurements were inverted to achieve the correlation of the factor with TC.

To get a prioritization of the retrieved factors, graphs and tables of all included studies were scanned to estimate the total absolute change in either TC (ΔTC) or TR (ΔTR) over the total measured factor range. For example, in the study by Zhu (2020) investigating the effect of moisture content (0 – 80 %) on TC, the corresponding TC values at 0 and 80 % were noted (resp. 0.022 and 0.09 W/mK). Absolute (Δ) and relative (Δ (%)) TC and TR increase over the measured factor range were calculated.

Furthermore, forensically relevant ranges were determined for the investigated

factors in cooperation with an expert of the Dutch National Police (Table 3). Absolute and relative TC and TR increases were either inter- or extrapolated to equate study results to the same forensically relevant factor range. For interpolation, TC or TR values could be read from the graphs. Extrapolation of the values was calculated assuming a linear relationship between the retrieved factor and TC or TR.

In general, SI units were used to note TC (W/mK) and TR (m^2K/W). When possible, TC- and TR-values were converted to these standard units. When this was not possible, studies were disregarded for effect size estimation.

Table 3. Used forensically relevant factor ranges determined in cooperation with an expert of the Dutch National Police; shown with the reason for the determined range.

Factor	Forensically relevant range	Reason for chosen range
Air layer thickness	0 – 30 mm	Maximum range used in literature is applicable during forensic practice.
Air pressure	690 – 800 mmHg	Maximum and minimum air pressure ever measured in Europe [20, 21]
Ambient temperature	-20 - +40 °C	Maximum outside temperature range in the Netherlands [22]
Emissivity of the plates	0,05 – 0,85	Maximum range used in literature is applicable during forensic practice.
Fabric compression	200 – 2100 Pa	Maximum range used in literature is applicable during forensic practice.
Fabric extension	10 – 80 %	Maximum range used in literature is applicable during forensic practice.
Fabric thickness	0,2 – 7,5 mm	Due to interpolation uncertainties, the maximum range of all studies was used, except for outlying factor ranges.
Horizontal heat leakage	6 – 11,2 %	Maximum range used in literature is applicable during forensic practice.
Moisture	0 – 100 %	Maximum range used in literature is applicable during forensic practice.
Molecular weight ambient gas	29,97 g/mol	Assume the gas surrounding the deceased during forensic practice is air.
Temperature difference between plates	10 – 40 °C	Maximum range used in literature is applicable during forensic practice.
Wind velocity	0 – 3 m/s	Due to interpolation uncertainties, the maximum range of all studies was used, except for outlying factor ranges.

3 Results

A total of 3.263 studies were identified (Figure 3). After the selection process, detailed in Table 1, 48 studies were included for data extraction.

3.1 Study characteristics

The complete data extraction table is provided in Annex I. As a general overview, Table 4 shows the main characteristics and outcomes of the included studies.

3.2 Factors affecting TC measurement of textile

Figure 4 shows the determined factors influencing TC measurement of clothing, with their incidence in the included studies. Figure 5 visualizes the correlation between the determined factor and TC. For all determined factors influencing TC or TR, the total range over which that factor was investigated in the included literature was reported (total literature range).

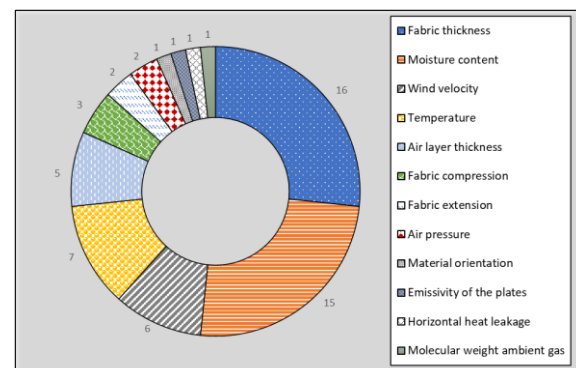


Figure 4. Factors influencing TC or TR measurement of textile with the number of studies determining it in literature. Note: some studies investigate multiple factors.

3.2.1 Fabric thickness

As expected by looking at equation (6) the initial fabric thickness L influences the obtained TC of textile, which has been shown by 17 studies. Of these, 16 found that the thickness of a fabric in uncompressed status is negatively correlated to TC: TC decreases as a result of an increased fabric thickness (total literature range 0 – 25 mm). These studies determined that thicker fabrics are more resistant to heat transfer.

Table 4. Characteristics of included studies (n = 48). **A:** Factors affecting TC. **B:** Factors affecting TR.

A: Studies investigating factors affecting TC measurement of clothing.

¹: See nomenclature for material abbreviations; C*: Correlation effect on TR (in cases of TR this is converted to TC); §: Differs: Fibers have higher TC in the longitudinal direction as compared to the transverse direction; ΔTC: Total TC difference over the measured factor range.

Study	Measurement method	Sample material ¹	Sample size	Affecting factors		Measured factor range	ΔTC full range	Relative ΔTC (%) full range
				C*	Factor			
Klemenčič et al. [23]	Selfmade GHP	CO	2	+	Moisture content	0 – 100 %	0,55	550%
Zhu [24]	Hot-disk method	PET and VC	2	+	Moisture content	0 – 100 %	0,07	309%
Wang et al. [25]	KAWABATA GHP	Blend of CO, NY, PES and EL	3	+	Fabric thickness	1,33 – 1,59 mm	0,01	19%
Shen et al. [26]	HFB-1 tester	50/50 KP/PES and 100 CO	2	+	Wind velocity	0 – 3 m/s	0,02	29%
Shen et al. [27]	KAWABATA GHP	PE, CO or WO	5	+	Horizontal heat leakage	6 – 11,2 %	-0,11	-76%
Akcagun et al. [28]	ALAMBETA GHP	100 WO and 30/70 PES/WO	6	+	Moisture content	0 – 100 %	0,11	275%
Siddiqui and Sun [10]	Selfmade GHP	Nomex III, Twaron, CO, WO and CV	NS	+	Ambient temperature	NS	-	-
				§	Material orientation	NS	-	-
Boughattas et al. [29]	ALAMBETA GHP	PC and PES	6	+	Moisture content	0 – 100 %	0,05	104 %
Tong et al. [30]	NS	CO with silver coated yarns	3	+	Wind velocity	0 – 2,2 m/s	-	-
Boguslawska-Baczek and Hes [31]	ALAMBETA GHP	PES, PA and PUR blends	5	+	Moisture content	0 – 100 %	0,13	255 %
Van Amber et al. [32]	Selfmade GHP	WO and PAN	27	-	Fabric thickness	1,53 – 4,62 mm	-	-
				+	Moisture content	NS	-	-
Karunamoorthy and Das [33]	Selfmade GHP	PES with PTFE coating	20	+	Fabric compression	200 – 2100 Pa	0,15	300 %
Boguslawska-Baczek and Hes [34]	ALAMBETA GHP	Nomex and their blends with Kevlar and carbon fibers	30	+	Moisture content	0 – 70 %	0,05	100 %
Boguslawska-Baczek and Hes [35]	ALAMBETA GHP	PAD, PAN, PES, PP, PVC and CV	136	+	Temperature difference plates	10 – 40 °C	0,002	4 %
				+	Emissivity of the plates	0,05 – 0,85	0,002	6 %
Naebe et al. [36]	KAWABATA GHP	Neoprene	20	-	Fabric thickness	3,20 – 4,30 mm	0,01	29 %
Romeli et al. [37]	Direct heating technique	CO	8	+	Moisture content	NS	-	-
Zhang et al. [38]	Selfmade GHP	CO, CA, SE and WO	23	-	Fabric thickness	0,17 – 0,95 mm	-	-

<i>Study</i>	<i>Measurement method</i>	<i>Sample material^l</i>	<i>Sample size</i>	<i>Affecting factors</i> <i>C*</i> <i>Factor</i>	<i>Measured factor range</i>	<i>ΔTC full range</i>	<i>Relative ΔTC (%) full range</i>	
Nawaz et al. [39]	Heat flow meter	100 WO, 60/40 WO/BA, 100 CO, 94/6 WO/EL, 100 PES, 52/48 WO/Biophyil	6	-	Fabric thickness	0,24 – 0,97 mm	-	-
Oğlakcioğlu and Marmarali [40]	ALAMBETA GHP	CO	6	+	Moisture content	10 – 60 %	0,06	130 %
Ramachandran et al. [41]	NS	CO	18	-	Fabric thickness	0,43 – 0,85 mm	-	-
Zhu and Li [42]	Heat flow meter	NomexIII	2	+	Temperature	0 – 400 °C	0,08	160 %
Vigneswaran et al. [43]	Lee's disk instrument	JU/CO (30/70, 40/60 and 50/50)	9	-	Fabric thickness	1,08 – 1,32 mm	0,00	-10 %
Dias and Delkumburewatte [44]	Selfmade GHP	NY 66 or PES	6	+	Moisture content	10 – 90 %	0,43	343 %
Zhu and Zhang [45]	Selfmade GHP	Flame resistant CO, Nomex IIIA, Panof and Moderate alkali GL	4	+	Air layer thickness	0,5 – 10 mm	0,02	100 %
				+	Temperature difference between plates	20 – 220 °C	0,07	140 %
Hes et al. [46]	ALAMBETA GHP	52/48 WO/PES; 100 CA, 60/40 PES/CO, 83/17 PAN/CO	11	-	Fabric thickness	NS	-	-
				-	Air layer thickness	NS	-	-
Schneider et al. [47]	Selfmade GHP	WO, PP, CO and porous PAN	4	+	Moisture content	0 – 100 %	0,16	361 %
Andersson [48]	Selfmade GHP	NY 66, NY 610, NY 6, NY 11, NY 12	15	+	Air pressure	0 – 1875139 mmHg	-	-
Zaslavskii and Ar'ev [49]	Selfmade GHP	NY 6	NS	-	Structure extension	0 – 40 mm	-0,01	-2 %
				-	Ambient temperature	20 – 130 °C	-0,03	-10 %
Hoge and Fonseca [50]	Selfmade GHP	WO and CO	1	+	Ambient temperature	15,5 – 60 °C	0,00	9 %
				+	Air pressure	0,01 – 1000 mmHg	0,03	140 %
				+	Moisture content	10 – 100 %	0,03	133 %
				+	Fabric compression	NS	0,02	33 %
				-	Molecular weight ambient gas	5 – 120 g/mol	-0,15	-81 %
Speakman and Chamberlain [51]	Lee's disk instrument	WO, WM, SE waste, CO, CV SE, CA SE	7	+	Fabric compression	NS	-	-
Rood [52]	Lee's disk instrument	WO and CO	NS	+	Moisture content	NS	-	-

B: Studies investigating factors affecting TR measurement of clothing.

¹: See nomenclature for material abbreviations; C*: Correlation effect on TC (the effect on TR is inverted to be applicable to TC); ΔTR: Total TR difference over the measured factor range.

Study	Measurement method	Sample material	Sample size	Affecting factors		Measured factor range	ΔTR full range	Relative ΔTR (%) full range
				C*	Factor			
Fung et al. [53]	PERMETEST	CO, PES, PP and their blends	7	-	Air layer thickness	0 – 16 mm	-	-
Tu et al. [54]	HFB-1 tester	KP, PES, CO, PET, LI and their blends	13	+	Wind velocity	0 – 3 m/s	-0,04	-33 %
				+	Ambient temperature	10 – 20 °C	-0,02	-15 %
Shaker et al. [55]	Selfmade SGHP	CO and EL	2	-	Fabric thickness	0,67 – 0,85 mm	0,01	137 %
He and Yu [56]	Selfmade SGHP	AR and CO	1	-	Air layer thickness	0 – 15 mm	0,14	280 %
				+	Ambient temperature	20 – 40 °C	-0,01	-8 %
Stoffberg et al. [57]	PERMETEST	WO, CO, PES, CV and their blends	26	-	Fabric thickness	0,23 – 0,65 mm	-	-
Mangat et al. [58]	ALAMBETA GHP	CO, PES blends	5	+	Moisture content	0 – 65 %	-0,02	-75 %
Kanat et al. [59]	ALAMBETA GHP	CO, PES, CMD and PAN blends	25	-	Fabric thickness	NS	-	-52 %
				-	Moisture content	0 – 100 %	-0,01	
Gupta et al. [60]	ALAMBETA GHP	CO, PES/CV blends and PES/CO blends	13	-	Fabric thickness	0,27 – 0,83 mm	0,01	108 %
Shabaridharan and Das [61]	Selfmade SGHP	Multilayer PES and PES with PTFE coating	18	-	Fabric thickness	0,23 – 7,5 mm	0,15	100 %
Salopek Čubrić et al. [62]	Selfmade SGHP	CO and EL	33	-	Fabric thickness	0,28 – 0,48 mm	0,01	67 %
Ding et al. [63]	Selfmade SGHP	CO and flame-resistant AR	2	+	Ambient temperature	-50 – 100 °C	-0,03	-29 %
				+	Wind velocity	0 – 30 m/s	-0,06	-29 %
				-	Air layer thickness	0 – 30 mm	0,14	117 %
				-	Fabric thickness	0 – 6 mm	0,06	60 %
Shekar et al. [64]	KAWABATA GHP	PES/PP blends and Nomex fabric	5	+	Wind velocity	0,25 – 1 m/s	-0,01	-8 %
Kothari and Bal [65]	Selfmade GHP	CV	1	+	Wind velocity	0 – 1,5 m/s	-0,01	-33 %
Gibson et al. [66]	Selfmade SGHP	CO, PA, PES, MAC, NY, PUR and their blends	12	+	Wind velocity	0 – 2 m/s	-0,06	-45 %
Holcombe and Hoschke [67]	Selfmade GHP	CO, PES/cellulosic blends, PVC, WO	31	-	Fabric thickness	0,81 – 4,63 mm	0,11	700 %
Aboalasaad et al. [68]	ALAMBETA GHP	CO, CO-PA-PUR, CV-PA and CV-EL	4	-	Fabric extension	10 – 80 %	-0,01	-37 %
Slater et al. [69]	Selfmade GHP	WO, CO, CV, SE and their blends	NS	-	Fabric thickness	5 -250 mm	0,48	400 %

One study, by Wang et al. (2020), determined a positive linear relationship for material thicknesses in the range of 1.33 – 1.59 mm [25]. In that study three fabricated socks were investigated, in which fabrics with a lower thickness simultaneously possessed a finer yarn count, resulting in a higher density which caused higher TC. Therefore, this positive relationship can be attributed to the density and will thus be disregarded further.

Stoffberg et al. (2015) and He and Yu (2018) justify the negative correlations between TC and fabric thickness mainly noting that there always is some air present within the fabric pores, which simply is increased in fabrics with a higher fabric thickness [56] [57]. Because TC of air (0.025 W/mK at 20 °C) is much smaller compared to TC of the investigated textiles (0.023 – 0.344 W/mK), the greater the thickness and with that the amount of air, the lower the TC and the better the heat retention [62] [70] [71]. Besides this rationale, it is clear that a higher fabric thickness results in lower TC due to the compactness of the yarns which hinders the diffusion of heat [43].

The size of this interaction is different per fabric, but the correlation is seen in wovens and non-wovens, as well as in multilayered fabrics [59, 61] [43]. Due to layering often present in woven fabrics, the effect of fabric thickness on TC in wovens is higher than in non-wovens [60].

3.2.2 Moisture content

In all 15 studies investigating the effect of moisture content on TC, the amount of moisture in or on a fabric turned out to have a positive correlation with TC. The term moisture content is quantified in each study in a slightly different way. In general, a 0% moisture content in a fabric induces an ‘ultra-dry state’, which is achieved after drying the fabrics in an oven (> 100 °C) to remove all moisture. Fabric in its normal state will always have some moisture (0 – 13.8 %) present due to the air humidity [23, 72].

To achieve 100% moisture content, ‘wet state’, samples were soaked in liquid (e.g. water) to their full volume [31]. Subsequently, samples were dried and weighted to achieve a moisture content between 0 - 100%.

With increasing moisture percentage (0 – 100%), TC first linearly increases when the water gets absorbed from the surface by the macropores of the sample [34]. The increase in TC can be more than three times the original TC of the fabric due to the addition of moisture. This finally stabilizes around the TC value of the absorbed liquid [23, 28].

When a saturation level of about 15-25% is reached, the increase in TC starts to slow down and a difference in behavior between absorbent and nonabsorbent fibers becomes apparent [23, 29, 34, 47]. Absorbent fibers and materials (e.g. cotton, wool and Nomex) also absorb liquid into the fibers and therefore ultimately obtain higher TCs [47]. Nonabsorbent materials however (e.g. polyester, acrylic and modacrylic) only retain free liquid in between fibers and yarns and achieve a slightly lower TC increase (max 0,09 W/mK) [47].

Bogusławska-Bączek and Hes (2017) concluded that the effect of moisture content on TC is caused by the substitution of air in fabric pores with water, because water (0.598 W/mK at 20 °C) is a better conductor than air (0.025 W/mK at 20 °C) [31, 70, 73]. The moisture content in fabric then greatly reduces the thermal insulation properties of the material. The correlation between TC and moisture, however, varies between clothing pieces, as it is highly dependent on the nature of the micro-pores in a fabric [37].

3.2.3 Wind velocity

All studies (n = 7) investigating the effect of wind velocity (total literature range 0 – 30 m/s) during TC measurement determined a positive correlation between wind velocity over the cold plate and apparent TC. The angle (0°, 45° and 90°) at which the air flows has little effect on TC of textile [30].

Most studies investigated low wind velocities (0 – 3 m/s). Only Shekar et al. (2011) and Ding et al. (2011) investigated higher wind velocities, with maximums of respectively 10 and 30 m/s [63, 64].

In all investigated studies the wind velocity acts as a cold plate, used in the GHP method (Figure 6). The wind accelerates convection on the textile surface and thus functions like a cold plate.

A high wind velocity enables increased penetration of air through the textile due to its air permeable properties. Thus, more air reaches the inside of the textile surface. Shen et al. (2020) showed that this would stimulate forced convection inside the textile, which increases heat transmission and therefore decreases thermal insulation of textile [26]. In other words, as the airflow carries energy from the textile to the surrounding environment, a faster thermal dissipation at a higher speed would be observed. Therefore, TC proportionally changes with wind velocity [30].

Ding et al. (2011) concluded that this effect was most significant at lower wind speeds (< 5 m/s). After that point, the parabolic correlation tends towards its asymptote [63]. At a speed of 25.6 m/s, an abrupt transition occurs due to the onset of turbulent flow over the textile surface, resulting in a greater increase in TC with wind velocity.

Textiles with a higher initial TR and thus a lower initial TC were relatively more affected by the increase in wind velocity than fabrics with a higher initial TC [64].

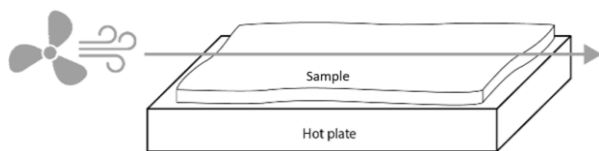


Figure 6. Wind acting as a cold plate in a TC measurement set-up.

3.2.4 Temperature

The effect of temperature on TC was investigated by different means; both the ambient temperature and the temperature difference between the measuring plates

were studied. Six studies investigated the effect of ambient temperature (total literature range $-40 - +400$ °C) on TC of clothing. One study investigated the effect of the temperature difference across the hot and cold plate of the measurement device (resp. 10 and 40 °C) and another one investigated the effect of an increase in hot plate temperature (40 – 240 °C) on TC.

Seven studies found a positive relationship between temperature (both ambient temperature and the temperature differences between the plates) and TC of textile. The only aberrant result was by Zaslavskii and Ar'ev (1968), showing a negative correlation between the ambient temperature and TC of NY6, due to the destruction of the crystalline formation of NY6 during heating [49].

Generally, the main reason for the positive correlation between temperature and TC is that the kinetic energy of the air molecules within the fabric sample increases with increasing ambient temperature [54]. This increased kinetic energy results in a decreased convective resistance which then increases TC.

3.2.5 Air layer thickness

The air layer thickness (total literature range 0 – 30 mm) between the sample area and measurement device negatively influences the apparent TC according to four studies (Figure 7). TC measurement of a textile sample gets biased by unintentionally including TC of air. This correlation is the highest when ambient temperatures are higher than the hot plate temperature of the measurement instrument [63]. Zhu and Zhang (2007) however found a positive correlation between a sample's TC and the enclosed air layer thickness (> 8 mm), which they attributed to natural convection increasing the system's heat transfer [45]. At smaller air gaps (> 8 mm), air movement does not exist within and around the fabric and convective heat transfer does not take place.

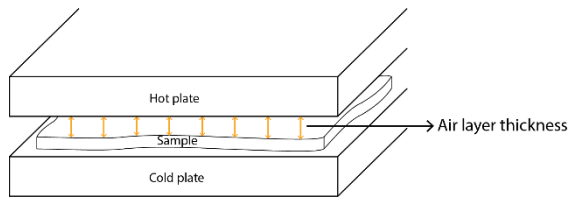


Figure 7. Visualization of the air layer thickness between the fabric sample and the hot plate.

3.2.6 Fabric compression

The effect of fabric compression on its TC was investigated in three studies. Fabric compression (total literature range 200 – 2100 Pa) has a positive correlation with TC. As the compression increases, the sample density and consolidation of fibers increase, leading to a decrease in fabric thickness, porosity and air volume fraction and therefore an increase in TC [33, 50]. Andersson (1976) observed that this correlation is more pronounced at lower air pressures (0 – ~0.3 GPa) due to its parabolic relation with TC [33, 48].

3.2.7 Fabric extension

Fabric extension or elongation (total literature range 10 – 80%) results in a decrease in the measured TC of textile. Aboalasaad et al. (2020) attribute this decrease in TC as a result of porosity increase due to fabric extension [68].

3.2.8 Horizontal heat leakage

Shen et al. (2019) defined the heat leaking percentage as the percentage of heat leaking from the edge and insulation material instead of going through the sample [27]. This study determined that horizontal heat leakage (range 0 – 11.2%) influences the

obtained TC measurement results. Samples with higher longitudinal TC, TC in the direction of the yarn, had a higher horizontal heat leakage percentage and vice versa (Figure 8). For TC measurement of textile, generally the value of transverse TC, TC perpendicular to the yarn direction, is desired. In most fabrics, this transverse TC value is lower than the horizontal TC value (see section 3.2.9). Yet, transverse TC was negatively related to the heat leakage percentage. Higher transverse TC would enable heat to transfer through the material easier and thus results in less horizontal heat leakage. This implies that a guard plate with high transverse TC could reduce the heat leakage and improve the accuracy of the TC measurement of the actual sample. The clothing itself, however, with its low transverse TC, would cause a higher heat leakage percentage, which should be considered during measurement.

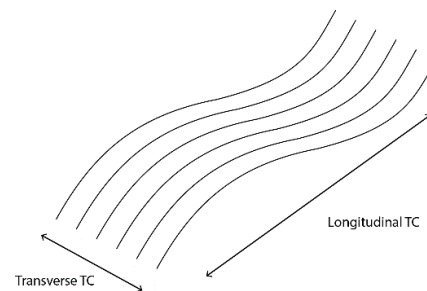


Figure 8. Fabric on yarn-scale elaborating on the transverse and longitudinal TC.

3.2.9 Material orientation

Siddiqui and Sun (2018) studied the effect of material orientation on TC of plain woven fabrics [10]. It was concluded that

Table 5. Overview of factors affecting TC measurement of clothing per measurement method.

	Fabric thickness	Moisture content	Wind velocity	Temperature	Air layer thickness	Compression	Fabric extension	Horizontal heat leakage	Material orientation	Emissivity of the plates	Air pressure	Weight ambient gas
Selfmade GHP	•	•	•	•	•	•	•		•		•	•
Alambeta	•	•		•	•		•			•		
Kawabata	•		•					•				
Selfmade SGHP	•		•	•	•							
HFB-1 tester			•	•								
Permetest	•				•							
Lee's disk	•	•				•						
Heat-flow meter	•			•								
Hot disk		•										
Direct heating		•										
NS*	•		•									

* Not specified

fibers have higher TC in the longitudinal direction, parallel to the yarn, than in the transverse direction, perpendicular to the yarn. This anisotropic behavior explains why heat also travels along the fiber direction in the yarn, resulting in horizontal heat leakage, when determining TC across the fabric thickness (section 3.2.8) [10].

3.2.10 Air pressure

Two studies investigated the effect of air pressure on TC measurement of textile [48, 50]. Hoge and Fonseca (1964) showed that with increasing pressure of the surrounding air (0 – 1.3 bar), the measured TC of clothing increased (0.15 – 0.36 W/mK). As the air pressure decreased, the mean free path of gas molecules was of the same order of magnitude as the distance across which the heat transfer is measured. Andersson (1976) observed that this correlation was higher at air pressures until 3 kbar, after which it decreased due to its parabolic relation with TC [33, 48].

3.2.11 Emissivity of the measuring plate

Bogusławska-Baczek and Hes (2014) determined the effect of surface emissivity of plates used in the measurement device on

the measured TC of fabrics [35]. The surface emissivity was defined as the ratio of radiated heat from the sample's surface to the heat radiation from a perfect emitter. A very small increase (about 1 – 5%) in TC was observed after an increase in emissivity of the plates (0.05 – 0.85). The positive correlation between TC and emissivity of the plates was linear, although almost negligible.

3.2.12 Molecular weight ambient gas

The effect of a change of gas surrounding the clothing sample on the apparent TC of clothing was investigated while preserving the same pressure (atmospheric) and temperature (33.9 °C). Hoge and Fonseca (1964) describe that measuring TC of clothing in environments with gasses with a molecular weight lower than air (e.g. Helium) results in higher apparent TCs of clothing and vice versa.

3.3 Factors affecting TC, split by measurement methods

A total of ten different measurement methods were used in the investigated studies to determine either TC or TR of a clothing sample. Table 5 visualizes the

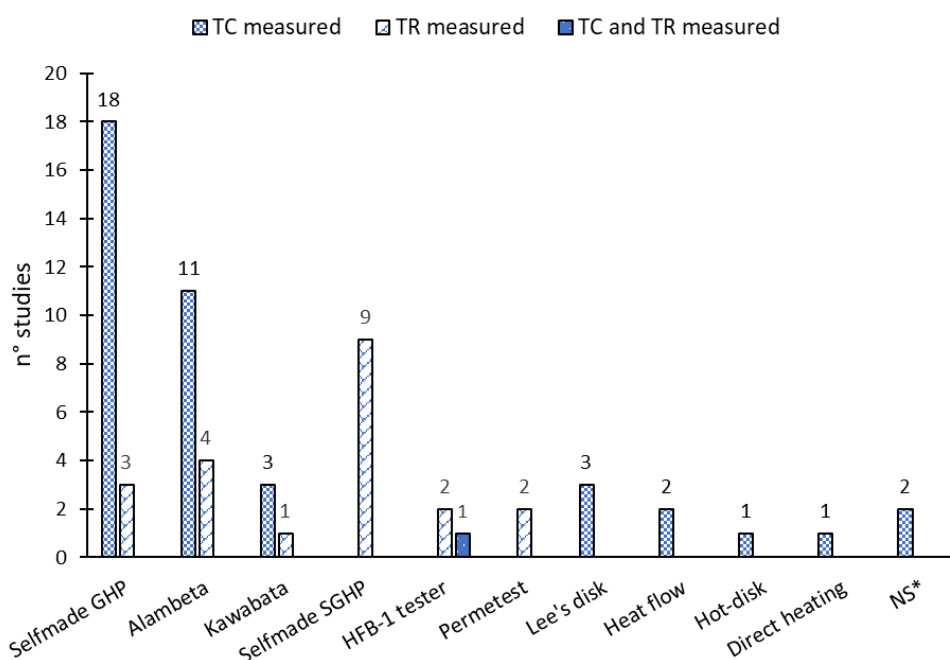


Figure 9. Distribution of the use of measurement methods used to determine TC or TR of clothing.

*NS: not specified.

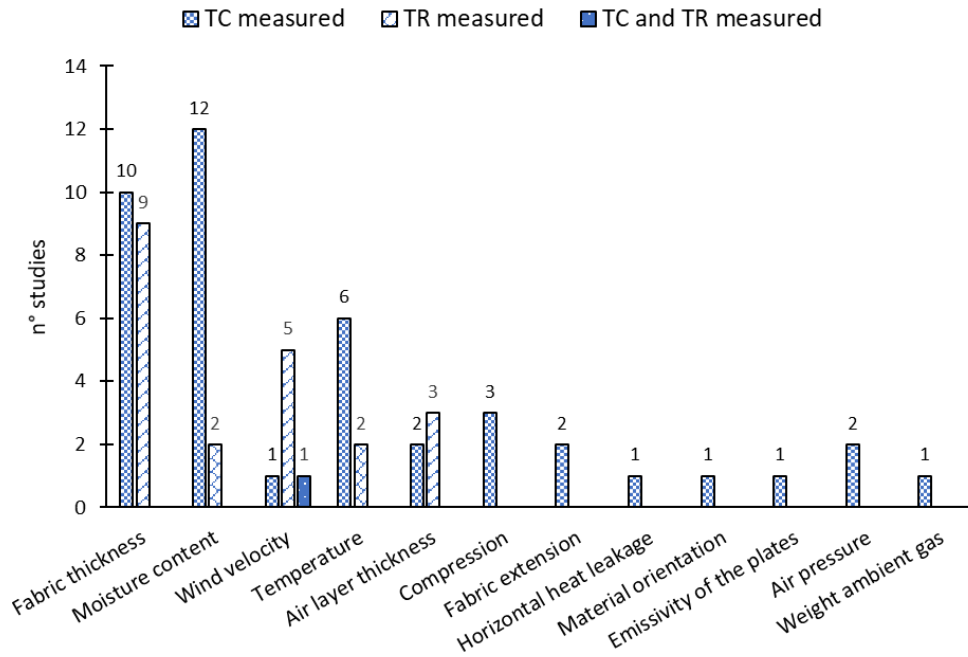


Figure 10. Distribution of the determined factors affecting TC of clothing for either TC or TR-specific measurements.

factors affecting TC measurements per measurement method.

3.4 Differences between TC and TR measurements

Distribution of the use of TC and TR measurement methods is depicted in Figure 9. For TC measurements, mainly the steady state GHP method was used, either via a self-made or a commercially available device. TR measurements most often used SGHP techniques. Likely due to the difference in measurement methods for TC and TR determination, a difference in affecting factors is observed (Figure 10).

3.5 Effect size estimation of the influencing factors

Results of the effect size estimation are shown in Figure 11. In 26 cases, a relative change in TC (ΔTC (%)) as a result of a change in factor size could be estimated. Similarly, this was possible for 16 factors influencing TR. In 14 studies, study outcomes did either not incorporate TC or TR values ($n = 10$) or these values could not be converted to SI units ($n = 4$).

Moisture content (0 – 100%) showed the greatest increase in TC in the total literature

range (Figure 11-A). When only considering the forensically relevant factor range, the effect of fabric thickness was dominant. Furthermore, the effect of air layer thickness increased when investigating the forensically relevant range. The effects of air pressure, ambient temperature, molecular weight of the ambient gas, and the temperature difference between the plates were negligibly small in the forensically relevant range (Figure 11-B).

Studies investigating the effect on TR showed most influence of the air layer thickness and fabric thickness effect (Figure 11-C). In the forensically relevant range, the effect of fabric thickness was further increased.

The moisture effect, investigated by multiple studies and having a relative large effect size as compared to other studies, does not follow a linear relationship (Figure 11). In most studies the relationship is approximately linear for a moisture content of 0 to 25% and thereafter flattens (concave form) till it reaches 100% moisture content. Therefore, the range was split into low (0 – 25%) and high (25 – 100%) moisture contents (Figure 12).

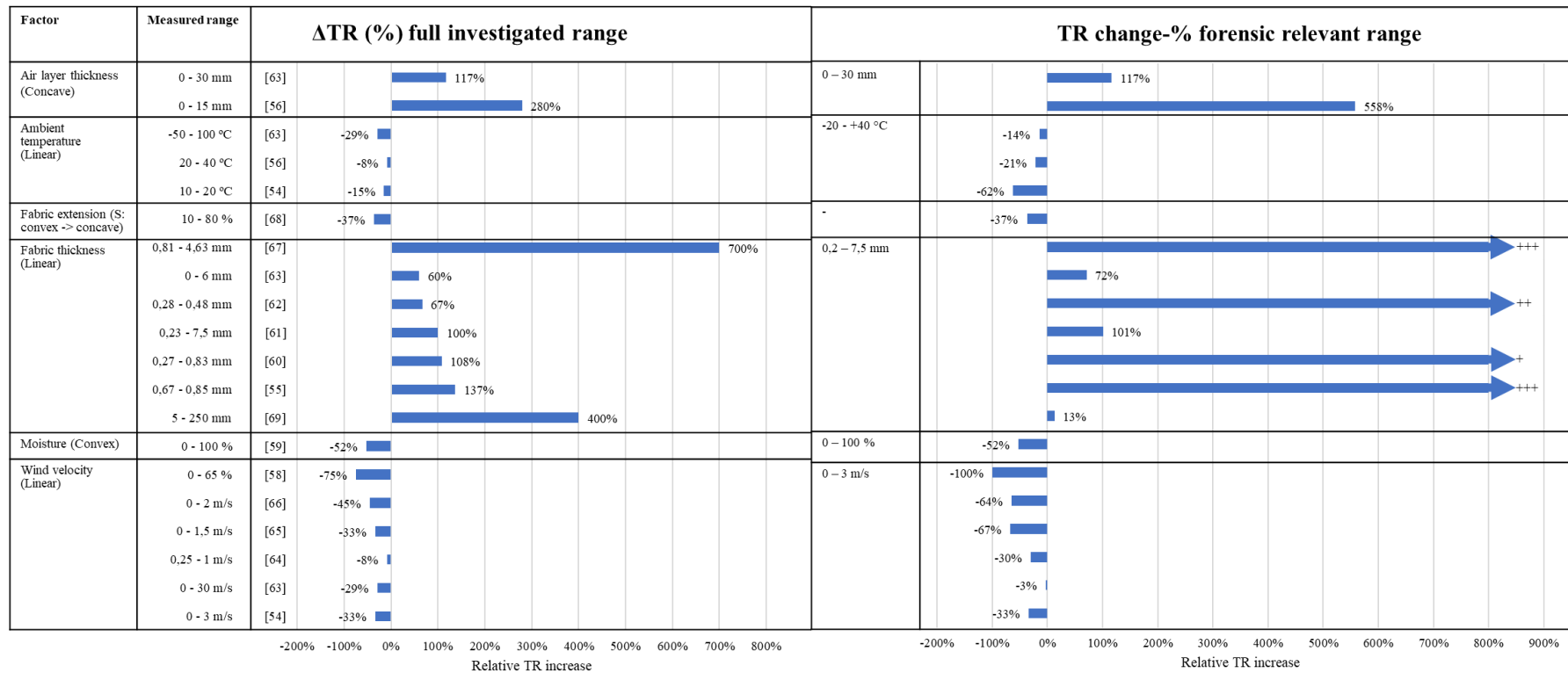


Figure 11B. Effect of factors influencing TR measurement of clothing, both for their full measured range and for an inter- or extrapolated forensically relevant range. Between brackets () the shape of the relationship between the determined factor and TR is reported. (-) indicates the shape of the relationship is unknown. +, ++ or +++ indicates a (very) high effect on TR, (much) more than the percentages on the given graph axis.

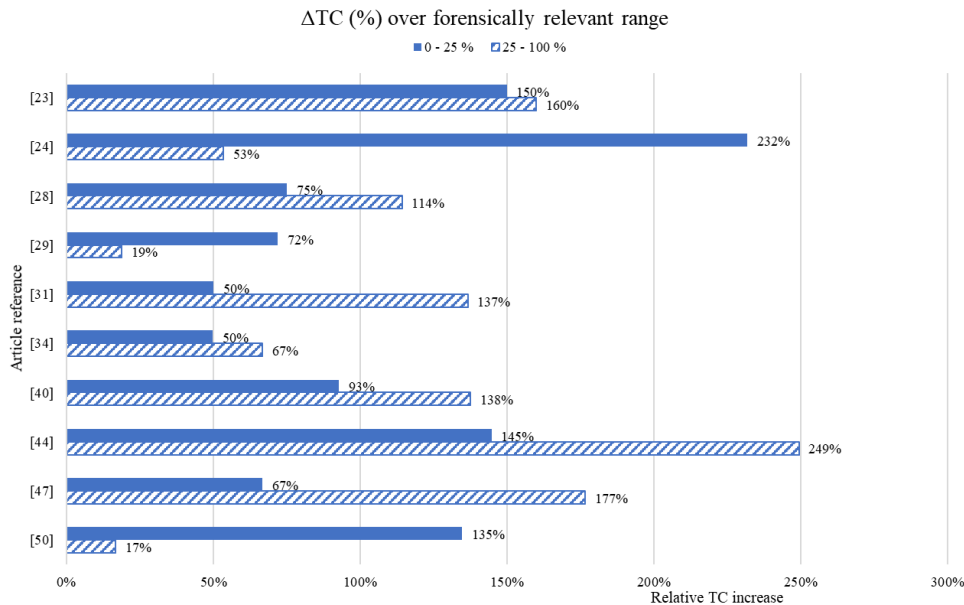


Figure 12. Moisture content effect on TC in forensically relevant range, split for low (0 – 25 %) and high (25 - 100 %) moisture contents.

3.6 Cross-correlations between factors

The effect of air layer thickness is important as it also influences the effect size of other factors influencing TC measurement. In particular, air layer thickness influences the effects of fabric thickness and temperature.

Ding et al. (2011) investigated the effect of both air layer thickness and fabric thickness. The air layer thickness between fabric sample surface and measurement device was more dominant than the effect of fabric thickness. When the air layer thickness increased, the effect of fabric thickness decreased [63].

Ding et al. (2011) also noticed an increase in the rate at which TC changes with temperature when the air layer thickness increased (> 12 mm) [63]. As there is an increased presence of air, its thermal properties naturally become the main contributor in the fabric's TC. This was confirmed by He and Yu (2018). In case of lack of air gaps, almost no change in TC occurred due to a change in temperature (20 – 40 °C) [56].

However, temperature itself does influence the effect size of fabric extension on TC. The effect of extension on TC is higher (absolute TC decrease at 40 mm extension: 0,026 W/mK) at higher ambient

temperatures (> 50 °C). At lower ambient temperatures (20 – 50 °C) the correlation is small (absolute TC decrease: 0,005 W/mK) [49].

4 Discussion

4.1 Interpretation of the results

The determined effect directions of the different factors influencing TC measurement of clothing were as expected. An insulating material has low TC and a conductor high TC. Only four of the determined factors decrease apparent TC and thus insulation; fabric thickness, air layer thickness, fabric extension and the molecular weight of the ambient gas. This is reasonable as a loose, thick, 100% wool sweater is a better insulator than a thin polyester/elastane swimsuit tightly enclosing one's body.

Five factors positively correlate with the determined TC of clothing, resulting in an increased TC value. Increased moisture content and higher wind velocity make textile a worse insulator. This, again, is understandable, as a rainy autumn storm will soak one's clothing and make one feel cold as a result of higher apparent TC of the clothing. The other factors (air pressure,

temperature, emissivity of the plates, fabric compression, horizontal heat leakage and molecular weight of the ambient gas) with a positive correlation with the determined TC did not make the textile layer more conductive, but merely influenced the measurement thereof.

Furthermore, an unequal distribution in the use of TC measurement methods was observed (Figure 9). GHP- and SGHP-based methods were used most often. Differences between methods for TC and TR measurements were present, even though it was assumed factors affecting TR of clothing would automatically affect their TC and thus need comparable measurement devices. TR was mainly determined using the SGHP method whereas TC measurements were most often performed with the GHP method or commercial derivatives thereof (Figure 9). However, the SGHP method includes an air flow in its measurement, whereas the GHP method does not. Therefore, it is understandable that studies investigating the effect of wind velocity prefer the SGHP method. Some factors were thus more dominant during TC measurements and others during TR measurements (Figure 10). It is therefore recommended to interpret these factors in within the context of the applied measurement method. Further, the empirically determined correlations and observations fit well with the theory discussed in sections 1.1 and 1.2. Steady state measurements, like GHP and SGHP, are often recommended due to their high accuracy and simple calculation compared to transient state techniques [15].

The effect size estimation of the retrieved factors is an order of magnitude estimation. It shows which factors have a more dominant effect on TC or TR than others. This estimation, however, is mainly based on graphs in the reviewed studies. Interpretation errors may have occurred when reading these graphs. Besides this, major differences between studies exist in terms of measurement protocol, measurement devices, type and material of

clothing and study aims. These would all affect TC and/or TR measurement in addition to the contact conductance which is always present and already decreases TC. Lastly, extrapolation of results was always done assuming a linear correlation over that range. As a result, the effect of air layer thickness and horizontal heat leakage might be underestimated. Also the effect of moisture might be wrongly estimated, although a distinction was made in effect size between low and high moisture content (Figure 12).

4.2 Recommendations for forensic practice

The results of this review should be carefully considered in forensics. The determined factors each play a role in the cooling rate of a deceased victim, affected by their clothing. To make an assessment of TC of a piece of clothing that represents the situation in which it was worn, it is important to control the factors that could potentially influence TC measurement. Both best-practices in performing the measurement and recommendations for the design of a measurement device were investigated. The most dominant factors (ΔTC and/or ΔTR (%) > 100%) in their forensically relevant range were fabric thickness, moisture content, air layer thickness and fabric compression, and are discussed below.

4.2.1 High effect factors

Fabric thickness

As the fabric thickness correlates with TC and as it could vary within a clothing piece, the measured clothing sample must have a thickness that is representative of the majority of the clothing [74]. Otherwise, multiple samples must be measured to ensure a complete TC documentation. Furthermore, adequate measurement of the sample's fabric thickness is indispensable. As the effect size of fabric thickness on TC is the highest, a small error in measured thickness could easily result in a large error in determined TC.

Moisture content

Partly wet clothing samples (blood, urine etc.) are often found in forensic practice. Therefore, the effect of moisture content on apparent TC of clothing is relevant to consider when determining TC.

The effect of moisture content has a linear relationship with TC until 25% moisture content, which weakens to a concave relationship at higher moisture contents. Especially in the low moisture content region (0 – 25 %), one cannot discriminate the presence and amount of moisture by eye. Therefore, it is important to measure the sample in the same humidity conditions as it was first worn in. This strongly demands for measuring directly at the crime scene or in an moisture controlled box.

The moisture content in a fabric might change over time, as a wet fabric dries when kept in a ‘dry’ environment. In order to minimize this physical change, it is advised to start TC measurements as quickly as possible once a deceased has been found [74]. Furthermore, a closed measurement chamber is recommended to avoid change in clothing properties during measurement.

In order to mimic the initial moisture content of the sample, one could rewet the sample. In that case, one should be mindful that the type of liquid determines the maximum TC the wetted fabric will achieve. A blood-soaked T-shirt should thus not be rewetted with water. However, it is hard to determine to what level the clothing sample should be rewetted. Therefore, one should recognize that the determined TC value may be an underestimation of the true TC of the clothing, when the sample dried over time.

Air layer thickness

It is important to avoid the presence of air layers between the clothing sample and the measurement device plates. Air layers increase the contact resistance and with that decrease apparent TC. The achieved apparent TC then strongly deviates from the real TC. This increases even more for open

measurement chambers, due to an increase in conductive and radiative heat leakage [75]. A system that precisely encloses the fabric sample with a controllable compression on the sample would be needed to achieve this.

Fabric compression

In general, clothing samples should not be compressed during measurement, as it highly increases apparent TC. However, one must ensure the clothing sample and the measuring plates connect to each other to avoid the effect of air layers on TC. A connection in which the sample and the top plate are just touching would be ideal if the clothing indeed was in an uncompressed state.

When clothing was in a compressed state, it should be simulated during TC measurement. That way, measurements with varying compressions could be performed for the same clothing; one measurement for a sample that was compressed (e.g. by body weight) and one measurement for clothing that was uncompressed (e.g. on top of the deceased). It is however challenging to determine the compression that was initially exerted on the clothing.

4.2.2 Moderate effect factors

Factors (ΔTC and/or ΔTR (%) 10 – 100%) with a less dominant influence than the ones mentioned above, include ambient temperature, fabric extension, horizontal heat leakage, temperature difference between the plates and wind velocity. For these factors, it mainly is advised to keep these factors constant during measurement and make use of a closed measurement system to avoid fluctuations in temperature and wind velocity.

Furthermore, it should be considered that the material’s stretch, and thus elongation, might change when a sample is cut out of the clothing. It is advisable to keep the tension in which the clothing was worn the same during sample measurement. If a leggings was worn stretched, the

apparent TC could differ from the TC for loosely hanging leggings.

Heat losses, found as horizontal heat leakage in this review, include convection and radiation to the surrounding and conduction through the wires of the temperature sensors [76]. As these heat losses affect the apparent TC measurement, it is important to minimize these in a TC measurement method. To minimize the effect of heat leakage, any TC measurement device should be adequately insulated with good insulating materials like polyisocyanurate (0.02 – 0.025 W/mK), and should have a sealed measurement chamber [77].

4.2.3 Negligible factors

Some factors are negligible in forensic use purposes due to their low effect (ΔTC and/or TR (%) < 10%): air pressure, emissivity of the plates and molecular weight of the ambient gas.

Material orientation of clothing samples was the only factor without any sizing information. However, it is clear the sample should be oriented in the plane the TC is demanded.

Two factors (temperature difference between the plates and fabric thickness)

affecting TC measurement are also an input in the calculation of TC by the measurement device (section 1.1). It is hence obvious that measurement errors of these factors should be minimized. Measurement standards by ASTM (C177-19) and ISO (8302:1991) help to establish accurate and reproducible measurements [17, 78].

4.3 Limitations of this literature review

The applied PRISMA search method, although transparent, might have induced some bias. Firstly, only one database (Scopus) was used for study selection. Secondly, only studies investigating TC or TR measurement of clothing were included. Factors affecting TC of other materials which are similar to clothing, such as building insulation materials, might also affect TC of textile. Therefore, some minor or even major factors might have been missed as a result of the applied search strategy.

Lastly, during full-text screening, 28 studies could not be accessed by the author. Besides this, 15 articles could not be interpreted due to non-familiar languages and were therefore excluded. Resultingly, some information might have been missed.

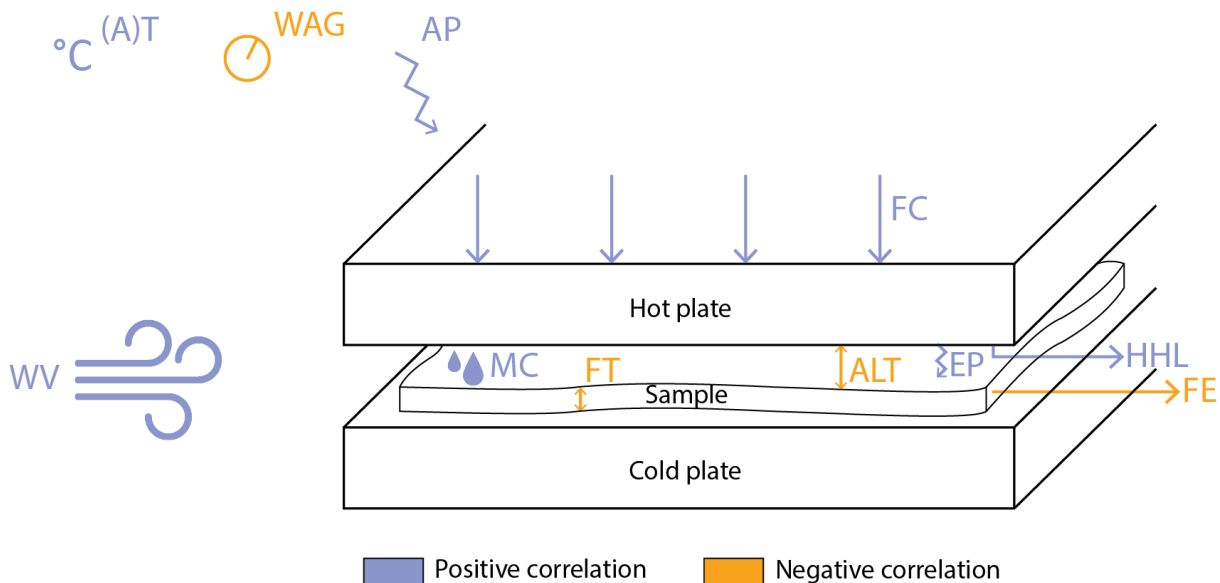


Figure 13. Visualization of all determined factors influencing the TC measurement of clothing, specified for a GHP set-up. Abbreviations: ALT, air layer thickness; AP, air pressure; (A)T, (ambient) temperature; EP, emissivity of the plates; FC, fabric compression; FE, fabric extension; FT, fabric thickness; HHL, horizontal heat leakage; MC, moisture content. WAG, weight ambient gas; WV, wind velocity.

5 Conclusion

A literature review of factors affecting TC measurement of clothing was conducted. Factors affecting TC measurement most during forensic purposes include fabric thickness, moisture content, air layer thickness and fabric compression (Figure 13). To achieve accurate TC values in forensic practice, it is important that the sample and the test circumstances are good representatives of the full clothing and the conditions the clothing was worn in. Furthermore, the clothing sample should be adequately positioned in the measurement device providing a good connection between sample and measurement plates.

The results of this review, including a rough factor size estimation, will guide in TC measurement for forensic practice. This will help in making a better PMI estimation at a crime scene.

Acknowledgements

I would gratefully like to thank dr. ir. A.J. Loeve and drs. C.A.W. Pellemans for their help and supporting advice.

Annex 1. Complete data extraction table

Supplementary data is available in a separate Excel document: 20211216_Data_extraction_table_Therminus_CI_Kaanen.xlsx

References

- [1] CBS. (2020, 26-06-2021). *1 811 zelfdodingen in 2019*. Available: <https://www.cbs.nl/nl-nl/nieuws/2020/27/1-811-zelfdodingen-in-2019>
- [2] CBS. (2020, 26-06-2021). *Overledenen, moord en doodslag, pleeglocatie Nederland*. Available: <https://www.cbs.nl/nl-nl/cijfers/detail/84726NED>
- [3] R. Shrestha, T. Kanchan, and K. Krishan, "Methods Of Estimation Of Time Since Death," in *StatPearls* Treasure Island (FL), 2021.
- [4] H. Vissers *et al.*, *Plaats en koers Forensische Opsporing 2018 - 2021*. Politie, 2018.
- [5] A. Hendrix *et al.*, *De opsporing verdient sporen*. Politie, 2018.
- [6] C. Henssge and B. Madea, "Estimation of the time since death in the early post-mortem period," *Forensic Sci Int*, vol. 144, no. 2-3, pp. 167-75, Sep 10 2004.
- [7] C. Henssge, "Death time estimation in case work. I. The rectal temperature time of death nomogram," *Forensic Sci Int*, vol. 38, no. 3-4, pp. 209-36, Sep 1988.
- [8] L. S. Wilk *et al.*, "Reconstructing the time since death using noninvasive thermometry and numerical analysis," *Sci Adv*, vol. 6, no. 22, p. eaba4243, May 2020.
- [9] S. Halaoua, Z. Romdhani, and A. Jemni, "Effect of textile woven fabric parameters on its thermal properties," *Industria Textila*, Article vol. 70, no. 1, pp. 15-20, 2019.
- [10] M. O. R. Siddiqui and D. Sun, "Thermal analysis of conventional and performance plain woven fabrics by finite element method," *Journal of Industrial Textiles*, Article vol. 48, no. 4, pp. 685-712, 2018.
- [11] R. Li, J. Yang, C. Xiang, and G. Song, "Assessment of thermal comfort of nanosilver-treated functional sportswear fabrics using a dynamic thermal model with human/clothing/environmental factors," *Textile Research Journal*, pp. 1 - 13, 2016.
- [12] Y. Kyosev and P. Reiners, "About the Thermal Conductivity of Multi-Layer Clothing," *ACC Journal*, vol. XIX, pp. 94 - 102, 2013. Technická univerzita v Liberci
- [13] Z. Misri, M. H. W. Ibrahim, A. S. M. A. Awal, M. S. M. Desa, and N. S. Ghadzali, "Review on factors influencing thermal conductivity of concrete incorporating various type of waste materials," (in English), *4th International Conference on Civil and Environmental Engineering for Sustainability (Iconcees 2017)*, vol. 140, 2018.

- [14] A. F. Mills, "Introduction and Elementary Heat Transfer," in *Basic Heat and Mass Transfer* 2 ed. England: Pearson, 2014, pp. 1 - 56.
- [15] Y. N. "Chapter 6: The Review of Some Commonly Used Methods and Techniques to Measure the Thermal Conductivity of Insulation Materials," in *Insulation Materials in Context of Sustainability* 1 ed. INTECH, 2016, pp. 113 - 140.
- [16] N. Yüksel, "The Review of Some Commonly Used Methods and Techniques to Measure the Thermal Conductivity of Insulation Materials," in *Insulation Materials in Context of Sustainability*: INTECH, 2016, pp. 113 - 140.
- [17] *C177-19 Standard Test Method for Steady-State Heat Flux Measurements and Thermal Transmission Properties by Means of the Guarded-Hot-Plate Apparatus*, 2019.
- [18] X. C. Tong, "Characterization Methodologies of Thermal Management Materials," in *Advanced Materials for Thermal Management of Electronic Packaging* New York: Springer Series in Advanced Microelectronics, 2011, pp. 59 - 130.
- [19] S. T. Czichos H., Smith L., "Measurement Methods for Materials Properties: Thermal Properties," in *Handbook Materials Measurement Methods* Germany: Springer Science+Business Media, 2006, pp. 399 - 430.
- [20] S. Burt, "The Highest of the Highs .. Extremes of barometric pressure in the British Isles, Part 2 - The most intense anticyclones," *Royal Meteorological Society*, vol. 62, no. 2, pp. 31 - 41, 2007.
- [21] T. Jónsson. (2007, 16-12-2021). *The lowest air pressure in Iceland*. Available: <https://www.vedur.is/vedur/frodleikur/greinar/nr/1056>
- [22] Rijksoverheid. (2020, 16-12-2021). *Temperatuurextremen in Nederland, 1907 - 2019*. Available: <https://www.clo.nl/indicatoren/nl0589-temperatuur-extremen>
- [23] E. Klemenčič, D. Zavec, and M. Slavinec, "Modelling the impact of moisture on the thermal conductivity of cotton jersey," *Fibres and Textiles in Eastern Europe*, Article vol. 29, no. 2, pp. 61-65, 2021.
- [24] F. L. Zhu, "Investigating the effective thermal conductivity of moist fibrous fabric based on Parallel-Series model: A consideration of material's swelling effect," *Materials Research Express*, Article vol. 7, no. 4, 2020, Art. no. 045308.
- [25] W. Wang *et al.*, "A study of thermal conductivity property of socks," in *Materials Science Forum* vol. 1007 MSF, ed, 2020, pp. 118-124.
- [26] H. Shen, Y. Xu, F. Wang, J. Wang, and L. Tu, "Numerical analysis of heat and flow transfer in porous textiles - Influence of wind velocity and air permeability," *International Journal of Thermal Sciences*, Article vol. 155, 2020, Art. no. 106432.
- [27] H. Shen *et al.*, "Analysis of heat transfer characteristics in textiles and factors affecting thermal properties by modeling," *Textile Research Journal*, Article vol. 89, no. 21-22, pp. 4681-4690, 2019.
- [28] E. Akcagun, M. Bogusławska-Bączek, and L. Hes, "Thermal insulation and thermal contact properties of wool and wool/PES fabrics in wet state," *Journal of Natural Fibers*, Article vol. 16, no. 2, pp. 199-208, 2019.
- [29] A. Boughattas, S. Benltoufa, L. Hes, M. Azeem, and F. Fayala, "Thermophysiological properties of woven structures in wet state," *Industria Textila*, Article vol. 69, no. 4, pp. 298-303, 2018.
- [30] J. Tong, Y. Zhao, C. Yang, and L. Li, "Comparison of air flow environmental effects on thermal fabrics," *Textile Research Journal*, Article vol. 88, no. 2, pp. 203-212, 2018.
- [31] M. Bogusławska-Bączek and L. Hes, "Thermophysiological properties of dry and wet functional sportswear made of synthetic fibres," *Tekstilec*, Article vol. 60, no. 4, pp. 331-338, 2017.
- [32] R. R. Van Amber, C. A. Wilson, R. M. Laing, B. J. Lowe, and B. E. Niven, "Thermal and moisture transfer

- properties of sock fabrics differing in fiber type, yarn, and fabric structure," *Textile Research Journal*, Article vol. 85, no. 12, pp. 1269-1280, 2015.
- [33] S. Karunamoorthy and A. Das, "Study on thermal resistance of multilayered fabrics under different compressional loads," *Journal of the Textile Institute*, Article vol. 105, no. 5, pp. 538-546, 2014.
- [34] M. Boguslawska-Baczek and L. Hes, "Thermal conductivity and resistance of nomex fabrics exposed to salty water," *Tekstil ve Konfeksiyon*, Article vol. 24, no. 2, pp. 180-185, 2014.
- [35] M. Boguslawska-Baczek and L. Hes, "Determination of heat transfer by radiation in textile fabrics by means of method with known emissivity of plates," *Journal of Industrial Textiles*, Article vol. 44, no. 1, pp. 115-129, 2014.
- [36] M. Naebe, N. Robins, X. Wang, and P. Collins, "Assessment of performance properties of wetsuits," *Proceedings of the Institution of Mechanical Engineers, Part P: Journal of Sports Engineering and Technology*, Article vol. 227, no. 4, pp. 255-264, 2013.
- [37] D. Romeli, G. Barigozzi, S. Esposito, G. Rosace, and G. Salesi, "High sensitivity measurements of thermal properties of textile fabrics," *Polymer Testing*, Article vol. 32, no. 6, pp. 1029-1036, 2013.
- [38] R. Zhang, J. Li, J. Xu, and J. Liu, "Dynamic heat conductivity property of fabrics," in *Advanced Materials Research* vol. 332-334, ed, 2011, pp. 845-849.
- [39] N. Nawaz, O. Troynikov, and C. Watson, "Thermal comfort properties of knitted fabrics suitable for skin layer of protective clothing worn in extreme hot conditions," in *Advanced Materials Research* vol. 331, ed, 2011, pp. 184-189.
- [40] N. Oğlakcioğlu and A. Marmarali, "Thermal comfort properties of cotton knitted fabrics in dry and wet states," *Tekstil ve Konfeksiyon*, Article vol. 20, no. 3, pp. 213-217, 2010.
- [41] T. Ramachandran, G. Manonmani, and C. Vigneswaran, "Thermal behaviour of ring- and compact-spun yarn single jersey, rib and interlock knitted fabrics," *Indian Journal of Fibre and Textile Research*, Article vol. 35, no. 3, pp. 250-257, 2010.
- [42] F. L. Zhu and K. J. Li, "Fractal analysis of effective thermal conductivity for woven fabrics used in fire fighters' protective clothing," *Journal of Fire Sciences*, Article vol. 29, no. 1, pp. 3-20, 2011.
- [43] C. Vigneswaran, K. Chandrasekaran, and P. Senthilkumar, "Effect of thermal conductivity behavior of jute/cotton blended knitted fabrics," *Journal of Industrial Textiles*, Article vol. 38, no. 4, pp. 289-307, 2009.
- [44] T. Dias and G. B. Delkumburewatte, "The influence of moisture content on the thermal conductivity of a knitted structure," *Measurement Science and Technology*, Article vol. 18, no. 5, pp. 1304-1314, 2007, Art. no. 016.
- [45] F. Zhu and W. Zhang, "Measuring the thermal conductive property of protective fabrics to radiant heat exposure," *Journal of Industrial Textiles*, Article vol. 37, no. 2, pp. 175-186, 2007.
- [46] L. Hes, M. de Araujo, and V. V. Djulay, "Effect of Mutual Bonding of Textile Layers on Thermal Insulation and Thermal Contact Properties of Fabric Assemblies," *Textile Research Journal*, Article vol. 66, no. 4, pp. 245-250, 1996.
- [47] A. M. Schneider, B. N. Hoschke, and H. J. Goldsmid, "Heat Transfer through Moist Fabrics," *Textile Research Journal*, Article vol. 62, no. 2, pp. 61-66, 1992.
- [48] P. Andersson, "Pressure dependence of the thermal conductivity of some polyamides," Article 1976.
- [49] N. N. Zaslavskii and A. M. Ar'ev, "Effect of extension on the structure and thermophysical properties of kapron (nylon 6)," *Polymer Mechanics*, Article vol. 4, no. 1, pp. 125-126, 1968.
- [50] H. J. Hoge and G. F. Fonseca, "The Thermal Conductivity of a Multilayer Sample of Underwear Material under a Variety of Experimental Conditions,"

- Textile Research Journal*, Article vol. 34, no. 5, pp. 401-410, 1964.
- [51] J. B. Speakman and N. H. Chamberlain, "The thermal conductivity of textile materials and fabrics," *J Text Inst Trans*, vol. 21, no. 2, pp. 29 - 56, 1930.
- [52] E. S. Rood, "Thermal conductivity of some wearing materials," *Physical Review*, Article vol. 18, no. 5, pp. 356-361, 1921.
- [53] F. Fung, L. Hes, R. Unmar, and V. Bajzik, "Thermal and evaporative resistance measured in a vertically and a horizontally oriented air gap by Permetest skin model," *Industria Textila*, Article vol. 72, no. 2, pp. 168-174, 2021.
- [54] L. Tu, H. Shen, and F. Wang, "The effective thermal resistance of permeable textile ensemble in windy environment," *International Journal of Thermal Sciences*, Article vol. 159, 2021, Art. no. 106644.
- [55] K. Shaker *et al.*, "Effect of fabric structural design on the thermal properties of woven fabrics," *Thermal Science*, Article vol. 2018, 2018.
- [56] H. He and Z. Yu, "Effect of Air Gap Entrapped in Firefighter Protective Clothing on Thermal Resistance and Evaporative Resistance," *Autex Research Journal*, Article vol. 18, no. 1, pp. 28-34, 2018.
- [57] M. E. Stoffberg, L. Hunter, and A. Botha, "The Effect of Fabric Structural Parameters and Fiber Type on the Comfort-Related Properties of Commercial Apparel Fabrics," *Journal of Natural Fibers*, Article vol. 12, no. 6, pp. 505-517, 2015.
- [58] M. M. Mangat, L. Hes, and V. Bajzik, "Thermal resistance models of selected fabrics in wet state and their experimental verification," *Textile Research Journal*, Article vol. 85, no. 2, pp. 200-210, 2015.
- [59] Z. E. Kanat, N. Özdil, and A. Marmarali, "Prediction of thermal resistance of the knitted fabrics in wet state by using multiple regression analysis," *Tekstil ve Konfeksiyon*, Article vol. 24, no. 3, pp. 291-297, 2014.
- [60] D. Gupta, A. Srivastava, and S. Kale, "Thermal properties of single and double layer fabric assemblies," *Indian Journal of Fibre and Textile Research*, Article vol. 38, no. 4, pp. 387-394, 2013.
- [61] M. Shabaridharan and A. Das, "Study on thermal and evaporative resistances of multilayered fabric ensembles," *Journal of the Textile Institute*, Article vol. 104, no. 10, pp. 1025-1041, 2013.
- [62] I. Salopek Čubrić, Z. Skenderi, A. Mihelić-Bogdanić, and M. Andrassy, "Experimental study of thermal resistance of knitted fabrics," *Experimental Thermal and Fluid Science*, Article vol. 38, pp. 223-228, 2012.
- [63] D. Ding, T. Tang, G. Song, and A. McDonald, "Characterizing the performance of a single-layer fabric system through a heat and mass transfer model - Part II: Thermal and evaporative resistances," *Textile Research Journal*, Article vol. 81, no. 9, pp. 945-958, 2011.
- [64] R. Shekar, T. M. Kotresh, M. S. Subbulakshmi, S. N. Vijayalakshmi, A. Patanaik, and R. D. Anandjiwala, "Experimental measurement and prediction of thermal resistance in paratrooper clothing," *Journal of Industrial Textiles*, Article vol. 40, no. 3, pp. 213-228, 2011.
- [65] V. K. Kothari and K. Bal, "Development of an instrument to study thermal resistance of fabrics," *Indian Journal of Fibre and Textile Research*, Article vol. 30, no. 4, pp. 357-362, 2005.
- [66] P. Gibson, M. Auerbach, J. Giblo, W. Teal, and T. Endrusick, "Interlaboratory Evaluation of a New Sweating Guarded Hot Plate Test Method (ISO 11092)," *Journal of Thermal Envelope and Building Science*, Article vol. 18, no. 2, pp. 182-200, 1994.
- [67] B. V. Holcombe and B. N. Hoschke, "Dry Heat Transfer Characteristics of Underwear Fabrics," *Textile Research Journal*, Article vol. 53, no. 6, pp. 368-374, 1983.

- [68] A. R. R. Aboalasaad, Z. Skenderi, S. Brigita Kolčavová, and A. A. S. Khalil, "Analysis of Factors Affecting Thermal Comfort Properties of Woven Compression Bandages," *Autex Research Journal*, Article vol. 20, no. 2, pp. 178-185, 2020.
- [69] F. P. Slater and W. H. Rees, "The protective value of clothing," *J Text Inst Proc*, vol. 37, no. 7, pp. 132 - 153, 1946.
- [70] W. E. Morton and J. W. S. Hearle, "Physical Properties of Textile Fibres, Fourth Edition," (in English), *Physical Properties of Textile Fibres, Fourth Edition*, no. 68, pp. 1-776, 2008.
- [71] S. K. Ghosh, S. Bairagi, R. Bhattacharyya, and M. M. Mondal, "Study on Potential Application of Natural Fibre Made Fabrics as Thermal Insulation Medium," *AIJRSTEM*, vol. 15, no. 1, pp. 8-13, 2016.
- [72] T. Aid. (10-12-2021). *Moisture Regain and Moisture Content of Different Fibers*. Available: <http://textileaid.blogspot.com/2013/12/moisture-regain-and-moisture-content-of.html>
- [73] M. L. Huber *et al.*, "New International Formulation for the Thermal Conductivity of H₂O," *J. Phys. Chem. Ref. Data*, vol. 41, no. 3, 2012.
- [74] K. J. Gross and B. Hardy, "Recommended Best Practices for Characterizing Engineering Properties of Hydrogen Storage Materials," H₂ Technology Consulting LLC2013, Available: https://www.energy.gov/sites/default/files/2014/03/f9/best_practices_hydrogen_storage_section_6_0.pdf.
- [75] J. Nadzeikiene, R. Milasius, J. Deikus, J. Eicinas, and P. Kerpauskas, "Evaluating thermal insulation properties of garment packet air interlayer," (in English), *Fibres & Textiles in Eastern Europe*, vol. 14, no. 1, pp. 52-55, Jan-Mar 2006.
- [76] D. L. Zhao, X. Qian, X. K. Gu, S. A. Jajja, and R. G. Yang, "Measurement Techniques for Thermal Conductivity and Interfacial Thermal Conductance of Bulk and Thin Film Materials," (in English), *Journal of Electronic Packaging*, vol. 138, no. 4, Dec 2016.
- [77] T. Makaveckas, R. Bliūdžius, and A. Levinskytė, "Analysis of the Variation of Thermal Conductivity of Rigid Polyisocyanurate Foam (PIR) in The Context of Aging " presented at the Current Topics and Trends on Durability of Building Materials and Components, Barcelona, 2020. Available: https://www.scipedia.com/wd/images/d/d4/Draft_Content_140487945p576.pdf
- [78] *ISO 8302:1991 Thermal insulation - Determination of steady-state thermal resistance and related properties - Guarded hot plate apparatus*, 1991.